# Trade and the End of Antiquity*

**Johannes Boehm**† Sciences Po

**Thomas Chaney**‡ USC

July 5, 2024

**Abstract**

What caused the end of antiquity, the shift of economic activity away from the Mediterranean towards northern Europe? We assemble a large database of coin flows between the 4th and 10th century. We build a dynamic model of trade and money where coins gradually diffuse along trade routes. We estimate the parameters of this model to recover time-varying bilateral trade flows and real consumption from data on the spatial and temporal distribution of coins. Our estimates suggest that reduced trade openness arising from the cost of crossing the newly formed border between Christianity and Islam, combined with technical progress and increased minting output in Muslim Spain and in the Frankish lands, explains the increased urbanization of western and northern Europe relative to the eastern Mediterranean from the 8th to the 10th century.

**JEL Classification:** F1, O1, N73.

**Keywords:** Gravity Models, International Trade, Market Access, Diffusion.

*We thank Marek Jankowiak, Ezra Oberfield, and Kevin O'Rourke for helpful comments. Malo Cadudal-Illy, Jinpei Tuchel, and in particular Ye Sun provided excellent research assistance. Boehm gratefully acknowledges financial support from the Banque de France/Sciences Po partnership, and Chaney gratefully acknowledges financial support from the European Research Council (ERC grant 884847). All remaining mistakes are our own.

† johannes.boehm@sciencespo.fr.

‡ thomas.chaney@gmail.com.

## Introduction

We quantify the extent to which disruptions in technology, coin production, and trade have contributed to the end of classical antiquity – the relative decline of Roman and Greek civilizations in the Mediterranean, and the subsequent shift of political and economic activity towards northern Europe.

What caused the end of antiquity has been a central question for centuries (see for instance Montesquieu, 1734; Voltaire, 1756; Gibbon, 1789). The current consensus among historians is that the conquest of Rome by Germanic invaders in the fifth century did not lead to an immediate decline of Roman institutions and commerce, as local institutions remained largely in place (Pirenne, 1927, 1939; Findlay and O'Rourke, 2009; McCormick, 2001). Instead, changes started to appear around the seventh century and culminate with the crowning of Charlemagne as Emperor at the end of the eighth century. It marks the dawn of a new era where political and economic power in Europe is no longer centered around the Mediterranean, but in the Frankish lands of northwestern Europe.

Some explanations point to changes in trade flows. Most famously, historian Henri Pirenne proposes that the expansion of the Arab Caliphate along the southern Mediterranean coast and into the Iberian peninsula disrupted commerce and political ties in the Mediterranean, and turned the emerging Carolingian Empire into a northern European power ("without Mohammed, Charlemagne would have been inconceivable," Pirenne, 1939, p.234). The evidence for these disruptions brought forward by Pirenne is mainly related to the disappearance of certain luxury goods north of the Mediterranean.[1]

In this paper we revisit Pirenne's thesis using the tools of modern quantitative trade models and novel data on the circulation of ancient coins. We structurally estimate a dynamic model of trade and money, recover time-varying trade costs, technology, coinage, and real consumption, and quantify the extent to which the Arab conquest coincides with changes in the ancient world economic geography.

We start with presenting new data. Building on decades of work by archaeologists and numismatists, we assemble a large database on coin finds from hoards that were deposited between AD 325 and AD 950, comprising observations from hundreds of thousands of coins that were found in hoards across Europe, North Africa, and the Middle East. Using data on coins to study changes in economic activity has three key advantages. First, coins were the key medium of exchange during Late Antiquity, particularly for long-distance trade. Second, coins offer rich quantitative information

[1] More precisely, Pirenne's argument is the near *absence* of mentions of silk and spices in historical texts written north of the Mediterranean, and the disuse of gold for coinage and papyrus for writings. These fragments of evidence, along with new archaeological findings, have been extensively studied and discussed by historians since Pirenne. See Lopez (1943), Ashtor (1970), Hodges and Whitehouse (1983), and, in particular, McCormick (2001)'s monumental work that synthesizes the existing literary and archaeological evidence on changes around the Mediterranean, including patterns of change in the flows of communications, objects, and travellers. The synthesis of Wickham (2006) interprets the evidence through the lens of social structures.

in a generally data-scarce setting,[2] as numismatists and archaeologists have deciphered, catalogued, and classified ancient coinage for over 200 years. Third, coin data contain information about where and when coins were minted and buried, which helps to resolve econometric identification challenges.

We document four stylized facts. First, the Arab conquest disrupted coin flows across the Mediterranean: Roman (including East Roman, i.e. Byzantine) coins dominate north-south and east-west Mediterranean crossings before the conquest; after the conquest, they are replaced by Islamic coins, which flow almost exclusively east-west, between the Caliphate's heartlands in the Middle East and the Maghrib (North Africa) and al-Andalus (the Iberian peninsula); coin flows between the Islamic and Christian worlds travel primarily between al-Andalus and the northern European Frankish lands. Second, the data display a familiar 'gravity' structure: fewer coins travel over longer distances and across political borders, holding origin (mint) and destination (hoard) sizes fixed. Third, coins travel longer distances as they age. Fourth, the fraction of coins of different ages decreases with coin age.

Informed by these stylized facts, we build a dynamic model of trade and money, which we structurally estimate using our coin hoard dataset. Agents across a discrete set of location hold coins to finance expenditure and to save, and they produce and sell goods in exchange for coins. We assume that coins are fungible,[3] and that they travel in opposite direction as trade. Trade across locations is governed by comparative advantages subject to trade costs as in Eaton and Kortum (2002). New coins are minted in a subset of mint locations at discrete minting events. The model features endogenous trade imbalances as in Dekle et al. (2007), where coin-rich locations may run a trade deficit financed by freshly minted coins. The model generates two unconventional features which are key to our structural estimation. First, the same coin may be used for multiple transactions throughout its life, so that the distribution of the stock of coins of different vintages evolves *dynamically* as coins percolate through the network of trading locations. A naive estimation that ignores the dynamics of coin diffusion would recover the Leontief inverse (Leontief, 1941, 1944) of the trade matrix instead of the trade matrix itself. Second, coins are used both as a medium of exchange (expenditures) and as a store of value (saving). A naive estimation that ignores saving would wrongly attribute the tendency of coins so stay locally because of local saving to a home bias in trade.

To bring our model to the data we partition the ancient world into 13 regions and 20-year time

[2] Due to the fact that no comprehensive data on production, consumption, trade, or demographics exists for the first millennium AD, historians of this period rely to a large extent on literary sources.

[3] The assumption that coins are fungible is key. We offer several (imperfect) validations of this assumption. First, we present a series of historical evidence that foreign coins were systematically accepted for domestic transactions (with the exception of tax collection). For instance, precise weights for foreign silver and gold coins were found in Cairo after the Arab conquest (Bates, 1991). Second, our estimates are robust to restricting our sample to gold coins only, which were widely accepted for transactions throughout the ancient world. This suggests that silver and bronze coins are just as fungible as gold coins. Third, our structural estimates of trade costs recovered from data on ancient coins are similar to estimates recovered from (limited) data on ancient trade in ceramics (Flückiger et al., 2022).

periods ranging from the 4th to the 10th century. We parameterize trade costs as a function of (optimal) travel time, and costs associated with crossing time-varying political and religious borders. We use travel time estimates from geospatial models of the Roman (Scheidel, 2015) and Arab worlds constructed by historians, and validate them by comparing them to travel times reported by the 10th century Arab geographer Al-Muqaddasī (1994). We collect data on time-varying borders between major political entities, and the time-varying religious border between Islamic and non-Islamic regions. Our structural estimation recovers time-varying trade *flows*, and the time-varying parameters governing them, using only data on the *stocks* of coins of different vintages. Importantly, although our data correspond, by construction, to *nominal* variables, bilateral trade flows contain information on relative factor prices, so that we are able to estimate time-varying regional *real* consumption. Inspired by Eaton and Kortum (2002) and Dekle et al. (2007), we estimate three economically meaningful terms: real consumption is fully partitioned into trade openness (up to the trade elasticity as in Eaton and Kortum, 2002; Arkolakis et al., 2012), technology, and seigniorage-financed trade deficits.

Our structural estimates reveal the joint importance of trade costs, shaped in part by religion, technology, and coin production. For instance, we estimate that the heartlands of the Byzantine empire experience a collapse in real consumption, due to a collapse in trade with regions newly conquered by the Arabs, a mild deterioration of technology, and a massive drop in minting output (our estimates match historical evidence on the "Byzantine dark ages," see Kazhdan, 1954; Ostrogorsky, 1959; Pennas, 1996; Zavagno, 2022). In contrast, western and northern Europe, including Islamic Spain (al-Andalus), are able to overcome the negative consequences of a reduced access to Mediterranean trade thanks to substantial improvements in technology (in line with the view that the Arabs brought along with them improvements in agricultural productivity, see Watson, 1974), and an commensurate increase in minting output which allows them to maintain almost constant trade deficits.

We further corroborate our findings by confronting our estimates of relative changes in real consumption from 620 to 900 AD to data on urbanization in Europe over the same period, under the presumption that urbanization is made possible by increased real consumption. We are able to match the relative urban decline of the Byzantine heartlands, the rapid increase in urbanization in western and northern Europe, and the relative stagnation of the Italian peninsula.

Our paper relates to the literature on the role of market access in shaping economic outcomes across space. Fogel (1964), Donaldson (2018), Donaldson and Hornbeck (2016), and Pascali (2017) evaluate the impact of improvements in transportation infrastructure in historical settings. Flückiger et al. (2022) use data on the flow of Roman pottery to argue for a persistent impact of Roman transportation infrastructure on the European economic geography, and Barjamovic et al. (2019)

use shipment records from Assyrian merchants archives in Bronze Age Anatolia, combined with a structural gravity model, to estimate the likely location of lost cities. In contrast, we do not observe prices, trade costs, or even trade flows directly. Instead, we recover trade flows and relative factor prices from data on the movement of coins over space and time, which we interpret through the lens of a dynamic model of trade and money. Liu and Tsyvinski (2024) features a related mechanism, where the dynamic transmission of shocks across an input-output network is subject to adjustment costs. This also distinguishes our work from classic applications of structural gravity models that use modern trade flow data to learn about trade barriers (see the survey in Head and Mayer, 2014). Similarly to Juhász (2018) we study the impact of trade barriers that result from political circumstances. Finally, the paper speaks to a literature in economic history that studies the patterns of change in Late Antiquity and early medieval times. This literature frequently uses numismatic evidence, although largely in a descriptive manner.[4] Closest to our paper, the textbook by Persson and Sharp (2015) discusses Pirenne's thesis and economic integration in Europe through the lens of a gravity model.[5]

The remaining of the paper is structured as follows. Section 1 lays out the historical context, describes our data, and presents four stylized facts on ancient coin flows. Section 2 presents our structural model of trade and money and estimation. Section 3 discusses our structural estimates.

# 1 Historical context, data, and stylized facts on ancient coins

## 1.1 Historical context

We study the economic and political developments that occurred in the Mediterranean between the 4th and the 10th century AD. At the start of this period, the fourth century, the Mediterranean was still entirely under control of the Roman Empire, albeit at times with multiple emperors and conflict between them, and under mounting pressure from Germanic invasions. The death of the eastern emperor Theodosius I in 395 divided the Roman Empire into a western and an eastern half. The fifth century saw increased Germanic incursions in the east and west, culminating with the Ostrogothic king Odoacer deposing the last West Roman emperor Romulus Augustulus in 476 and ending the Western Roman Empire. Italy was ruled by the Ostrogoths until the 550s, and later by the Lombards; Spain was taken over by the Visigoths, France by the Merovingian dynasty of the Franks, and North Africa, Sicily, and Sardinia by the Vandals. The Eastern Roman (Byzantine) Empire at times reconquered parts of the former Western Roman territory, but in the sixth century became increasingly under pressure

[4] A notable exception is Thomas Noonan's study of Islamic coin finds of different vintages and origins in Eastern Europe and Scandinavia (Noonan, 1980), which is similar in spirit to our exercise, but stops short of using a formal econometric model.

[5] See Shatzmiller (2018) for a qualitative application of the gravity model to medieval trade in the Middle East.

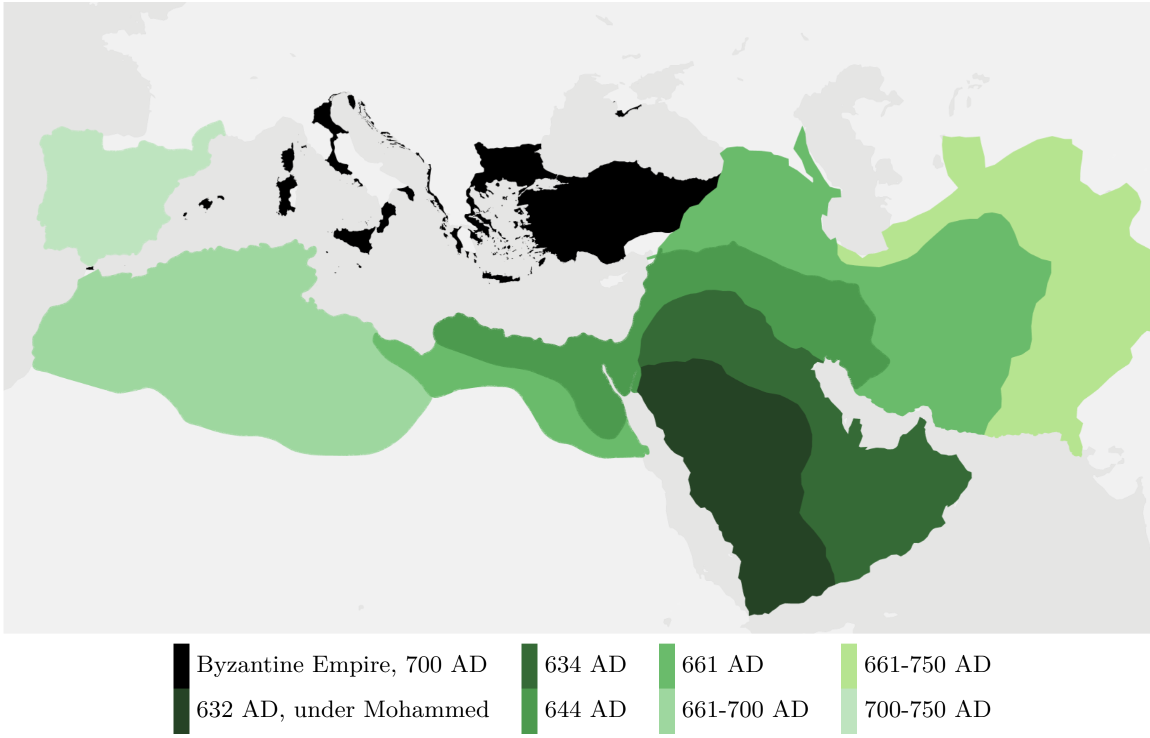


Figure 1: The Arab Conquests, 623-750

by wars with the Sasanian Empire in the east. The Byzantine-Sasanian wars of 602–628 depleted the resources of both empires, leaving a vacuum that was filled by the emerging Arab caliphate.

Figure 1 shows the rapid Arab expansion, starting in 622. By 634 the Arabs had the entire Arabian Peninsula under their control. The Levant followed in the late 630's and Egypt in the 640's. By the end of the Rashidun Caliphate in 661, the Arabs controlled a territory from Tripoli in the west to Balkh in the east. The expansion continued under the Umayyad dynasty. In 698 the Arab army razed Carthage and by 709 they had fully conquered the Maghreb. In 711 they crossed the Strait of Gibraltar and defeated the Visigoths at the Battle of Guadalete. In 732 they were stopped by Charles Martel at Tours, and driven back across the Pyrenees. When the Abbasid family overthrew the ruling Umayyads in 750, the Umayyads retained control of most of Iberia (al-Andalus). While the Arab conquest effectively ended Sasanian rule in the east, advances into Byzantine territory in Anatolia did not lead to sustained shifts in the land border. Meanwhile the Arabs strengthened their naval capabilities, ended the Byzantine naval control of the western Mediterranean and contested its control of the east. Arab sea raids on Mediterranean cities became frequent in both the east and the west.

## 1.2 Data

To study the impact of these political changes on the Mediterranean economy we construct a large dataset on the flows of coins around the Mediterranean between AD 325 and AD 950.[6] For the period from AD 325 to AD 725 we mostly rely on data from the *Framing the Late Antique and Early Medieval Economy* project (FLAME, 2023b),[7] a large-scale effort by historians and numismatists to record harmonized information on the location, dating, and composition of coin finds up to the year 725. FLAME covers hoards[8] from the Mediterranean and beyond, contributed by specialists working on the coinage of their geographical and temporal expertise. We use the most recent release of FLAME (January 2023) which covers 9,831 coin hoards. We remove hoards that fall outside our area of interest, continental western Europe up to the modern-day German-Polish border and including Bohemia, southern Europe up to the line between Vienna and Odessa, and North Africa and the Middle East up to the maximum extent and area of influence of the Umayyad Caliphate (stretching from the Maghreb in the West to the Indus in the east, and up to Bulgar in the north).[9] We also remove all hoards that only consist of incompletely described coins (no mint or mint date information).

We supplement FLAME's data, in particular for the period after AD 725, with hand-coded records of 100,478 coins from 797 finds, which we assemble using hoard catalogues from the archaeological and numismatic literature, similarly to the source documents that underlie FLAME. These additional records include the time period when the expansion of the Caliphate has ended, so that we can assess the impacts of these changes on the patterns of exchange in the Mediterranean. Together these data cover the vast majority of published information on coin finds in our geographic and temporal scope.

The structure of the coin hoard data is ideally suited for an analysis of dynamic bilateral spatial flows. Each unit of observation – a coin – contains the following attributes: (*i*) the location where the coin has been minted, "mint" (birth place), (*ii*) a year interval when the coin was minted, "mint date" (birth date), (*iii*) the identifier and the location of the hoard that the coin is part of (death place), (*iv*) a year interval when the coin was deposited (death date). These pieces of information are typically recorded by the author of the original numismatic or archaeological publication. Figure 2 shows an example. Mints are typically inferred from mint marks on the coins.[10] The mint date is

[6] Appendix A contains extensive information on the assembly, harmonization, and cleaning of the coin flow data.

[7] https://coinage.princeton.edu/

[8] FLAME also includes finds from excavations and single finds. Unless explicitly mentioned, we will treat all records in the same way and just use the word "hoard" to describe deposits of any size.

[9] The precise definition and construction is given in Appendix E, along with maps. Note that our area of study excludes the Viking lands, and therefore does not speak to the discussion on the potential role of the Vikings (and the inflow of Islamic silver through trade via eastern and northern Europe) in the changing economic geography during Late Antiquity (Bolin, 1953). Recent archaeometric studies indicate that Carolingian silver is largely not of Arab origin (Sarah, 2008; Sarah et al., 2008; Naismith et al., 2023), suggesting a limited role for silver inflows via the Viking route in affecting Carolingian mint output.

| No. | MINT | DATE | DIAM. | WEIGHT | NUMB. |
|---|---|---|---|---|---|
| 51 | الأندلس | 114 | 29. | 2.93 | 4 |
| 52 | " | 115 | 29.5 | 2.92 | 1 |
| 53 | " | 116 | 26.5 | 2.92 | 3 |

Figure 2: Coin hoard data, an example from al 'Ush (1972)

*Notes:* The figure shows an excerpt of an original publication from which we assemble hoard data: al 'Ush (1972) gives the content of the Damascus silver hoard in tabular form. From left to right, for the first row: the record number (51), the mint (al-Andalus), the date (year 114 of the Hijri calendar), diameter (29mm), weight (2.93g), and the number of coins with these attributes (4). The issuing dynasty (Umayyad) is given in the table headings and the denomination and material (silver *dirham*) is stated in the text.

often indicated on the coin. When this is not the case, it can be approximated from the ruler (or dynasty or empire) under whose authority the coin was issued and other information, like the mint mark. Finally, we follow the common approach of historians to estimate the date of deposit of each hoard using the *terminus post quem*, *tpq* for short, the date of the youngest object in the hoard that can be dated. In our case that is typically the most recent end year of the time intervals of the coins in the hoard.

In coding the mint location and date we typically follow the coding of the author of the original publication which catalogues the content of the hoard.[11] In some cases this information is imprecise: the author of the publication may not have been able to inspect the coin or inspected only a fragment. We conduct robustness checks to investigate whether our findings are driven by endogenous selection.

We have data on 5,600 hoards and 514,349 coins. After removing from FLAME large hoards found in the 19th century or earlier for which not much besides rough coin counts are known, 286,035, or 55.6% of coins are complete with a mint and minting year interval; on average 86% of coins in a hoard are complete. We define the age of coins at time of deposit as the difference between the midpoint of the coin's minting interval and the *tpq* of the hoard. Figure 3 shows the distributions of the number of hoard by *tpq*. Appendix tables A.1 and A.2 contains summary statistics on coins and hoards.

**Discussion.** The interpretation of coin flows as relating to trade, despite having a long tradition among numismatists and historians,[12] deserves some discussion. The Roman and subsequently Byzantine empire were generally fairly monetized economies, with coinage taking a pre-eminent role and

[10] Mint marks have been in use since ancient Greek times to be able to monitor the weight and precious metal content of coins issued by a mint.

[11] Sometimes these interpretations are critically evaluated and corrected by subsequent scholars. Appendix A lists the extensive sources we use for each of the hand-coded hoards.

[12] See, in particular, the discussions by Grierson (1959) and, more recently, Naismith (2014).

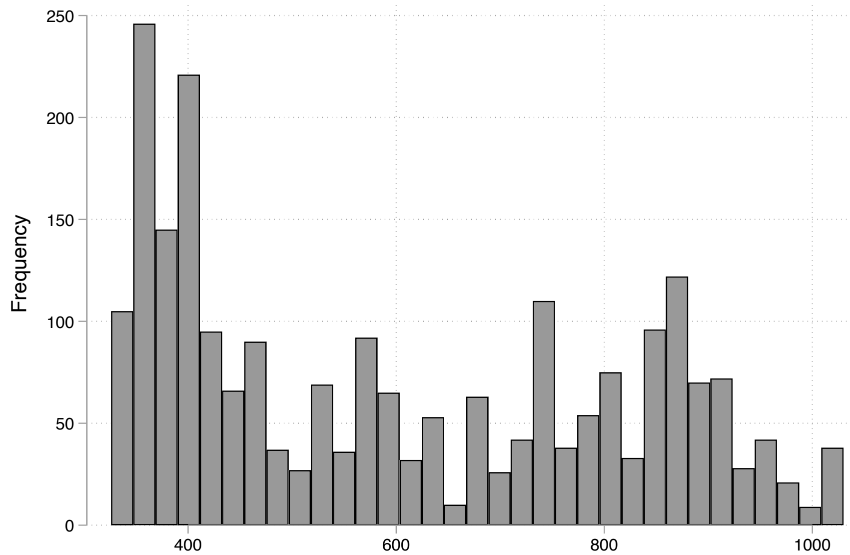


Figure 3: Distribution of coin hoards by Terminus Post Quem (*tpq*), 325-950 AD

*Notes:* This figure shows the number of hoards per 20-year period.

credit being very limited (Morrisson, 2002).[13] The situation was similar in the caliphate (Bessard, 2020) and in the Carolingian empire (Coupland, 2014). The fact that coins were light, durable, and — because they were made from precious metal, which could be easily reminted — accepted within and across borders made them particularly suitable for long-distance trade.[14] This is particularly the case for gold coins, which were traded throughout the Mediterranean and were valued by their weight in gold (Banaji, 2016).[15] Of course coins did not travel solely because of commerce; theft, gift-exchange, tribute, dowry, and ransom are other explanations for coin flows. We subsume those alternative motives for exchanges within a model of trade driven by comparative advantages.[16]

A potential source of bias comes from the fact that our data do not cover the universe of coin flows, but instead only hoards that have been created (i.e. the coins were either deliberately or accidentally deposited, which may depend on warfare, natural disasters, and property rights protection), subsequently found (which may depend on modern-day institutions, such as whether metal detecting is

[13] A possible exception was the eighth century, where Byzantine mint output collapsed.

[14] Examples of the use of currency in foreign empires abound. Bates (1991) discusses how Byzantine coins kept circulating (and even being minted) in Egypt following the Arab takeover in 641. Tribute and ransom payments between the Arabs and Byzantines following periods of conflict often included domestic currency. See also Chapter 12 of McCormick (2001), who discusses the circulation of Arab and Byzantine coins in the west.

[15] We conduct robustness checks of all our main results that restrict the sample to gold coins.

[16] Other data-driven approaches used by economic historians to measure economic activity include urbanization rates, the flows of consumption goods, notably ceramics (Wickham, 2006, Flückiger et al., 2022), communication flows and movements of people (McCormick, 2001), pollen grain measurements (Izdebski et al., 2016), and ice core readings (McConnell et al., 2018, Loveluck et al., 2018). Coin flows bring several econometric advantages and are plausibly more directly related to comprehensive patterns of exchange than ceramics or communications flows.

allowed, and modern-day market prices for historical coins), and finally documented by experts (which may depend on the local presence of experts, the "novelty" of the hoards' contents, and the demand for research on these topics).[17] Our model-based estimation is designed to correct those statistical biases, and differs from the more descriptive methods employed by historians.

Finally, an important characteristic of our data is that — in contrast to standard trade data — we do not observe flows at each point in time, but only when and where a coin was minted, and where and when a coin is deposited into a hoard. Our structural model in section 2 is specifically designed to identify the parameters governing trade flows from data on coin stocks, and to reconstruct the possibly numerous successive trips a coin took throughout its life.

### 1.3 Four stylized facts on ancient coins

We present reduced-form evidence on four stylized facts, which inform our structural model in section 2.

**The Arab conquest disrupted Mediterranean coin flows.** We first show suggestive evidence that the Arab conquest had a profound impact on coin flows across the Mediterranean. Figure 4 illustrates the changes in the flow of coins across the Mediterranean before and after the Arab conquests. Panel (a) shows flows between 450 and 630 AD. Constantinople, Thessalonica, Rome, Ravenna, and Carthage are important mints whose coins flow across the entire Mediterranean. Coins from Carthage cross the sea into Europe, and coins from Rome and Constantinople cross into Africa and the Middle East. Panel (b) shows that the patterns of coin flows change abruptly after 713, when the Arabs conquer the eastern Mediterranean coast (up to and including Antioch), the southern Mediterranean coast, and most of the Iberian peninsula. Most coins flow east to west within the Islamic Caliphate, within the Arab heartlands of Syria, Mesopotamia, and Egypt, and within the Frankish lands of northern Europe. The coin flows emanating from the remaining Byzantine mints in Constantinople, Syracuse, and Italy are much smaller than in the earlier period.[18] Besides a few coins from the mints of Ifriqiya and al-Abbasiyya that end up in the hoards of Ilanz and Steckborn (McCormick, 2001), there are almost no north-south flows across the Mediterranean. Flows that cross the border between Christianity and Islam primarily do so in the the West across the Pyrenees (Parvérie, 2014, 2018).

Figure 5 shows the number of coins crossing the Mediterranean, and their composition. The time

[17] FLAME (2023a) discusses potential sources of biases in FLAME's data, which also apply to our combined data.

[18] The changes in the magnitude and location of Byzantine coin production has been the topic of a large literature. Kazhdan (1954) was the first to argue for a decline of Byzantine cities in the 8th and 9th century based on archaeological evidence. Several authors (including Kazhdan, Zavagno (2022), and Pennas (1996)) relate these changes to Arab military pressure. Grierson (1973) notes that the eastern mints of Nicomedia, Cyzicus, Thessalonica, Cyprus, as well as Catania, were closed in 629-630, before the Arab conquests, and production was relocated to Constantinople. Nevertheless, a number of provincial mints, including Syracuse, Ravenna, and Rome, remained active until at least the mid-8th century (in the case of Sycracuse until 878 when it fell to the Aghlabids).

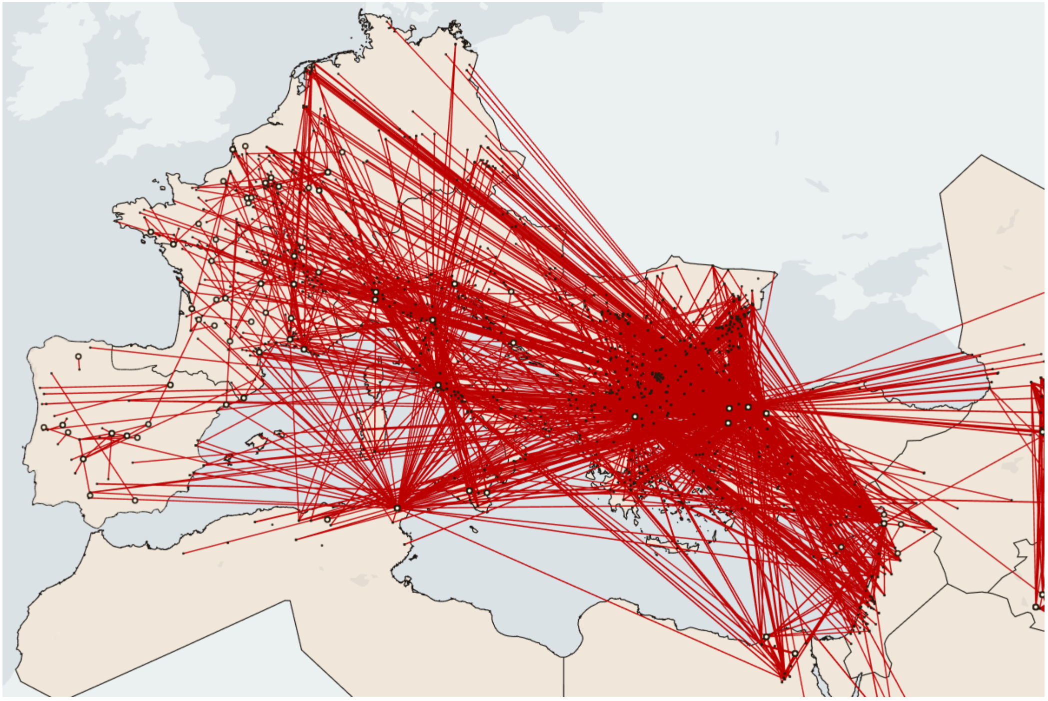

(a) Before the Arab conquests: 450-630 AD

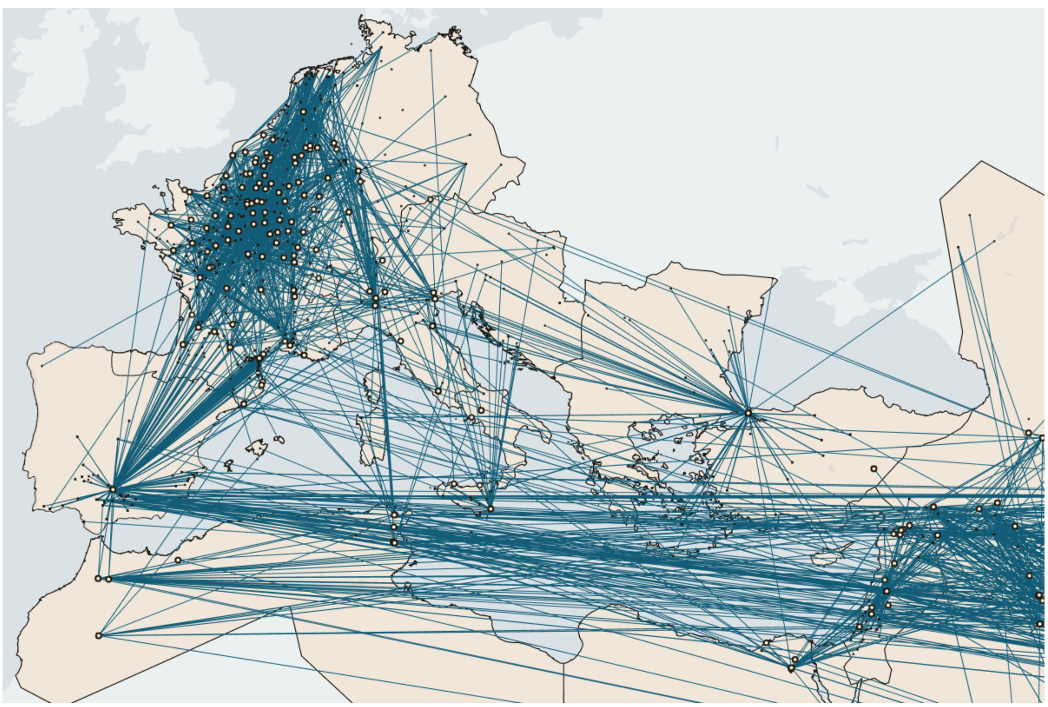

(b) After the Arab conquests: 713-900 AD

Figure 4: Changes in coin flows in the Mediterranean

*Notes:* The figure shows coin flows, indicated by a straight line, between mints and find spots. The sample consists of all coin groups where both the lower end of the mint interval and the *tpq* of the hoard lie between 450 and 630 AD (panel (a)) and 713 and 900 AD (panel (b)). Hoards from outside the shaded area are excluded.

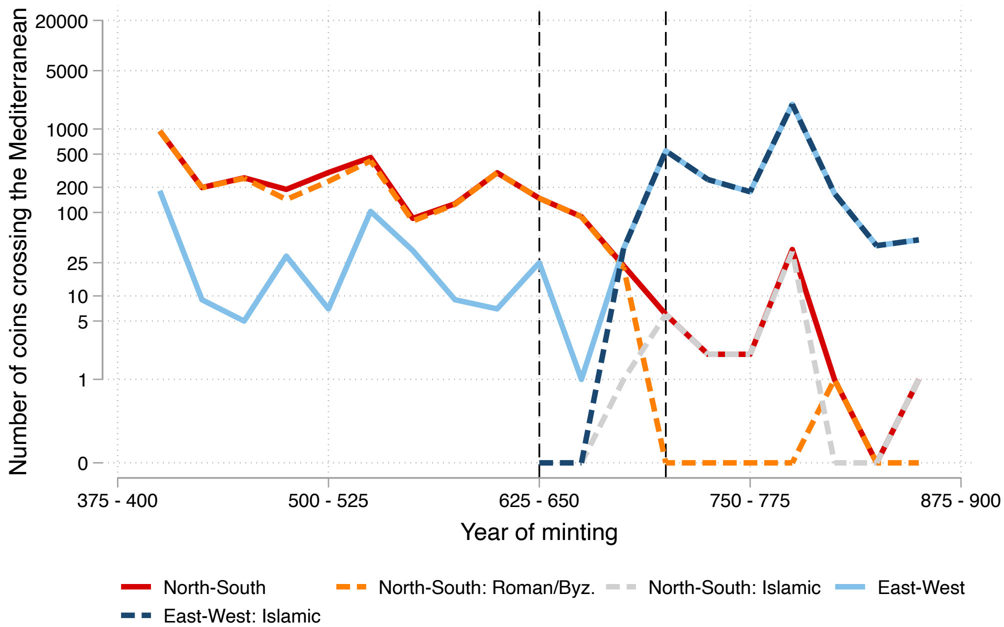


Figure 5: Number of coins flowing across the Mediterranean

*Notes:* The figure shows the number of coins minted in the 25-year interval on the horizontal axis, that are minted on one side of the Mediterranean, and are found on the other. Flows include both directions. The north is defined to go from the Pyrenees to Byzantine Turkey, east from Byzantine Turkey to Egypt, south from Egypt to the Maghreb, and west from Maghreb to Aquitaine. Border regions are included in these definitions, so regions are partly overlapping.

of the Arab conquests, indicated by two dashed vertical lines, corresponds to a decline of north-south flows (almost entirely flows of Roman/Byzantine coins), and an increase in east-west flows. The new flows along both axes are almost entirely made of Islamic coins. Despite the fact that in some historical sources the Arabs called the Mediterranean the "Sea of the Romans" (*Baḥr al-Rūm(ī)*), after the Arab conquests the Mediterranean became, at least when it comes to coin flows, an Arab dominated sea.[19]

To isolate changes in the Mediterranean from origin-destination effects, we estimate by PPML

$$\begin{aligned} \text{count}_{mhpt} = \exp\Big(& a_{mh} + a_{mp} + \\ & b_1 \text{Mediterranean}_{mh} \times \text{After}_t + b_2 \text{Mediterranean}_{mh} \times \text{After}_t \times \text{Islamic}_p + u_{mhpt}\Big). \end{aligned} \quad (1)$$

We aggregate all hoard ($h$) and mint ($m$) locations to $1° \times 1°$ cells, separately for each time period ($t$), and note for each coin which one of fourteen aggregate political blocks $p$ had issued it.[20] Count$_{mhpt}$ is the number of coins issued in cell $m$ under empire/dynasty $p$ and found in a cell $h$, within time period

[19]Paraphrasing Pirenne (1939). We take the Arab conquests as a proximate cause for these changes, and do not attempt to explain why the Arabs were successful. The commonly held view is that the Byzantine-Sasanian war of 602–628 exhausted the forces of both empires and paved the way for Arab military success (Foss, 1975).

[20]These political blocks are: Eastern Roman Empire, Western Roman Empire, Roman Empire (pre-division), Sasanians, Umayyads, Spanish Umayyads, Abbasids, Fatimids, Samanids, Visigoths, Ostrogoths, Vandals, Merovingians, and Carolingians. See Appendix Figure A.1 for a breakdown of these and more aggregate political entities.

Table 1: The Mediterranean Before and After the Conquests

| | Dependent variable: Number of Coins | | | |
|---|---|---|---|---|
| | (1) | (2) | (3) | (4) |
| Crossing Mediterranean × After Conquests | -1.774** | -3.141** | -0.712 | -1.751 |
| | (0.46) | (0.53) | (0.66) | (1.24) |
| Crossing Mediterranean × After Conquests × Islamic Coin | | 7.171** | 4.835** | 8.382** |
| | | (0.91) | (0.97) | (1.15) |
| Crossing Mediterranean × After Conquests × Roman Coin | | | -3.108** | -2.976** |
| | | | (0.79) | (0.71) |
| Mint Cell × Empire FE | Yes | Yes | Yes | Yes |
| Mint Cell × Hoard Cell FE | Yes | Yes | Yes | Yes |
| After Conquests FE | Yes | Yes | Yes | |
| Mint Cell × After Conquests FE | | | | Yes |
| Hoard Cell × After Conquests FE | | | | Yes |
| Estimator | PPML | PPML | PPML | PPML |
| Observations | 10350 | 10350 | 10350 | 6023 |

Standard errors in parentheses, clustered at the hoard × era and mint × era level.
$^{+}$ $p < 0.10$, $^{*}$ $p < 0.05$, $^{**}$ $p < 0.01$

*Notes:* This table presents various specifications of equation (1). The dependent variable is the number of coins in a hoard cell from a mint cell × dynasty × era (where era is before vs after the conquests). The regression drops all mint × dynasty combinations that have zero emitted coins. Hoard and mint cells are 1° × 1°. Flows before the conquests are those with mint date after 400 and *tpq* before 630; flows after the conquests are those with mint date after 713 and *tpq* before 900. Observation counts only include those that remain after dropping singletons and separated observations. "Crossing Mediterranean" is a dummy that is one if the geodesic line between hoard and mint cell intersects with the Mediterranean. "Islamic Coin" and "Roman Coin" are dummies equal to one if the coin is of Islamic issue (any dynasty) or Roman/Byzantine issue, respectively. "Empires" here are categorized as Sasanian, Roman-Byzantine, Franks, Islamic, Germanic Tribes, and Other Christian.

$t$. Mediterranean$_{mh}$ is a dummy that is one if the geodetic line between cells $m$ and $h$ intersects the Mediterranean; After$_t$ is a dummy equal to one if $t$ is between 713 and 900, and zero if between 400 and 630; Islamic$_p$ is one if the coin is of Islamic issue (any dynasty); $a_{mh}$ and $a_{mp}$ denote mint cell × hoard cell and mint-cell × dynasty/empire fixed effects, respectively. The objective is to investigate whether the Mediterranean acts differentially as a barrier to coin flows after the Arab conquests, and if so, for coins of which issue. Table 1 presents the results. We drop all mint cell × empire/dynasty combinations that did not produce coins. Column (1) shows a negative coefficient on the interaction of the Mediterranean and post-conquest dummies, so that after the Arab conquests coin flows declined in cell pairs across the sea. Column (2) shows a positive coefficient on the triple interaction: Islamic coins were facing disproportionately lower barriers on sea routes in the post-conquest world, conditional on origin and destination characteristics. Column (3) contrasts this with Roman/Byzantine coins, which experience disproportionately higher barriers. Column (4) shows similar estimates with hoard cell × time and mint cell × time fixed effects, neutralizing potential location-time-specific confounders.

Our structural estimation leverages the timing and spatial extent of the Arab conquest to estimate

Table 2: Distance and Border Effects in Coin Flows

| | Dependent variable: # $\text{Coins}_{mdh}$ | | | | | |
|---|---|---|---|---|---|---|
| | (1) | (2) | (3) | (4) | (5) | (6) |
| Log Distance | -1.138$^{**}$ | -1.002$^{**}$ | -1.140$^{**}$ | -0.955$^{**}$ | -0.727$^{**}$ | -0.694$^{**}$ |
| | (0.12) | (0.13) | (0.10) | (0.077) | (0.10) | (0.10) |
| Political border | | -1.945$^{**}$ | | -2.073$^{**}$ | | -1.540$^{**}$ |
| | | (0.62) | | (0.47) | | (0.41) |
| Hoard Cell FE | Yes | Yes | Yes | Yes | Yes | Yes |
| Mint × Empire Cell FE | Yes | Yes | Yes | Yes | Yes | Yes |
| Sample | | | Gold only | Gold only | Int. Marg. only | Int. Marg. only |
| Estimator | PPML | PPML | PPML | PPML | PPML | PPML |
| Pseudo-$R^2$ | 0.766 | 0.778 | 0.809 | 0.825 | 0.737 | 0.744 |
| Observations | 216809 | 216809 | 57457 | 57457 | 6306 | 6306 |

Standard errors in parentheses, clustered at mint cell × empire and hoard cell level.
$^{+}$ $p < 0.10$, $^{*}$ $p < 0.05$, $^{**}$ $p < 0.01$

*Notes:* This table presents various specifications of equation (2). The dependent variable is the number of coins in a hoard cell $h$ from a mint cell $m$ issued by a political entity $p$. The regression drops all $(m, d)$ combinations that have no emitted coins. Hoard and mint cells are $1° \times 1°$. Observations only include those that remain after dropping singletons and separated observations. Political entities here are categorized into fourteen divisions.

the changes in trade costs it induced.

**Distance and political borders disrupt trade.** The bilateral structure of our dataset, with a mint-origin and hoard-destination for each coin, allows us to explore the geography of coin flows. We aggregate hoard ($h$) and mint ($m$) $1° \times 1°$ cells across all periods, and model the flows of coins between these cells as a function of distance between cells and a political border dummy,

$$\text{count}_{mhp} = \exp\left(a_{mp} + a_h + b_1 \log \text{distance}_{mh} + b_2 \text{PoliticalBorder}_{hp} + u_{mhp}\right). \tag{2}$$

We estimate this model by PPML using data on all triplets $(m, h, p)$ where some coins of political block $p$ were minted in mint cell $m$.[21] The political border dummy is one if the region[22] where the center of the hoard cell $h$ is located in has never and to no extent been under the political control of $p$. Table 2 shows the results. Distance between mint and hoard is negatively correlated with coin flows, whether we combine extensive and intensive margins, columns (1) and (2), or use only the intensive margin, column (3). The political border effect coefficient is large and statistically significant. The point estimate from column (2) suggest that crossing a political border is equivalent to a ten-fold increase in distance.[23] Columns (3) and (4) show almost identical results when limiting the sample to the flow of

[21] We exploit the extensive margin of flows and include triplets when no coins of $p$ from $m$ were found in a hoard cell $h$.

[22] See Appendix E.2 for our division of the combined Arab and Mediterranean world into 13 regions.

[23] An alternative explanation for the significance of the border effect would be that coins first get administratively redistributed within a political entity before entering circulation. Appendix B.1 shows gravity regressions with hoard × empire effects that suggest that this is unlikely to be the case at a large scale.

Table 3: Coin age and distance travelled

| | Dependent variable: Log Distance between Mint and Hoard | | | | |
|---|---|---|---|---|---|
| | (1) | (2) | (3) | (4) | (5) |
| Log Age of Coin | 0.160** | 0.0942** | 0.0882** | 0.178** | 0.0623** |
| | (0.050) | (0.025) | (0.031) | (0.049) | (0.020) |
| Sample | | | | No non-hoards | No non-hoards |
| Hoard FE | Yes | Yes | Yes | Yes | Yes |
| Mint × 50-year-interval FE | | Yes | | | |
| Mint × 25-year-interval FE | | | Yes | | Yes |
| $R^2$ | 0.762 | 0.863 | 0.869 | 0.775 | 0.899 |
| Observations | 287235 | 287018 | 286860 | 250133 | 249806 |

Standard errors in parentheses, clustered at the hoard level.
$^{+}$ $p < 0.10$, $^{*}$ $p < 0.05$, $^{**}$ $p < 0.01$

*Notes:* The dependent variable is the log distance between the mint location and the location of the hoard. The independent variable is the log age of the coin at the date of the *tpq* of the hoard (where the age is defined as the difference between the midpoint of the minting interval and the maximum of the endpoints of the minting intervals). In the rare cases where this age is zero (the youngest coin in the hoard is dated to a precise year) we set the log age to zero. Mints are identified as all Nomisma or FLAME-recorded entities that have been geocoded to the same $0.1° \times 0.1°$ cell. Columns (4) and (5) exclude FLAME finds that are tagged as not being hoards.

gold coins, which were universally valued throughout the Mediterranean for their metal content and were therefore particularly favoured for long-distance trade. Despite accounting for only about 7% of the coins in our sample, distance and border effects for gold coins are remarkably similar.[24]

Columns (5) and (6) shows similar results when using the intensive margin of coin flows only.

Combined, those estimates suggest that coin flows contain information related to trade costs (e.g. distance and border effects). The key contribution of our structural model is to isolate features of the geography of coin flows that are driven by trade.

**Older coins travel further.** Coins are found, on average, in hoards 800 kilometers from their mint. But within hoards, older coins are also coins that have on average travelled farther. Table 3 shows results from a regression of log distance between a coin's mint and hoard place on the log age between minting and the hoard's *tpq*, with hoard fixed effects to isolate within hoard variations. The coefficient of coin age is positive and significant, and remains so even when including mint × mint year interval fixed effects, to control for the average distance travelled and age of coins of a particular mint and issue. This fact suggests that older coins have been used on average for more transactions, with each transaction taking them further away from their mint origin. Our structural model is designed to disentangle the many transactions of old coins from the few transactions of young coins.

[24] Results are also very similar when weighing coins by their value. See Appendix Table B.3 for details.

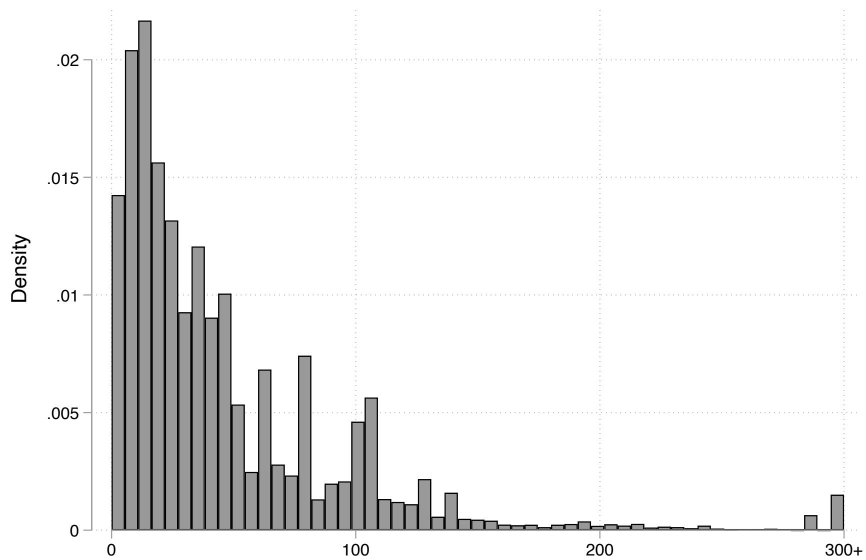


Figure 6: Coin age at time of deposit (*tpq*), in years

*Notes:* This figure displays the (annual) density of coins of different ages. We define the age of a coin at the time of deposit as the difference between the midpoint of the coin's minting interval and the *tpq* of the hoard it is found in.

**The fraction of coins in a hoard declines with coin age.** Figure 6 shows the distribution of coin ages within a hoard.[25] The average coin in our data is deposited 47 years after it was struck, and we sometimes observe coins that are hundreds of years old. On average, hoards contain fewer older coins than younger coins. This suggests that coins can be used over many years but also that they may eventually disappear. This fact will prove useful to our estimation, as it allows us to observe coins in circulation over different, overlapping, lengths of time.

# 2 Model and estimation

We now introduce a quantitative model of trade, money, and the diffusion of coins. This model forms the basis for the estimation of trade costs, mint outputs, and technology, from which we can quantify the importance of political changes for the economic geography of the ancient western world.

## 2.1 Model

**Set up.** There is a discrete set of $N$ locations, denoted by a subscript. Time is discrete, denoted in square brackets. Each time period is decomposed into three sub-periods: beginning, middle, and end.

At the end of period $t-1$, location $n$ sets aside a coin stock $S_n[t]$ for consumption and saving at $t$.

[25]To further support the view that the hoards in our data reflect coin circulation during Late Antiquity, Appendix A.4.3 compares the coin age distribution in our hoards with the one in twelve Byzantine hoards that Banaji (2016) labels as circulation hoards, i.e. that are known to have originated from coins that were in circulation.

At the beginning of period $t$, an exogenous fraction $\lambda_n[t]$ of the coins in this stock $S_n[t]$ ceases to circulate, either lost or melted into fresh new coins.[26] In addition, some locations own a mint which exogenously generates fresh new coins if it is active in period $t$, $M_n[t] \geq 0$.

In the middle of period $t$, $L_n[t]$ identical workers save a fraction $s_n[t]$ of their coins, and spend the rest for expenditures on consumption, $X_n[t]$. Importantly, expenditures contain spending on all goods, possibly including capital goods. What we label saving, $s_n[t]$, solely captures saving into nominal financial assets (coins), not saving for investment into physical capital. Workers face the following budget constraint,

$$X_n[t] = (1 - s_n[t])\Big((1 - \lambda_n[t])\, S_n[t] + M_n[t]\Big), \text{with } s_n[t] \geq 0, \tag{3}$$

where we assume workers cannot borrow ($s_n[t] \geq 0$). This is a 'coin-in-advance' economy where consumption is financed by available coins, and not by promised future income.[27]

At the end of period $t$, workers earn a competitive wage $w_n[t]$ selling goods in exchange for $w_n[t]\, L_n[t]$ worth of coins. The stock of coins set aside for the subsequent period evolves recursively,

$$S_n[t+1] = (1 - \lambda_n[t])\, S_n[t] + M_n[t] + w_n[t]\, L_n[t] - X_n[t]\,. \tag{4}$$

**Trade.** Within each period comparative advantages (Eaton and Kortum, 2002) shape trade flows. Consumers in $n$ allocate a fraction $\pi_{ni}[t]$ of their expenditures $X_n[t]$ to imports from $i$, $X_{ni}[t]$,

$$\pi_{ni}[t] = \frac{X_{ni}[t]}{X_n[t]} = \frac{T_i[t]\,(w_i[t]\, d_{ni}[t])^{-\theta}}{\sum_k T_k[t]\,(w_k[t]\, d_{nk}[t])^{-\theta}} \tag{5}$$

**Inter-temporal allocations.** Workers have log-utility over real consumption,

$$U_n[t] = \mathbb{E}_t\left[\sum_{\tau \geq t} \beta^{\tau - t} \ln\left(\frac{X_n[t]}{p_n[t]}\right)\right], \text{with } p_n[t] = \gamma\left(\sum_k T_k[t]\,(w_k[t]\, d_{nk}[t])^{-\theta}\right)^{-1/\theta}.$$

where $p_n[t]$ is the ideal price index in $n$ at $t$ (Eaton and Kortum, 2002). Each location chooses a sequence of coins stocks, $\{S_n[\tau]\}_{\tau \geq t}$, to maximize utility, given wages, and subject to the coins-in-advance constraint (3), their inter-temporal budget constraint (4), the optimal within-period allocation

[26] We think of $\lambda$ primarily as coins melted into bullion for their precious metal content, possibly as a segnioriage tax to be re-minted into fresh new coins. A very small fraction of $\lambda$ is literally lost, buried into a hoard and forgotten. Some of those lost coins will be found by archaeologists and become part of our dataset.

[27] The 'coin-in-advance' constraint is both plausible and necessary. Any relaxation of this constraint would imply that agents have access to financial markets, which were underdeveloped or even non-existent in the ancient world. Moreover, if relaxed, workers in one location would send their income (coins) to pay for consumption on goods from another location; those coins would become the income of workers in those locations, which they would send to other locations, etc, all within the same period. Coins would travel infinitely many times within each period and data on coin holdings would no longer contain any information on trade. Similarly, if coins were used only to clear bilateral imbalances, data on coins would contain information on net trade but not on gross trade flows.

of spending across imports (5), and a transversality condition which prevents holding coins forever,

$$\max_{\{S_n[\tau]\}_{\tau\geq t}} \mathbb{E}_t \left[ \sum_{\tau\geq t} \beta^{\tau-t} \ln \left( \frac{(1-\lambda_n[\tau]) S_n[\tau] + M_n[\tau] + w_n[\tau] L_n[\tau] - S_n[\tau+1]}{\gamma \left( \sum_k T_k[\tau] (w_k[\tau] d_{nk}[\tau])^{-\theta} \right)^{-1/\theta}} \right) \right] \tag{6}$$

$$\text{s.t. } S_n[\tau+1] \geq w_n[\tau] L_n[\tau], \forall (\tau \geq t), \text{ and } \lim_{\tau\to\infty} \beta^\tau \frac{S_n[\tau+1]}{X_n[\tau]} = 0.$$

In this model, saving ($s_n[\tau] > 0 \Leftrightarrow S_n[\tau+1] \geq w_n[\tau] L_n[\tau]$) is used only for consumption smoothing.

**Equilibrium.** Wages are determined by market clearing each period, given the trade equilibrium, $\pi_{ni}[t]$ from equation (5), and the coin stock policy function, $S_n[t]$ from equation (6),

$$w_i[t+1] L_i[t+1] = \sum_n \pi_{ni}[t] \Big( (1-\lambda_n[t]) S_n[t] + M_n[t] + w_n[t] L_n[t] - S_n[t+1] \Big). \tag{7}$$

**Steady state equilibrium.** We use the following steady state characterization when simulating counterfactual equilibria in section 3. In a steady state all aggregate variables are constant, in particular $w_n[t] L_n[t] = w_n L_n$ and $M_n[t] = M_n, \forall (n,t)$. If agents correctly anticipate they are in a steady state, there is no consumption smoothing motive for saving, $s_n = 0$ and $X_n = (1-\lambda_n) w_n L_n + M_n$. If agents anticipate shocks and save for precautionary motives, the same equality between expenditure and income (inclusive of minting) holds to a first order, $X_n = \frac{1-s_n}{1-s_n+\lambda_n s_n} ((1-\lambda_n) w_n L_n + M_n)$ with $\frac{1-s_n}{1-s_n+\lambda_n s_n} \approx 1$.[28] Equilibrium wages jointly clear markets,

$$w_i L_i = \sum_n \pi_{ni} \Big( (1-\lambda_n) w_n L_n + M_n \Big), \text{ and } \pi_{ni} = \frac{T_i (w_i d_{ni})^{-\theta}}{\sum_k T_k (w_k d_{nk})^{-\theta}}, \tag{8}$$

such that the aggregate stock of coins in circulation is constant, $\sum_n M_n = \sum_n \lambda_n w_n L_n$.[29]

## 2.2 Dynamic accumulation in coin hoards

We assume in our estimation that coin hoards found by archaeologists, our dataset, are drawn uniformly at random from the stock of coins set aside, $S_n[t]$ in each location $n$ and period $t$. Our aim is to keep track of the composition of those coin stocks, made of coins of different vintages, minted in different locations at different dates, which have traveled over time through the trade network.

[28] We estimate $\lambda = 1.7\%$ p.a. (section 2.3), and Scheidel (2015) calculates a savings rate $s = 1.5\%$ for Roman times.

[29] We do not impose any constraint on using arbitrarily small coin denominations: if aggregate minting, $\sum_n M_n$, decreases (increases), wages denominated in coins will be decrease (increase), leading to deflation (inflation).

Note that this model is analogous to Dekle et al. (2007), where some locations run a trade deficit and some a trade surplus. The trade deficit of location $n$, equal to the net creation of coins, is $D_n \equiv X_n - w_n L_n = M_n - \lambda_n w_n L_n$. Any non-mint location runs a trade surplus ($D_n < 0$), and a mint location runs a trade deficit if minting is large enough, with at least one mint location running a trade deficit.

We denote by $S_{mi}[t,\tau]$ the number of coins minted in location $m$ at time $t$ which are part of the coin stock of location $i$ at time $\tau$, with $S_i[\tau] = \sum_{m=1}^{N} \sum_{t \leq \tau} S_{mi}[t,\tau]$. Coins start their 'coin life' when they are minted, so $S_{mm}[t,t] = M_m[t]$. Subsequently, they circulate across locations as they are used for transactions or saved. $S_{mi}(t,\tau)$ evolves recursively,

$$S_{mi}[t,\tau+1] = \sum_{n=1}^{N} (1 - s_n[\tau])(1 - \lambda_n[\tau]) S_{mn}[t,\tau] \pi_{ni}[\tau] + s_i[\tau](1 - \lambda_i[\tau]) S_{mi}[t,\tau], \forall (\tau \geq t). \quad (9)$$

At time $\tau$, each location $n$ has a stock of coins set aside. A fraction $(1 - s_n[\tau])$ is spent on goods (non-saved). Of those coins, $(1 - \lambda_n[\tau]) S_{mn}[t,\tau]$ were minted in location $m$ at time $t$. Consumers in $n$ send a fraction $\pi_{ni}[\tau]$ of their non-saved coins to $i$ to pay for imported goods. We assume that coins are fungible so that buyers draw from their coin stock at random, and $(1 - s_n[\tau])(1 - \lambda_n[\tau]) S_{mn}[t,\tau] \pi_{ni}[\tau]$ coins minted in location $m$ at time $t$ move from $n$ to $i$ at time $\tau$ in expectation. Summing across all (coin) origins we derive the first term (sum) in equation (9). In addition, a fraction $s_i[\tau]$ of coins is saved locally and remains in region $i$, the second term in equation (9). We can express the dynamic evolution of the composition of coin stocks in a compact matrix form and solve it forward,

$$\begin{aligned} \mathbf{S}[t,t] = \mathbf{M}[t], \text{and } \mathbf{S}[t,\tau+1] = \mathbf{S}[t,\tau]\left((\boldsymbol{I} - \boldsymbol{\lambda}[\tau])\tilde{\mathbf{\Pi}}[\tau]\right), \forall \tau > t, \\ \text{with } \tilde{\mathbf{\Pi}}[\tau] \equiv (\boldsymbol{I} - \boldsymbol{s}[\tau])\mathbf{\Pi}[\tau] + \boldsymbol{s}[\tau], \\ \Rightarrow \mathbf{S}[t,T] = \boldsymbol{M}[t]\left(\prod_{\tau=t}^{T-1} (\boldsymbol{I} - \boldsymbol{\lambda}[\tau])\tilde{\mathbf{\Pi}}[\tau]\right) \forall T \geq t. \quad (10) \end{aligned}$$

$\mathbf{S}[t,T]$ is the square $N \times N$ matrix of coin stocks with $(n,i)^{th}$ element $S_{ni}[t,T]$. $\boldsymbol{M}[t]$ is a diagonal $N \times N$ matrix of minting with $n^{th}$ element $M_n[\tau]$. $\boldsymbol{I}$ is the $N \times N$ identity matrix and $\boldsymbol{\lambda}[\tau]$ is a diagonal $N \times N$ matrix of coin loss with $n^{th}$ element $\lambda_n[\tau]$. $\tilde{\mathbf{\Pi}}[\tau]$ is the square $N \times N$ matrix, which governs bilateral coin flows. This 'augmented' trade matrix $\tilde{\mathbf{\Pi}}[\tau]$ is a function of $\boldsymbol{s}[\tau]$, the diagonal $N \times N$ matrix of net saving rates with $n^{th}$ element $s_n[\tau]$, and $\mathbf{\Pi}[\tau]$, the trade matrix with $(n,i)^{th}$ element $\pi_{ni}[\tau]$, the classical Eaton and Kortum (2002) trade share from equation (5).

Equation (10) forms the basis of our estimation. Before describing our estimation strategy, we isolate two original features of our model, which helps gain intuition on how we can extract information about trade from coins, but also clarifies the inherent distinctions between data on coins and trade.

**Coins as a medium of exchange versus a store of value.** The stock of coins $\mathbf{S}$ in equation (10) diffuses across locations not according to the trade matrix $\mathbf{\Pi}$, but to the 'augmented' trade matrix $\tilde{\mathbf{\Pi}}$. Both matrices have almost the exact same structure, with one distinction: coins, unlike goods, have an additional tendency to stay locally, because they are also used as a store of value for (local) saving.

To make this distinction explicit, we decompose the 'augmented' trade share $\tilde{\pi}_{ni}$ into an origin-specific term, $\tilde{\alpha}_n$, a destination-specific term, $\tilde{\beta}_i$, and a bilateral term $\tilde{\delta}_{ni}$,

$$\begin{aligned}
\tilde{\pi}_{ni}[\tau] &= \tilde{\alpha}_n[\tau]\,\tilde{\beta}_i[\tau]\,\tilde{\delta}_{ni}[\tau], \\
\tilde{\alpha}_n[\tau] &= \frac{1}{\sum_k \tilde{\beta}_k[t]\,\tilde{\delta}_{nk}[t]}, \\
\tilde{\beta}_i[\tau] &= T_i[t]\,(w_i[t])^{-\theta}, \\
\tilde{\delta}_{ni}[\tau] &= \frac{(d_{ni}[t])^{-\theta}}{(d_{nn}[t])^{-\theta}} \times \begin{cases} 1 & \text{if } n = i, \\ (1 - s_n[t]/\tilde{\pi}_{nn}[t]) & \text{if } n \neq i. \end{cases}
\end{aligned} \tag{11}$$

The classical Eaton and Kortum (2002) trade matrix $\mathbf{\Pi}$ has a similar structure: $\pi_{ni} = \alpha_n \beta_i \delta_{ni}$ with $\alpha_n = 1/\sum_k \beta_k \delta_{nk}$, $\beta_i = T_i(w_i)^{-\theta}$, and $\delta_{ni} = (d_{ni})^{-\theta}/(d_{nn})^{-\theta}$. In the absence of saving, $s_n = 0$, both matrices are identical. But if $s_n > 0$ the home bias for coins flows is magnified compared to the home bias in trade flows, i.e. the gap between the (high) within-location flows versus the (low) between-location flows increases. In practice this distinction is of little consequence, as the ancient saving rate into nominal financial assets was likely very low.[30]

**Coin stocks versus coin flows.** The second key distinction between coin and trade flows is that coins do not travel just once: they may be used for multiple transactions throughout their stochastic lifespan. This is made explicit by the product of 'augmented' trade matrices in equation (10). Our structural estimation unpacks the different elements of the product of matrices in equation (10), leveraging the overlapping yet distinct information contained in 'young' coins —which have only traveled through a few iterations of the 'augmented' trade matrix— and in 'old' coins —which have traveled through many iterations of the 'augmented' trade matrix.

A naive estimation that would wrongly ignore the inherently dynamic nature of coin flows, simply combine all coins of different ages, and run a gravity regression on the shares of coins from different origins (mints) in different destinations (hoards), would not identify the parameters of the 'augmented' trade matrix. This can be most easily seen in a simple stationary version of our model, though the result extends to non-stationary cases. In a stationary steady state, there is no net saving in any location, $\boldsymbol{s}[\tau] = 0, \forall \tau$, all variables are time-invariant, and equation (10) governing the dynamics of the composition of coin stocks simplifies into

$$\mathbf{S}[t, t+a] = \mathbf{S}[a] = \boldsymbol{M}\Big((\boldsymbol{I} - \boldsymbol{\lambda})\,\mathbf{\Pi}\Big)^a, \forall (t, a). \tag{12}$$

[30]The savings rate of 1.5% that Scheidel (2020) calculates for Roman times is likely an upper bound for Late Antiquity, where property rights were weaker and conflict was widespread.

In this stationary steady state, only age, $a$, matters. Combining coins of different ages, we get

$$\sum_{a=0}^{A}\mathbf{S}\left[a\right]=\boldsymbol{M}\left(\sum_{a=0}^{A}\Big(\left(\boldsymbol{I}-\boldsymbol{\lambda}\right)\boldsymbol{\Pi}\Big)^{a}\right)\underset{A\to+\infty}{=}\boldsymbol{M}\Big(\boldsymbol{I}-\left(\boldsymbol{I}-\boldsymbol{\lambda}\right)\boldsymbol{\Pi}\Big)^{-1}. \tag{13}$$

The share of coins from different mint origins ($\boldsymbol{M}$) in different locations depends not on the trade matrix $\boldsymbol{\Pi}$, but on the Leontief inverse of the trade matrix discounted by $(\boldsymbol{I}-\boldsymbol{\lambda})$: $\left(\boldsymbol{I}-\left(\boldsymbol{I}-\boldsymbol{\lambda}\right)\boldsymbol{\Pi}\right)^{-1}$. The reason is simple: newly minted coins percolate through the trade network, just as value added shocks percolate through the input-output network in the work of Wassily Leontief (Leontief, 1941, 1944). The intensity with which coins flow from one location to another depends on bilateral trade shares, just as the intensity with which one upstream sector affects the production of a downstream sectors depends on bilateral input shares. The same coin will travel multiple times through the trade network (until hit by a Poisson death shock $\lambda$), just as value added travels multiple times through the input-output network. However, unlike in conventional static models of input-output linkages, coins take time to percolate through the system, as inputs do in Liu and Tsyvinski (2024).

Figure 7 illustrates the potential bias from wrongly interpreting coin stocks as coin flows. Within the first period of their life, coin flows mirror trade flows ($\boldsymbol{\Pi}$ in figure 7). The same trade elasticity $\theta$ governs both coin and trade flows, $S_{ni}\left[t,t+1\right]\propto\pi_{ni}\propto\left(d_{ni}\right)^{-\theta}$. In the second period of their life, coins have traveled twice through the trade network ($\boldsymbol{\Pi}^2$ in figure 7). Trade costs have a weaker impact over short distances as coins have traveled longer, and have started diffusing within nearby destinations. The trade elasticity falls below $\theta$. As coins age, their flows gradually escape the negative effect of trade costs, as coins diffuse through the trade network and converge towards a uniform distribution.[31] The trade elasticity falls towards zero (see the flattening slopes of $\boldsymbol{\Pi},\boldsymbol{\Pi}^2,\cdots\boldsymbol{\Pi}^{100}$ in figure 7). A naive estimation using coins of all ages combined, i.e. wrongly interpreting the Leontief inverse $\left(\boldsymbol{I}-\left(\boldsymbol{I}-\boldsymbol{\lambda}\right)\boldsymbol{\Pi}\right)^{-1}$ as if it were the trade matrix $\boldsymbol{\Pi}$, would infer incorrect parameters. In our numerical example, if we assume that trade costs depend on travel times, $\left(d_{ni}\right)^{-\theta}=\left(TravelTimes_{ni}\right)^{-\zeta}$, with a true elasticity $\zeta=2.2$, we would wrongly estimate a travel times elasticity of 1.1. This corresponds approximately to the discrepancy between our naive reduced form estimate combining coins of all ages (1.138 in column 1 of table 2) and our upcoming structural estimate (2.22 in section 3).[32] Appendix figure B.1 shows additional reduced form evidence suggestive of this phenomenon. We estimate a naive gravity regression (as in table 2) separately for different vintages of coins. The travel time elasticity of coin flows falls towards zero as we move from younger to older coins.

[31] Our model of gradual diffusion of coins through a trade network is intimately related to the model of diffusion of information through a trade network in Chaney (2018).

[32] Figure 7 is not a structural exercise. Our numerical example is a very stylized example, with symmetric locations around a regular polygon at a steady state, which is not meant to resemble the real ancient world.

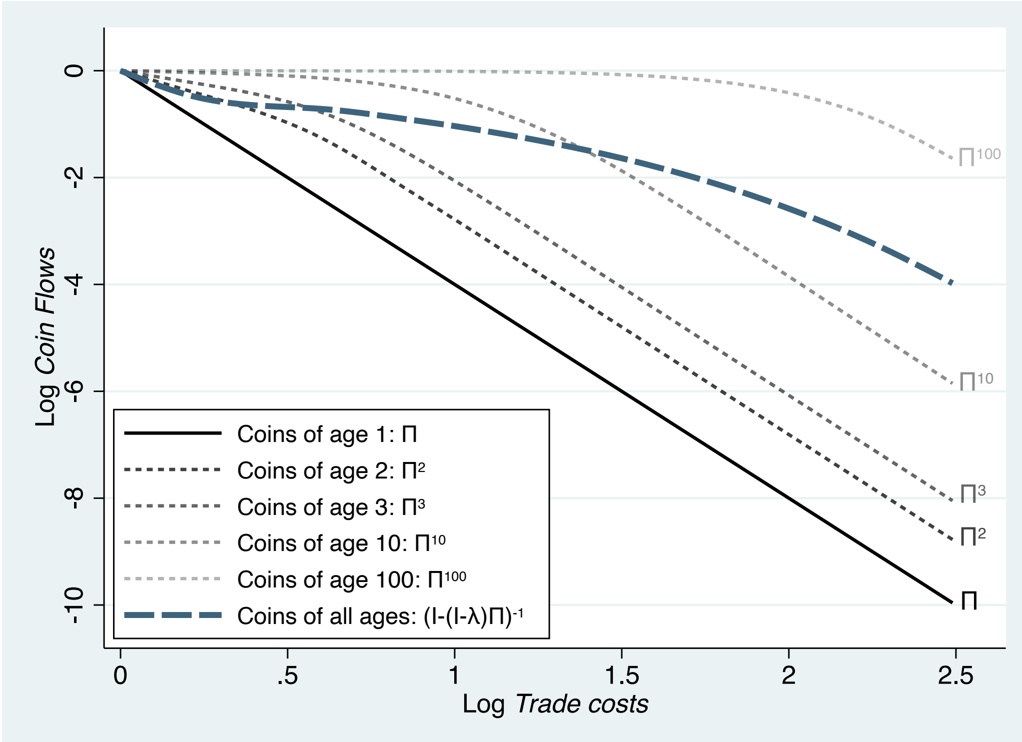


Figure 7: Flows of coins of different ages

*Notes:* This figure presents a numerical illustration of the flow of coins of different ages as a function of trade costs. We use equations (12) and (13), and the trade model (5) to simulate an economy with 200 locations around a regular polygon, with same technology $T_n = T, \forall n$, a trade elasticity $\theta = 4$, and a coin loss rate $\lambda = 0.017$. Locations are symmetric so wages are equalized and trade shares simplify to $\pi_{ni} = \alpha\,(d_{ni})^{-\theta}$ with $\alpha = 1/\sum_k (d_{nk})^{-\theta}$. Log trade costs ($\ln d_{ni}$) are on the x-axis; and log flows of coins of different ages on the y-axis ($\ln S_{ni}\,[t, t+a]$) for age $a$). To ease comparisons, we normalize the smallest log flows and log costs to zero. 'Naively' treating the flows of coins of all ages combined as trade flows, i.e. treating the Leontief inverse $(\boldsymbol{I} - (\boldsymbol{I} - \boldsymbol{\lambda})\,\boldsymbol{\Pi})^{-1}$ as if it were the trade matrix $\boldsymbol{\Pi}$, gives a misspecified trade elasticity of 1.95, substantially below the true $\theta = 4$.

### 2.3 Mapping the model to the data

**Definition of time periods.** We aggregate mint and hoard dates (*tpq*) to 20-year intervals.

**Definition of locations.** We next partition the world into $N = 13$ regions which we interpret as the locations in our model. In the Islamic world they correspond to the regions associated with graph nodes in al-Ṯurayyā (Romanov and Seydi, 2022); in the Roman world they are based partly on Roman provincial borders, and partly on 9th-century political borders (see appendix E for details). In order to facilitate the identification of the parameters, we choose a level of disaggregation so that each region has some minting and some hoarding activity both before and after the conquests.

**Assumption: constant loss rate $\lambda$.** Under the assumption that the stock of existing coins depreciates at a constant rate, $\lambda = \lambda_n\,[t]\,, \forall\,(n,t)$, any collection of coins minted at time $t$ will gradually disappear from the monetary system as those coins are (randomly) 'lost' at a rate $\lambda$. At time $t+1$, only a fraction $(1-\lambda)$ remains; at time $t+2$, a fraction $(1-\lambda)^2$; etc. The same exponential decay over age holds for any starting date $t$, and it holds for the random sample found by archaeologists. We aggregate all the coins in our dataset, and express the density of coins of age $a$ as $f(a) \propto (1-\lambda)^a$, corresponding to panel (b) in figure 3. Taking logs, we estimate $\lambda$ by OLS,

$$\ln f(a) = constant + \ln(1-\lambda) \times a + \varepsilon(a). \tag{14}$$

The stock of coins depreciates at a rate of 1.7% per year, derived from a 15% depreciation rate for a 10-year intervals, $\hat{\lambda}_{10-year} = 0.15$, or a 30% rate for a 20-year intervals, $\hat{\lambda}_{20-year} = 0.301$.[33]

**Parameterization of trade costs.** We assume that bilateral trade costs properly scaled by the trade elasticity $\theta$ solely depend on (directed) bilateral travel times, $TravelTime_{ni}$, and on a possible proportional penalty incurred when crossing political and religious boundaries, $\forall(n \neq i, t)$,

$$\ln\left((d_{ni}[t])^{-\theta}\right) = \gamma_0 - \zeta \ln(TravelTime_{ni}) - \kappa_1 PoliticalBorder_{ni}[t] - \kappa_2 ReligiousBorder_{ni}[t]. \tag{15}$$

We normalize $d_{nn}[t] = 1, \forall n, t$, as in Eaton and Kortum (2002). $PoliticalBorder_{ni}[t]$ is a dummy variable equal to 1 if regions $n$ and $i$ are separated by a political border in period $t$. $ReligiousBorder_{ni}[t]$ is a dummy variable equal to 1 if in period $t$ one region, $n$ or $i$, is in the Islamic world and the other is not.[34] $\gamma_0$ is a scaling constant which adjusts travel time units, and governs the home bias in trade. From our 'augmented' trade model, which describes coin flows driven both by transactions (trade) and saving, we derive the bilateral determinants of coin flows, the $\tilde{\delta}_{ni}[t]$'s in equation (11), $\forall(n \neq i, t)$,

$$\ln\left(\tilde{\delta}_{ni}[t]\right) = \tilde{\gamma}_0 - \zeta \ln(TravelTime_{ni}) - \kappa_1 PoliticalBorder_{ni}[t] - \kappa_2 ReligiousBorder_{ni}[t], \tag{16}$$

and $\tilde{\delta}_{nn}[t] = 1, \forall(n, t)$. The bilateral determinants of external trade flows, $(d_{ni}[t])^{-\theta}$, and coin flows, $\tilde{\delta}_{ni}[t]$, only differ by a multiplicative scalar due to saving. In our baseline we assume that this scalar is constant, equal to $e^{\tilde{\gamma}_0 - \gamma_0}$, but also explore alternative specifications.

Given estimates for within region coin flows, $\tilde{\pi}_{nn}[t]$, this scalar directly maps into the saving rates,

$$s_n[t] = \tilde{\pi}_{nn}[t]\left(1 - e^{\tilde{\gamma}_0 - \gamma_0}\right). \tag{17}$$

$\tilde{\pi}_{nn}[t]$ controls the home bias in coins, and $\left(1 - e^{\tilde{\gamma}_0 - \gamma_0}\right)$ adjusts for the discrepancy (due to saving $s_n[t]$) between the home bias in coins (governed by $\tilde{\gamma}_0$) and the home bias in trade (governed by $\gamma_0$).

[33]See appendix table B.2 for the formal estimation results.

[34]Our parameterization for the trade cost function is potentially inconsistent with the assumption of arbitrage trade. This is because we compute optimal travel routes once and for all, without taking into account the additional costs associated with potentially multiple border crossings. In practice, this does not happen: we manually verify that the estimated costs in equation (15) cannot be lowered by taking a longer route avoiding unnecessary border crossings.

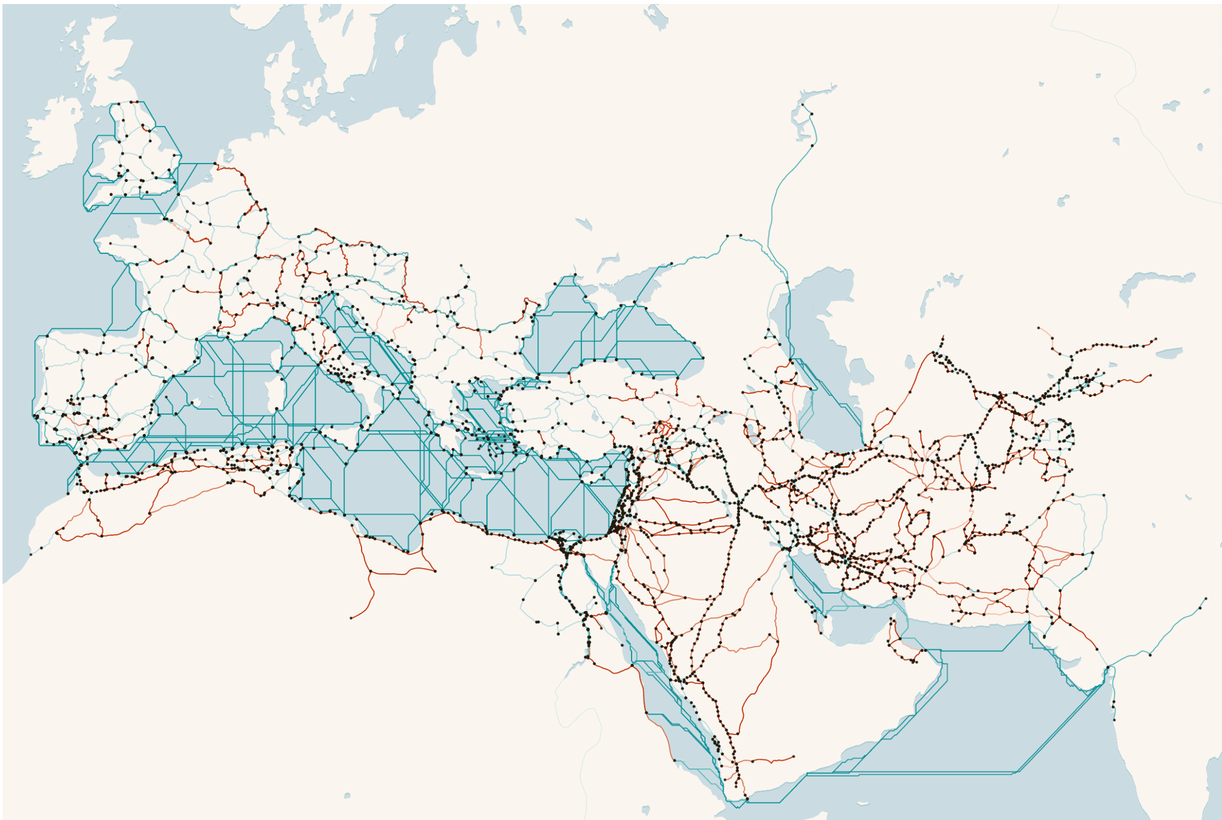

Figure 8: The combined geospatial model

*Notes:* The figure shows the combined geospatial models from Orbis and al-Ṯurayyā. Edges in more reddish colors indicate lower travel speeds; edges in darker blue tones indicate faster travel speeds.

In the absence of direct evidence on ancient trade, we cannot directly estimate $\gamma_0$. Instead, we choose $\gamma_0$ to match the average ancient saving rate into nominal assets of 1.5% (Scheidel, 2020).

**Travel times.** To compute (optimal) travel times given the transportation network and technology we use two geo-spatial models constructed by historians to provide quantitative estimates of (shortest) distances, trade routes, and trade costs. The first is the Orbis (Scheidel, 2015), a directed graph of cities and trade routes of the Roman world (i.e. from Britannia in the north-west to Egypt, Palestine, and Syria in the south-east) along with a calibrated model of trade costs, in monetary units and units of time, along the edges to allow for the calculation of shortest paths. The second is al-Ṯurayyā (Romanov and Seydi, 2022), a digitalization of the Atlas of the Islamic World of Cornu (1983), which, similarly, contains the coordinates of cities and trading posts connected by trade routes, but without estimates of travel times. We combine the nodes of al-Ṯurayyā and Orbis and extend Scheidel (2015)'s methodology from Orbis to calculate travel times for the Islamic world. We validate the resulting travel times by comparing them to those reported by the 10th-century Arab geographer Al-Muqaddasī (1994). Figure 8 shows the combined graph (see appendix D for details).

For each region, we calculate the weighted average of mint locations (with the shares of each location in total coin output as weights) and project it to the closest vertex on the road network graph. The shortest travel time between two vertices $n$ and $i$ is our time-invariant measure of $TravelTime_{ni}$.

**Political and religious borders.** We construct political border and religious border dummies by coding the start and end years of the presence of political entities in our regions. We define $PoliticalBorder_{ni}[t]$ to be one if the set of political entities that occupy at least some part of the regions $n$ and $i$ for some part of the 20-year time interval is completely disjoint. We code $ReligiousBorder_{ni}[t]$ to capture the border between the emerging religion of Islam and the rest of the world, coding the dummy to be one if all political entities in region $n$ (defined in the same way as for the political border dummy) are Islamic and none in $i$ are, or vice versa.

**Coin hoard data generating process.** We assume that our hoard dataset $\boldsymbol{H}$ is a random sample from the stocks of coins in each region and period. We group coins into coin hoards, with $H_h[T]$ the total number of coins found in location $h$ and buried at time $T$ (*tpq*), which we decompose into coin types, with $H_{m,h}[t,T]$ the number of coins minted in $m$ at time $t$ within that hoard. Our random sampling assumption means that the expected share of coins of different types within a hoard is equal to the share of coins of different types within a coin stock in our model (10). Formally, we assume

$$\mathbb{E}\left[\frac{H_{m,h}[t,T]}{H_h[T]}\right] = \frac{S_{m,h}[t,T]}{S_h[T]}. \tag{18}$$

As we discuss in section 1, we recognize that the probability that a coin ends up in our dataset may vary systematically between regions and periods, depending on whether coins were lost and deposited in the ground, found by archaeologists, and documented by experts. By using only information on the composition of coins *within* hoards, we condition on those events being realized (lost, found, documented), and we purge any variation in the probability of those events.

### 2.4 Estimation

We estimate the structural parameters of our model by maximum likelihood. Given our assumption of random sampling in equation (18), the probability of observing $(\cdots, H_{m,h}[t,T], \cdots)_{m,t}$ coins minted in different regions ($m$'s) at different times ($t$'s) among the total of $H_h[T]$ coins within a hoard buried in region $h$ at time (*tpq*) $T$ is multinomial, and depends on coin stocks,

$$\Pr(\cdots, H_{m,h}[t,T], \cdots) = \frac{H_h[T]!}{\prod_{m',t'} H_{m',h}[t',T]!} \prod_{m,t} \left(\frac{S_{m,h}[t,T]}{S_h[T]}\right)^{H_{m,h}[t,T]}.$$

It depends on the model parameters through the model-predicted share of coin types, ${}^{S_{m,h}[t,T]}/_{S_h[T]}$. Assuming a constant loss rate $\lambda$ (14), the stocks of coins evolve recursively according to equation (10),

$$\mathbf{S}[t,T] = \boldsymbol{M}[t]\left(\prod_{\tau=t}^{T-1}(1-\lambda)\,\tilde{\mathbf{\Pi}}[\tau]\right)\forall(T \geq t).$$

We decompose the elements of the coin flow matrix ('augmented' trade matrix) $\tilde{\mathbf{\Pi}}[\tau]$ into destination, origin, and bilateral terms according to equation (11),

$$\tilde{\pi}_{ni}[\tau] = \frac{\tilde{\beta}_i[\tau]\,\tilde{\delta}_{ni}[\tau]}{\sum_k \tilde{\beta}_k[\tau]\,\tilde{\delta}_{nk}[\tau]}, \forall(n,i,\tau)$$

We parameterize the bilateral component of coin flows in equation (16), $\tilde{\delta}_{nn}[t] = 1, \forall(n,t)$, and

$$\ln\left(\tilde{\delta}_{ni}[t]\right) = \tilde{\gamma}_0 - \zeta\ln\left(TravelTime_{ni}\right) - \kappa_1 PoliticalBorder_{ni}[t] - \kappa_2 ReligiousBorder_{ni}[t], \forall(n \neq i, t).$$

We collect all parameters to be estimated in the vector $\mathbf{\Theta}$, consisting of the time-varying minting output, the $M$'s in (10), the time-varying destination terms, the $\tilde{\beta}$'s in (11), and the parameters governing saving and trade costs, $\tilde{\gamma}_0$, $\zeta$, $\kappa_1$, and $\kappa_2$ in (16),

$$\mathbf{\Theta} = \Big((\cdots, M_n[t], \cdots)_{n,t}, (\cdots, \tilde{\beta}_n[t], \cdots)_{n,t}, \tilde{\gamma}_0, \zeta, \kappa_1, \kappa_2\Big).$$

As we target coin shares within hoards, we can never recover the total number of coins minted over 320-950. We normalize mint output $M_{n_0}[t_0] = 100$ for an arbitrary region $n_0$ (Northern Italy) and period $t_0$ (320-340). Similarly, only *relative* origin terms matter for coin flow shares, so we normalize $\tilde{\beta}_{n_0}[t] = 100, \forall t$, for region $n_0$ (northern Italy).

We estimate $\widehat{\mathbf{\Theta}}$ by maximizing the log-likelihood of observing a sample of coin hoards $\boldsymbol{H}$,

$$\widehat{\mathbf{\Theta}} = \arg\max_{\mathbf{\Theta}} \sum_{h,T}\sum_{m,t} H_{m,h}[t,T]\Big(\ln S_{mh}[t,T](\mathbf{\Theta}) - \ln\sum_{m',t'} S_{m'h}\left[t',T\right](\mathbf{\Theta})\Big). \tag{19}$$

Given those structural estimates, we can recover the parameter $\gamma_0$ governing bilateral trade costs (possibly distinct from the parameter $\tilde{\gamma}_0$ governing bilateral coin flows in the presence of saving). We use equation (17) and target an average net saving rate into coins of 1.5% (Scheidel, 2020),

$$\gamma_0 \;\; s.t. \;\; \left(1 - e^{\tilde{\gamma}_0 - \gamma_0}\right)\mathbb{E}_{n,t}\Big[\tilde{\pi}_{nn}[t]\Big] = 0.015. \tag{20}$$

With those estimates, we can compute all remaining structural variables, including real consumption.

Table 4: Determinants of ancient trade costs

| | Log Trade Costs | | | |
|---|---|---|---|---|
| | (1) | (2) | (3) | (4) |
| Log Travel Time | 3.04 | 3.06 | 1.41 | 1.09 |
| | (0.01) | (0.02) | (0.04) | (0.04) |
| Political Border | 0.64 | 0.47 | 2.51 | 3.19 |
| | (0.02) | (0.02) | (0.05) | (0.05) |
| Religious Border | 3.85 | | 2.94 | |
| | (0.11) | | (0.16) | |
| Religious Border: East | | 1.99 | | 0.12 |
| | | (0.12) | | (0.30) |
| Religious Border: West | | 4.69 | | 14.63 |
| | | (0.21) | | (147.22) |
| Religious Border: Mediterranean | | 5.20 | | 2.72 |
| | | (0.19) | | (0.19) |
| Sample | All | All | Gold/Silver | Gold/Silver |
| Coin Accounting | Number | Number | Value | Value |
| Estimator | MLE | MLE | MLE | MLE |
| Observations | 4,389 | 4,389 | 2,010 | 2,010 |

*Notes:* The table shows the coefficient estimates in the trade cost function, equation (15). "Political Border" is one if the sets of political entities that occupy at least some part of the regions during the 20-year time period are completely disjoint, and zero otherwise. "Religious Border" is one if all political entities in one region are Islamic and all are non-Islamic in the other region, and zero otherwise. "Religious Border: East" is one iff the religious border dummy is one and the regions are al-Andalus and Aquitaine or Francia/Germania, or vice versa. "Religious Border: West" is one iff the religious border dummy is one and the regions are the Byzantine Heartlands and one of the Caliphal regions east of Egypt, or vice versa. "Religious Border: Mediterranean" is one for all other region pairs where the religious border dummy is one. "Observations" denotes the number of observations $(m, h, t, T)$ in equation (19) where $H_{m,h}[t, T] > 0$, i.e. which enter the loglikelihood.

# 3 Trade and the end of antiquity

## 3.1 Parameter estimates

Table 4 shows the estimates of the parameters governing ancient trade costs. We consider two specifications for the religious border effect: either a single parameter governing the cost of crossing from Islamic to non-Islamic regions (colums 1 and 3), or we distinguish the cost of crossing the religious border overland in the east (in and out of Byzantium) and in the west (in and out of al-Andalus), and the cost of crossing the Mediterranean in and out of its non-Islamic northern shore (columns 2 and 4). In addition, we use two accounting methods for our coin hoard data: we either use a simple count of coins (columns 1 and 2), or use only gold and silver coin and measure the value of coins, accounting both for weight (or denomination) and metal content (columns 3 and 4).

**Travel time elasticity of trade.** In our main specification (column 1), the travel time elasticity of trade, $\zeta = 3.04$ (s.e. 0.01), is somewhat larger but close to the 2.05-2.89 range of estimates from Flückiger et al. (2022) using bilateral trade in terra sigillata in ancient Rome and optimal travel times along the Roman transportation network, and to the 1.9 distance elasticity from Barjamovic et al. (2019) using merchant records in Bronze Age Anatolia. This proximity to estimates using actual (though partial) ancient trade data is reassuring, as we do not use any direct information on trade flows, but only indirect information on coin flows. Interestingly, $\zeta$ is also larger than the 1.1 elasticity estimated in table 2 using the same data on coin hoards. The reason is that in table 2 we use a naive gravity model, combining coins of all ages, and doing so ignore the fact that older coins have a tendency to travel longer distances. Our structural model (10) corrects this misspecification.

This travel time elasticity is robust to alternative specifications for the religions border effect, $\zeta = 3.04$ versus $\zeta - 3.06$. Our estimate is significantly lower when we restrict our sample to gold and silver coins, and measure their relative values, e.g. $\zeta = 1.41$ in column 3 versus $\zeta = 3.01$ in column 1. We conjecture that the stronger reliance of Byzantium on gold, and the exclusion of any information on bronze coins, induces a systematic bias in our estimates.

**Political and religious border effects.** In our baseline specification (column 1), the political ($\kappa_1$) and religious ($\kappa_2$) border effects are large, but of the same magnitude as estimates for modern border effects. All else equal, bilateral trade is $\exp(0.64) \approx 2$ times larger within than across political borders, and $\exp(3.85) \approx 40$ times larger within than across religious borders. If we assume, somewhat arbitrarily, a trade elasticity $\theta = 4$ (Simonovska and Waugh, 2014), those correspond to a 17% tax for crossing a political border ($d_{across}/d_{within} = e^{\kappa_1/\theta} = 1.17$), and a 155% tax for crossing a religious border ($d_{across}/d_{within} = e^{\kappa_2/\theta} = 2.55$), similar to the estimated 49% cost of crossing the modern US-Canada border (Anderson and van Wincoop, 2003).[35]

Changing the specification of the religious border effect, distinguishing the eastern land border, the Meditteranean border, and the western land border (column 2) does not affect our estimate of the political border effect, which remains relatively small (0.64 in column 1 versus 0.47 in column 2). It does however reveal different estimated penalties associated with crossing from Islamic to non-Islamic regions. The religious border effect is strongest for crossing the Mediterranean ($\kappa_2^{Med.} = 5.20$, s.e. 0.19) and for the western border from al-Andalus ($\kappa_2^{West} = 4.61$, s.e. 0.21), and lowest for the eastern border into Byzantium ($\kappa_2^{Med.} = 1.99$, s.e. 0.12).

Columns 3 and 4 drop all information on bronze coins, and compute the value shares within hoards

[35] Anderson and van Wincoop (2003) estimate that trade is $\exp(1.59) \approx 5$ times larger within the US or Canada than between them. For a trade elasticity $\theta = 4$ it corresponds to a $d_{across}/d_{within} - 1 = e^{1.59/4} - 1 = 49\%$ border tax.

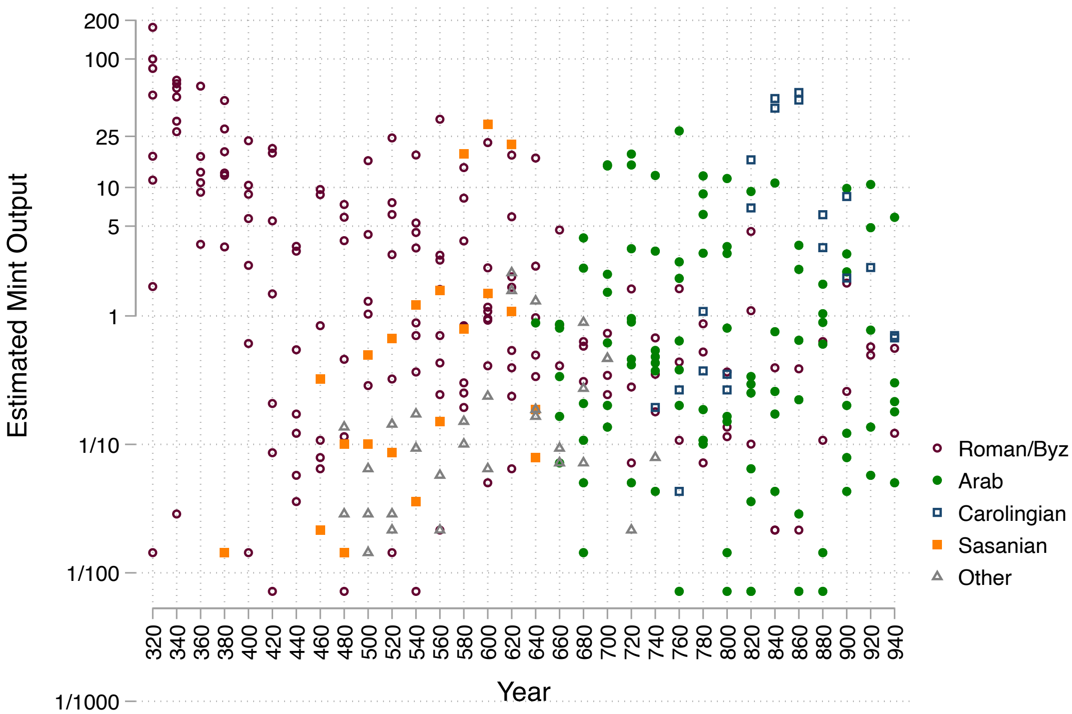


Figure 9: Estimated mint output, 320-960 AD

*Notes:* The figure shows the estimated coin output $M_n[t]$ by time $t$ (horizontal axis) and region $n$, broken down by the political entities that locations are – at that time – primarily associated with. The units are relative to northern Italy in 320-340, which we normalize to have a mint output of 100.

for gold and silver coins using their weights or denominations. Under this accounting of the coins data, the political border effect is larger ($\kappa_1 = 2.51$, s.e. 0.05, in column 3 and 3.19, s.e. 0.05, in column 4). The religious border effect instead is smaller ($\kappa_2 = 2.94$, s.e. 0.16 in column 3 versus 3.85, s.e. 0.11, in column 1). We also estimate statistically insignificant easter and western religious border effects, and a smaller Mediterranean religious border effect using coin values than counts ($\kappa_2^{Med.} = 2.72$, s.e. 0.19, in column 4, versus 5.20, s.e. 0.19, in column 2). As for our estimate of the travel time elasticity, we conjecture that selectively dropping bronze coins biases our estimates.

**Minting output.** Figure 9 shows estimates of mint output by region and time interval. Our estimates line up with several patterns described in the numismatic literature: (*i*) the decline of coin production in the western Mediterranean following the demise of the West Roman Empire in the late 5th century; (*ii*) the large decline of Byzantine mint output in the "Byzantine dark ages" of the eighth century; (*iii*) the gradual increase in Arab mint output starting from the late seventh century.

### 3.2 Real consumption in the ancient world: technology, minting, and trade

Our full set of structural estimates further allows us to recover all equilibrium variables in our model.

To do so, we must impose structure on the dynamics of the model-predicted economy. First, in the absence of any direct evidence on how ancient agents form expectations – and therefore how endogenous wages dynamically clear markets in equation (7) – we solve a steady state version of our model as in equation (8). Second, our parameter estimates only allow us to recover the combination $L_n T_n^{1/\theta}$, but not population ($L_n$) and technology ($T_n$) separately. In the absence of any direct evidence on population, technology, or wages, we assume a simple Malthusian benchmark, $L_n = T_n$.

From the parameters of the trade cost function ($\gamma_0, \kappa_1, \kappa_2$), data on the determinants of trade ($TravelTime_{ni}, PoliticalBorder_{ni}$ and $ReligiousBorder_{ni}$), and the destination terms ($\tilde{\beta}_n$), we recover all bilateral trade shares ($\pi_{ni}$). Using the goods market clearing condition in equation (8), estimated bilateral trade shares, the coin loss rate ($\lambda$), and estimates of minting output ($M_n$), we recover aggregate regional income ($w_n L_n$). Finally, under our Malthusian assumption ($L_n = T_n$), we recover population ($L_n$) and technology ($T_n$) from the destination terms ($\tilde{\beta}_n$).[36]

We can fully characterize real consumption per capita in any equilibrium, realized or counterfactual, and partition real consumption into three economically meaningful components,

$$\underbrace{\frac{X_n/p_n}{L_n}}_{\text{Real Consumption}} = \gamma^{-1} \underbrace{(\pi_{nn})^{-1/\theta}}_{\text{Openness}} \underbrace{(T_n)^{1/\theta}}_{\text{Technology}} \underbrace{\left(1 + \frac{M_n - \lambda w_n L_n}{w_n L_n}\right)}_{\text{Trade Deficit}}. \tag{21}$$

Real consumption ($^{X_n}/_{p_n}$) is the quantity that contributes to flow utility in our dynamic model in equation (6). As in Eaton and Kortum (2002) and its generalization in Arkolakis et al. (2012), real consumption depends on trade openness ($\pi_{nn}^{-1/\theta}$) and technology ($T_n^{1/\theta}$). As in Dekle et al. (2007), real consumption also depends on trade deficits, expressed as the ratio of expenditure to income ($^{X_n}/_{(w_n L_n)} = 1 + {}^{(M_n - \lambda w_n L_n)}/_{(w_n L_n)}$).[37] A region with a superior technology has a higher consumption. For a given technology, the more open to trade a region is, the higher its real consumption. Finally, for a given technology and trade openness, a region able to mint more coins than it loses runs a trade deficit, i.e. can afford to consume more real goods than it produces.

While the 'openness' and 'trade deficit' terms in equation (21) are unit-free, technology depends on arbitrary units. We choose those units such that real consumption is normalized to one for northern

[36] Technical appendix B explains in detail how to recover all equilibrium variables from our parameter estimates.

[37] The first two components of the decomposition of consumption in equation (21) are the same as in equation (15) on page 1756 in Eaton and Kortum (2002). The last term is the same as in the (all important) unnumbered equation on page 354 in Dekle et al. (2007), where they label trade deficits as $D_n$. In our model, trade deficits are financed by minting output in excess of coin losses, $D_n = M_n - \lambda w_n L_n$, so that so $1 + D_n/Y_n = 1 + (M_n - \lambda w_n L_n)/(w_n L_n)$.

Table 5: Real consumption in the ancient world, from 460-620 AD to 720-900 AD

| | Real consumption $\Delta \log \left(\frac{X_n/p_n}{L_n}\right)$ (1) | Openness $\Delta \log \left(\pi_{nn}^{-1/\theta}\right)$ (2) | Technology $\Delta \log \left(T_n^{1/\theta}\right)$ (3) | Trade Deficit $\Delta \log \left(1 + \frac{M_n - \lambda w_n L_n}{w_n L_n}\right)$ (4) |
|---|---|---|---|---|
| al-Andalus | 0.79 | -0.04 | 0.97 | -0.13 |
| Aquitaine and Basque Country | 1.34 | -0.05 | 1.52 | -0.13 |
| Francia and Germania | 1.63 | -0.05 | 1.87 | -0.18 |
| Northern Italy and Balkans | 0 | -0.03 | 0.10 | -0.06 |
| Southern Italy | 0.03 | 0.00 | -0.11 | 0.13 |
| Byzantine Heartlands | -0.87 | -0.15 | -0.11 | -0.61 |
| al-Sham (Greater Syria) | 0.40 | -0.00 | 0.19 | 0.21 |
| Northern Syria and Caucasus | 0.55 | 0.04 | 0.07 | 0.43 |
| al-Iraq, al-Jibal, Khuzistan, Kirman | 0.44 | -0.01 | 0.50 | -0.04 |
| Eastern Caliphate | 0.73 | -0.00 | 0.74 | -0.01 |
| Jazirat al-arab and al-Yaman | 1.26 | 0.04 | 0.66 | 0.56 |
| Misr (Egypt) | -0.03 | -0.00 | -0.01 | -0.02 |
| al-Maghrib | 0.35 | 0.01 | 0.19 | 0.15 |

*Notes:* TBD.

Italy.[38] Our model informs us on cross-sectional *differences* in real consumption between regions. This is true despite the fact that we only have information on nominal variables (coins): bilateral trade flows reveal real differences in factor prices, which our structural estimation is able to recover. Unfortunately our model, as any trade model, offers no guidance on the absolute *levels* of real consumption.

**Consumption changes in the ancient world.** We begin with an exploration of the changes in the economic geography of the ancient world, from before to after the rise of Islam. We average our structural estimates over the period 460-620 AD (`pre`), just after the fall of Rome but before the birth of Islam, and over the period 720-900 AD (`post`), after the Arabs have conquered a territory from the Indus to the Atlantic. We use equation (21) to compute the change in real consumption and its components from the `pre` to the `post` period. The results are presented in table 5 (see appendix table B.4 for details on aggregate consumption). We focus our discussion on a few important regions.

*Egypt*: the Arab conquest of Egypt (Misr) has almost no impact on real consumption per capita. Although Egypt is partially cut off from trade with the northern side of the Mediterranean by the Arab conquest, its proximity to central regions of the eastern Caliphate compensates this loss, so that the Egyptian access to trade is nearly unaffected. Egypt is a large producer of grain in the ancient world, both before and after the Arab conquest, and the Egyption production efficiency revealed by the patterns of trade pre and post Arab conquest confirm this. Finally, Egypt is also home to large mints, which operate both under Byzantine (pre Arab conquest) and Arab rule (post conquest).

*Syria*: as a province of the Byzantine empire, Syria is one of the larger regions of the ancient world

[38] We must impose this normalization for any realized (estimated) equilibrium. However, in counterfactual simulations, we are free to allow technology to change in such as way that real consumption in northern Italy differs from one.

before the rise of Islam (appendix table B.4). Similarly to Egypt, the loss of trade access to Byzantium and Europe is compensated by its privileged access to the heart of the eastern Caliphate. Syria also benefits from an improved relative technology and larger trade deficits financed by a large minting output. Combined, they contribute to a 50% ($e^{0.40} - 1 \approx 0.49$) relative increase in real consumption.

*Arabian peninsula (Jazirat al-Arab)*: the birthplace of Islam, the Arabian peninsula, initially the smallest region of the ancient world, experiences a sustained growth in real consumption ($e^{1.26} - 1 \approx +250\%$), primarily driven by improved technology and a larger minting output.

*Byzantine heartlands*: by contrast, the core of the Byzantine empire in the eastern Mediterranean experiences the most dramatic economic collapse, a 60% ($e^{-0.87} - 1 \approx 0.58$) drop in real consumption per capita. Initially the most open to trade region of the ancient world, it is partly cut off from trade, and the share consumption that relies solely on locally sourced goods increases by more than 80% ($e^{0.15\times\theta} - 1 \approx 0.82$). In addition, Byzantium's sharp drop in minting output prevents it from financing consumption through trade deficits and contributes to a fall in consumption by 46% ($e^{0.61} - 1$).

*Western and northern Europe*: on the other end of the ancient world both Islamic (al-Andalus) and non-islamic western European regions (Aquitaine and the Basque Country, and the Frankish lands of Francia and Germania) experience the most spectacular relative rise in real consumption. Initially among the smallest regions of the ancient world (4 to 100 times smaller than northern Italy), they grow to become the largest ones over the course of a few centuries (10 to 50 times larger than northern Italy, see appendix table B.4). This growth is entirely fueled by improvements in technology. Regional minting grows substantially, but not enough to keep up with the larger increase in aggregate income, so that trade deficits decrease somewhat (around 10-15%). Finally, the reduction in trade openness caused by the religious border has only a minor negative impact on real consumption: the reduced access to European trade for al-Andalus is partly compensated by its continued access to the growing regions of the Caliphate, and the reduced access to southern Mediterranean trade for northern Europe is partly compensated by local trade among booming neighbors. Trade openness falls by around 20% ($e^{0.5\times\theta} - 1 \approx 0.22$), which contributes to a 5% reduction in real consumption.

**Counterfactual changes.** We then leverage our fully specified structural model to explore the causal impact of specific shocks to real consumption changes. They are causal in the sense that we simulate counterfactual equilibria, changing only one set of parameters at a time. The results are presented in table 6. Column 1 shows real consumption per capita in the estimated `pre` equilibrium (460-620 AD). We then compute (log) changes in real consumption between this initial `pre` equilibrium and various counterfactual equilibria. In column 2 we turn on the religious border to its `post` level (720-900 AD), while keeping all other parameters unchanged. In column 3, we only change technology

Table 6: Counterfactual changes in real consumption per capita

| | Log consumption | Counterfactual log consumption change if: | | |
|---|---|---|---|---|
| | All parameters 460-620 AD (1) | Religious border 720-900 AD (2) | Technology 720-900 AD (3) | Minting 720-900 AD (4) |
| al-Andalus | -0.35 | 0.02 | 0.20 | 0.86 |
| Aquitaine and Basque Country | -0.71 | -0.17 | 0.61 | 3.26 |
| Francia and Germania | -0.97 | -0.15 | 1.03 | 4.02 |
| Northern Italy and Balkans | 0 | -0.16 | 0.43 | -0.35 |
| Southern Italy | -0.38 | -0.02 | 0.20 | -0.01 |
| Byzantine Heartlands | 0.95 | -0.42 | 1.33 | -1.27 |
| al-Sham (Greater Syria) | 0.00 | 0.03 | -0.02 | -0.04 |
| Northern Syria and Caucasus | -0.53 | 0.01 | -0.06 | 0.06 |
| al-Iraq, al-Jibal, Khuzistan, Kirman | 0.08 | 0.03 | 0.11 | -0.02 |
| Eastern Caliphate | -0.62 | 0.01 | 0.25 | 0.24 |
| Jazirat al-arab and al-Yaman | -1.71 | 0.00 | 0.34 | 1.10 |
| Misr (Egypt) | 0.06 | 0.01 | -0.13 | -0.06 |
| al-Maghrib | -0.07 | 0.00 | 0.25 | -0.14 |

*Notes:* TBD.

to its `post` level. And in column 4, we only change minting output to its `post` level.

The increase in trade costs associated with crossing the border in and out of Islam has an asymmetric impact on real consumption. Non-Islamic regions see a large drop in trade, which contributes to substantial reductions in real consumption. The most severely hit region is Byzantium (34% drop in real consumption), the region that benefits the most from access to trade before the Arab conquests. Other European regions also experience a sharp reduction in consumption (15% drop), as they benefit from trading with more developed regions before the Arab conquests. In contrast, Islamic regions are almost unaffected by the reduced access to trade with regions north of the Mediterranean.

Changes in technology and minting induce more heterogeneous changes in the economic geography of the ancient world. Western and northern Europe (including Islamic Spain) would have benefited from a large technological improvement. Given their relatively small initial size, a counterfactual increase in minting to post Arab conquests levels would also have allowed those regions to finance large trade deficits, which would have contributed to large gains in real consumption. Byzantine real consumption would have increased if technology moved to its post Arab conquests level for all regions. Interestingly, this is not because Byzantine technology itself improves (it actually declines by approximately 10%, see table 5). Instead, foreign technologies improve in many neighboring regions, and the pre Arab conquest trade openness allows Byzantium to reap the benefits from those foreign improvements through trade. On the other hand, the collapse of minting output during the "Byzantine dark ages" would have prevented Byzantium from acquiring foreign wares using locally minted coins (a collapse in seigniorage-financed trade deficits), and would have severely reduced real consumption.


(a) Relative real consumption changes: pre- to post-conquests

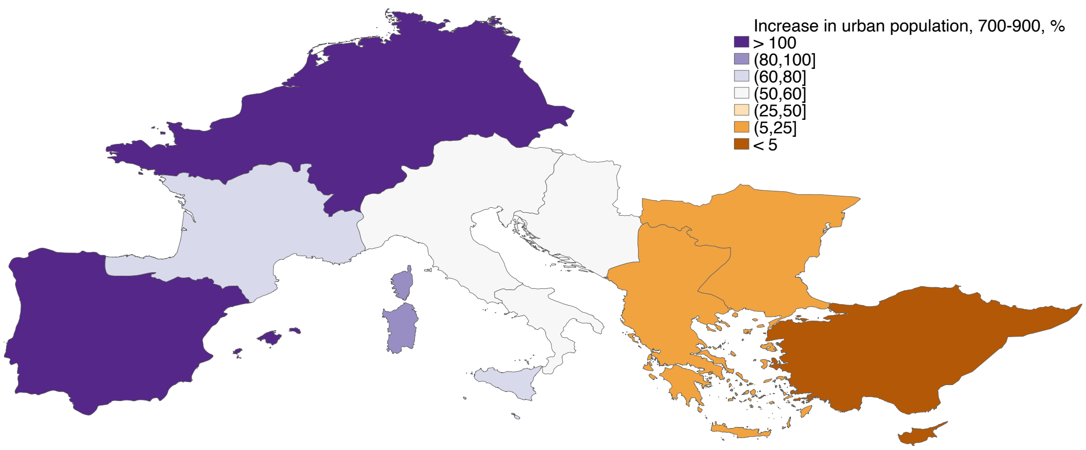


(b) Urban Population Growth in European Regions, 700-900 AD

Figure 10: Real consumption and urbanization

*Notes:* Panel (a) shows the relative real consumption change from the pre-conquest period to the post-conquest period, column 1 of Table 5, relative to Northern Italy (=0). Panel (b) shows the percentage growth of the urban population between 700 and 900 AD. City size data from Buringh (2021), except for Byzantine Anatolia, which is not covered. We construct measures of urban decline in Anatolia (calculations available upon request) based on the shrinking surface area of cities described in Brandes (1989). The resulting figure of a 10% decline in urban population over this time interval seems to be a conservative estimate in light of the fact that many coastal cities saw large amounts of destruction and depopulation as a consequence of Arab attacks.

### 3.3 Urbanization and trade in ancient Europe

We conclude this section by confronting our estimates for changes in real consumption to realized changes in urbanization in Europe. While our model does not feature any explicit notion of urbanization, we conjecture that a higher real consumption per capita allows to sustain a larger urban population. This exercise is illustrative, meant to verify that our estimates for real consumption derived solely from information on coin flows are line with independent evidence on economic growth.

Figure 10 shows our estimates for changes in real consumption per capita (top panel) together with the patterns of urban population growth between 700 and 900 AD in the regions north of the Mediterranean (bottom panel). Comparing both maps suggests that our estimates for real consumption are qualitatively in line with direct and independent evidence on urbanization. Our estimated drop in real consumption in the heartlands of the Byzantine empire, and substantial increase in western and northern Europe, relative to Northern Italy, are in line with the decline in urban population in Asia Minor and Cyprus, low urban population growth in Greece, Thracia, and Dacia, medium urban population growth in the Balkans, Italy, and Aquitaine, and strong urban population growth in Iberia and Francia/Germania.

## Conclusion

In this paper we study the patterns of change in trade relationships in the Mediterranean during Late Antiquity through the lens of coin flows. Pirenne's thesis claims that a disruption for trade linkages caused by the Arab conquests triggered a shift in economic activity towards northern Europe. A descriptive analysis of a large dataset spanning most known coin deposits between the 4th and the 10th century around the Mediterranean reveals large changes in the geography on coin flows before and after the Arab conquests in line with an increase in trade costs due to the emergence of new political and religious border. To serve as a quantitative framework through which we can interpret coin movements, we propose a model of trade where agents hold coins to make transactions (cash-in-advance constraint) and where coins diffuse over space in proportion to trade flows. We show that when enough coin types are present, trade shares are identified from random samples drawn from the distribution of coins in different locations. We estimate the structural parameters that determine trade costs and perform counterfactuals as a means of decomposing the changes in market access before and after the conquests. Our estimates reveal patterns of reductions in market access that are consistent with observed measures of relative urbanization across European regions.

## References


Al-Muqaddasī (1994): *Aḥsan al-taqāsīm fi maʾarfat al-aqalīm (The Best Divisions for Knowledge of the Regions)*, Garnet Publishing (transl. B.A. Collins).

al 'Ush, A.-F. (1972): *The silver hoard of Damascus: Sasanian, Arab-Sasanian, Khuwarizmian, and Umayyad kept in the National Museum of Damascus*, Damascus: Direction General of Antiquities and Museums.

Anderson, J. E. and E. van Wincoop (2003): "Gravity with Gravitas: A Solution to the Border Puzzle," *American Economic Review*, 93, 170–192.

Arkolakis, C., A. Costinot, and A. Rodríguez-Clare (2012): "New Trade Models, Same Old Gains?" *American Economic Review*, 102, 94–130.

Ashtor, E. (1970): "Quelques observations d'un orientaliste sur la thèse de Pirenne," *Journal of the Economic and Social History of the Orient*, 13, 166–194.

Banaji, J. (2016): *Exploring the Economy of Late Antiquity: Selected Essays*, Cambridge University Press.

Barjamovic, G., T. Chaney, K. Coşar, and A. Hortaçsu (2019): "Trade, merchants, and the lost cities of the bronze age," *The Quarterly Journal of Economics*, 134, 1455–1503.

Bates, M. (1991): "Coins and money in the Arabic Papyri," *Documents de l'Islam Medieval*, 43–643.

Bessard, F. (2020): "Money Supply and Currency," in *Caliphs and Merchants: Cities and Economies of Power in the Near East (700-950)*, Oxford University Press.

Bolin, S. (1953): "Mohammed, Charlemagne and Ruric," *Scandinavian economic history review*, 1, 5–39.

Brandes, W. (1989): *Die Städte Kleinasiens im 7. und 8. Jahrhundert*, De Gruyter.

Buringh, E. (2021): "The population of European cities from 700 to 2000: Social and economic history," *Research Data Journal for the Humanities and Social Sciences*, 6, 1–18.

Chaney, T. (2018): "The Gravity Equation in International Trade: An Explanation," *Journal of Political Economy*, 126, 150–177.

Cornu, G. (1983): *Atlas du monde Arabo-Islamique à l'époque classique: IX.-X. siècles*, Brill.

Coupland, S. (2014): "The use of coin in the Carolingian Empire in the ninth century," *Early Medieval Monetary History: Studies in Memory of Mark Blackburn, Farnham*, 257–93.

Dekle, R., J. Eaton, and S. Kortum (2007): "Unbalanced Trade," *American Economic Review, Papers and Proceedings*, 97, 351–355.

Donaldson, D. (2018): "Railroads of the Raj: Estimating the impact of transportation infrastructure," *American Economic Review*, 108, 899–934.

Donaldson, D. and R. Hornbeck (2016): "Railroads and American economic growth: A "market access" approach," *The Quarterly Journal of Economics*, 131, 799–858.

Eaton, J. and S. Kortum (2002): "Technology, Geography, and Trade," *Econometrica*, 70, 1741–1779.

Findlay, R. and K. H. O'Rourke (2009): *Power and Plenty: Trade, War, and the World Economy in the Second Millennium*, Princeton University Press.

FLAME (2023a): "Biases in FLAME's data," https://coinage.princeton.edu/biases-in-flames-data/.

——— (2023b): "Framing the Late Antique and early Medieval Economy," https://coinage.princeton.edu/, accessed: 2023-07-01.

Flückiger, M., E. Hornung, M. Larch, M. Ludwig, and A. Mees (2022): "Roman transport network connectivity and economic integration," *The Review of Economic Studies*, 89, 774–810.

Fogel, R. W. (1964): *Railroads and American economic growth*, Johns Hopkins Press Baltimore.

Foss, C. (1975): "The Persians in Asia Minor and the end of Antiquity," *The English Historical Review*, 90, 721–747.

Gibbon, E. (1789): *The history of the decline and fall of the Roman Empire*, vol. I-VI, London: Strahan & Cadell.

Grierson, P. (1959): "Commerce in the Dark Ages: a critique of the evidence," *Transactions of the Royal Historical Society*, 9, 123–140.

——— (1973): *Catalogue of the Byzantine Coins in the Dumbarton Oaks Collection and in the Whittemore Collection, 3: Leo III to Nicephorus III, 717-1081*, Dumbarton Oaks.

Head, K. and T. Mayer (2014): "Gravity equations: Workhorse, toolkit, and cookbook," in *Handbook of international economics*, Elsevier, vol. 4, 131–195.

Hodges, R. and D. Whitehouse (1983): *Mohammed, Charlemagne & the origins of Europe: archaeology and the Pirenne thesis*, Cornell University Press.

Izdebski, A., G. Koloch, T. Słoczyński, and M. Tycner (2016): "On the use of palynological data in economic history: new methods and an application to agricultural output in Central Europe, 0–2000 AD," *Explorations in Economic History*, 59, 17–39.

Juhász, R. (2018): "Temporary protection and technology adoption: Evidence from the napoleonic blockade," *American Economic Review*, 108, 3339–3376.

Kazhdan, A. (1954): "Vizantijskie goroda v VII-IX vv," *Sovetskaja arkheologija*, 21, 164–188.

Leontief, W. W. (1941): *The Structure of the American Economy, 1919–1929*, Cambrige, MA: Harvard University Press.

——— (1944): "Output, Employment, Consumption, and Investment," *The Quarterly Journal of Economics*, 58, 290–314.

Liu, E. and A. Tsyvinski (2024): "A Dynamic Model of Input–Output Networks," *The Review of Economic Studies*.

Lopez, R. S. (1943): "Mohammed and Charlemagne: a revision," *Speculum*, 18, 14–38.

Loveluck, C. P., M. McCormick, N. E. Spaulding, H. Clifford, M. J. Handley, L. Hartman, H. Hoffmann, E. V. Korotkikh, A. V. Kurbatov, A. F. More, et al. (2018): "Alpine ice-core evidence for the transformation of the European monetary system, AD 640–670," *Antiquity*, 92, 1571–1585.

McConnell, J. R., A. I. Wilson, A. Stohl, M. M. Arienzo, N. J. Chellman, S. Eckhardt, E. M. Thompson, A. M. Pollard, and J. P. Steffensen (2018): "Lead pollution recorded in Greenland ice indicates European emissions tracked plagues, wars, and imperial expansion during antiquity," *Proceedings of the National Academy of Sciences*, 115, 5726–5731.

McCormick, M. (2001): *Origins of the European economy: communications and commerce AD 300-900*, Cambridge University Press.

Montesquieu, C. (1734): *Considérations sur les causes de la grandeur des Romains et de leur décadence*.

Morrisson, C. (2002): "Byzantine money: its production and circulation," *The Economic History of Byzantium*, 3, 909–966.

Naismith, R. (2014): "The Social Significance of Monetization in the Early Middle Ages*," *Past & Present*, 223, 3–39.

Naismith, R., J. Kershaw, and S. Merkel (2023): "Byzantine plate and Frankish mines: the provenance of silver in north-west European coinage during the Long Eighth Century (c. 660–820)," *Antiquity*.

Noonan, T. S. (1980): "When and how dirhams first reached Russia: a numismatic critique of the Pirenne theory," *Cahiers du monde russe et soviétique*, 401–469.

Ostrogorsky, G. (1959): "Byzantine cities in the early Middle Ages," *Dumbarton Oaks Papers*, 13, 45–66.

Parvérie, M. (2014): "Corpus des monnaies arabo-musulmanes des VIII et IX siècles decouvertes dans le Sud de la France," *Revista Numismática OMNI*, 79–100.

——— (2018): "La circulation des deniers de l'Aquitaine carolingienne en Al-Andalus; un réexamen des trésors 'Espanya-1, 2 et 3'," *Bulletin de la Société numismatique de Limousin*, 25, 4–16.

Pascali, L. (2017): "The wind of change: Maritime technology, trade, and economic development," *American Economic Review*, 107, 2821–2854.

Pennas, V. (1996): "Life in Byzantine Cities of Peloponnesos: The Numismatic Evidence (8th-12th Century)," in *Mneme Martin Jessop Price*, Hellenic Numismatic Society.

Persson, K. G. and P. Sharp (2015): *An economic history of Europe*, Cambridge University Press.

Pirenne, H. (1927): *Medieval Cities: Their Origins and the Revival of Trade*, Princeton University Press.

——— (1939): *Mohammed and Charlemagne*, London: G. Allen & Unwin.

Romanov, M. and M. Seydi (2022): "al-Thurayyā," https://althurayya.github.io/ [Accessed: (1 July 2023)].

Sarah, G. (2008): "Caractérisation de la composition et de la structure des alliages argent-cuivre par ICP-MS avec prélèvement par ablation laser. Application au monnayage carolingien." Ph.D. thesis, Université d'Orléans.

Sarah, G., M. Bompaire, M. McCormick, A. Rovelli, and C. Guerrot (2008): "Analyses élémentaires de monnaies de Charlemagne et Louis le Pieux du Cabinet des Médailles: l'Italie carolingienne et Venise," *Revue numismatique*, 164, 355–406.

Scheidel, W. (2015): "ORBIS: The Stanford geospatial network model of the Roman world," Tech. rep.

——— (2020): "Roman wealth and wealth inequality in comparative perspective," *Journal of Roman Archaeology*, 33, 341–353.

Shatzmiller, M. (2018): "At the origins of Middle Eastern trade, 700-1000 AD: An application of the gravity theory of trade," in *Economic integration and social change in the Islamic world system*, ed. by H. Kennedy and F. Bessard, 800–1000.

Simonovska, I. and M. E. Waugh (2014): "The elasticity of trade: Estimates and evidence," *Journal of International Economics*, 92, 34–50.

Voltaire (1756): *Essai sur les mœurs et l'esprit des nations*, Geneva: Frères Cramer.

Watson, A. M. (1974): "The Arab agricultural revolution and its diffusion, 700–1100," *The Journal of Economic History*, 34, 8–35.

Wickham, C. (2006): *Framing the early middle ages: Europe and the Mediterranean, 400-800*, Oxford University Press.

Zavagno, L. (2022): "A Lost World That Never Died," *Dumbarton Oaks Papers*, 76, 281–310.

# Online Appendix for

# Trade and the End of Antiquity

## by Johannes Boehm and Thomas Chaney

# A Coin hoard data

Our numismatic data consists of two datasets: first, the set of hoards from the current release of the *Framing the Late Antique and Early Medieval Economy* project (FLAME, 2023). FLAME is a large collaborative effort of historians and numismatists that records data on coin hoards around the Mediterranean and Europe from between 325 AD and 725 AD. We use the most recent release (January 2023) which has data on about 1.7m coins belonging to more than 9,000 hoards. Since the temporal and spatial focus of our study does not entirely overlap with that of FLAME, we complement their data by constructing a hand-coded dataset on hoards between 700 AD and 900 AD, and hoards with a heavier emphasis on near eastern coins. We describe the hand-collected data and FLAME's data in turn.

## A.1 Hand-collected data

We search the numismatic and archaeological literature for descriptions of coin hoards or coin finds with a *terminus post quem* (= date of the most recent content) of roughly between 700 AD and 950 AD, that were discovered in Europe, North Africa, or the Middle East. For the sake of brevity we will refer to a single coin or a collection of coins that was found together in one place as a "hoard" (i.e. unless specifically mentioned, we do not distinguish between single finds, stray finds, mini-hoards, or full hoards). We exclude hoards that largely contain silver that was brought via the Viking route or that clearly have a Viking connection.[39] We likewise exclude records from excavations, unless they are described as a hoard or constitute a set of coins that were found together in the same location (e.g. in the same room of an excavated building).

An (at least approximate) findspot must be known for a hoard to be of use in our analysis. For each hoard we record the latitude and longitude of its findspot. When the findspot is known only with a low level of precision (e.g. at the country or region level) we code this in a separate dummy variable. Importantly, we do not record coins in museums or collections that have unknown findspots. While we digitize many descriptions of hoards that are incomplete, we omit hoards of which no information on the vast majority of coins has been published.

For each coin (or group of coins with identical properties) in a hoard we record, if documented by the authors of the hoard catalogue:

- The mint where the coin was minted, or believed to have been minted. When a coin is believed to have been an imitation, we note this separately.

- A time interval (consisting of a start year and end year) during which the coin was minted or is believed to have been minted. For some coins, such as most Islamic dirhams, this information is imprinted on the coin. For others, we code this as the shortest time interval during which the coin could have been minted, taking into account the denomination of the coin, the ruler under whose authority it has been issued, as well as his/her dynasty, and other information about coin types (e.g. pre/post-reform coinage). When the coin has been dated through the regnal year of the ruler or in the Islamic calendar, we convert this to Gregorian calendar years.

Beyond the attributes above, we record denomination, material, and issuing rulers and dynasties (mostly with dating of the coins in mind). This information, if known, is typically furnished by the authors of hoard catalogues in the numismatic literature. We do not distinguish between fragments and entire coins.

The geocodes of the hoards and mints are only approximate. We code Nomisma IDs for the mints based on the proximity of the place of minting, not based on the dynasty, e.g. "Siqilliyah" (Sicily) can be also used for non-Islamic issue.

### A.1.1 Hoards in the Near East and North Africa

Table A.5 shows the list of hand-coded hoards from the Near East and North Africa, along with references. These hoards consist mainly of Sasanian and/or Islamic coins, and sometimes Byzantine issue. We code approximate mint

[39] Among the list from Appendix 3 of McCormick (2001), these are the hoards in Britain, Scandinavia, and Schleswig-Holstein (Germany). We also digitized the 10th century Máramaros county hoard (Fomin and Kovács, 1987), but drop it as its content (consisting of many imitations, as well as dirhams from the Samarkand and al-Shash mints) indicate that it was clearly brought in from the east.

locations based on the proposals in the literature, typically giving preference to the suggestions of the authors of the original hoards.

A couple of notes on specific hoards:

- We digitize the Umm-Hajarah hoard based on the description by al 'Ush (1972a) but follow Noonan (1980) in treating the isolated Seljuk coin that Al-'Ush dates to 689-690 AH as not belonging to the hoard.
- We digitize Hoge (1997)'s description of a hoard from "North Africa (or Spain?)", and assign Kairouan as approximate location (and note that the precise location of the hoard is immaterial to our exercise). We treat the Safavid dinar that is 650 years younger than the other coins (Hoge: "no doubt added to the other pieces 'in trade'.") as extraneous to the hoard.

### A.1.2 Islamic hoards in Spain and France

Tables A.6 and A.7 show the hand-digitized hoards from Islamic Spain (al-Andalus) and Islamic coin finds from southern France.

### A.1.3 Other Islamic and Byzantine hoards in Europe

We digitize the hoards, mini-hoards, and stray finds from McCormick (2001)'s survey of Arab and Byzantine coins in Europe (Appendix 3) between 668 and 900. We add those to our dataset, except when already covered in our other sources. We update hoard descriptions for which newer catalogues are available.[40] Finally, we exclude the contested Odoorn/Zuidbarge (1859–60) hoard, as the identity of it as a single hoard is not clear, some of the coins had been converted into jewellery, and the contents are not well described.[41]

### A.1.4 Byzantine hoards

The hoards reported in the corpora by Pennas (1991), Füeg (2007), and Nikolaou and Touratsoglou (2019) form the basis of our collection of Byzantine hoards (the corpus on earlier finds by Morrisson et al. (2006) is mostly already incorporated into FLAME). Information on particular regions come from Mirnik (1981) (Balkans), Arslan (2005) (Italy), Kovács (1989) (Hungary), and Wołoszyn (2009) (Central Europe). Hoard catalogues typically refer to collection catalogues (Sabatier, 1862, Wroth, 1908, Grierson, 1968, 1973) which we use to retrieve mint date intervals and likely mints.[42] We exclude coin finds from running excavations, unless the coins were found as individual parcels in a specific location. Tables A.8 and A.9 show our hand-coded byzantine hoards.

### A.1.5 Carolingian hoards

We follow Simon Coupland's *Checklist* (Coupland, 2011a, 2014, 2020) and digitize hoards and finds primarily based on the corpora presented by Völckers (1965), Duplessy (1985), and Haertle (1997), giving priority to more recent descriptions. Tables A.10 to A.14 show details. We follow the mint codings of Louis the Pious' *Christiana religio* coins given by Coupland (2011b). As mentioned above, we exclude the contested Odoorn/Zuidbarge hoard.

## A.2 FLAME

FLAME records their data in three different tables: coin finds, coin groups, and mints. In the coin find table each observation is a find that contains one or more coin groups; in the coin group table each observation is a set of coins with common recorded attributes (and linked to the coin find ID), including a mint and an interval for the year of minting. In the mint table each observation is a mint, and the mint name string allows these to be matched to coin groups. Mints and coin finds are geocoded.

[40] A35 (Steckborn): Ilisch (2005), A8 (Cagliari): Saccocci (2005), who also mentions an Aghlabid semi-dirham of Muhammad I found in Crotone, Sicily. We update A28 (Porto Torres, Sardinia) based on the number and datings reported in Füeg (2007)'s corpus, likewise the dates from A34 (Reno River).

[41] See Coupland (2011a) for a discussion of these issues.

[42] For a large part of the time interval that is not covered by FLAME, Byzantine gold and silver coins are believed to have been exclusively issued at Constantinople (Grierson, 1968).

The records in FLAME thus include a superset of the attributes in the hand-coded data above, except (i) the material of the coin, which we code based on the denomination; (ii) the weight and dimensions of the coins, which are sometimes (but not systematically) coded in the comments. We convert the FLAME data to the same structure as our handcoded data, including the following cleaning steps:

- A small number (6) of coin groups has a start year that's after the end year; we switch those around.
- FLAME contains start and end dates for the coin find itself. For a small number of coin groups the end date of the coin find falls in between the start and end dates of the coin group. This is often the case when very broad ranges have been given for the coin group, and so we truncate the coin group interval at the end date of the find.
- For Sasanian coins, we adhere to the mint codings in FLAME. A number of coins report the mint abbreviation but not the mint, we code and locate them analogously to how we coded them in the hand-coded coins (see below).
- A number of coin groups record a mint string that is not included in FLAME's mint file. We code Nomisma ID's for those mints, wherever possible.
- A large fraction of FLAME coins don't have mints or dates: often large hoards are not recorded by coin (just the total number of coins). Out of 1.7m coins, about 340k have mint and dates.

## A.3 Locating mints

For FLAME data, we follow the attribution of mint locations done by the authors of the respective FLAME entries. For hand-collected data, we attempt to map the hand-coded mints to Nomisma (2023) IDs for the mints (`nmo:Mint`). Whenever a geocode for a mint is not available in Nomisma, or whenever the mint is not represented in Nomisma, we hand-code the geocodes. These geocodes should only be regarded as approximate and with a degree of precision required for our particular application in mind. Table A.3 shows the mints we add to Nomisma, along with our codings, and Table A.4 shows the codings for existing Nomisma mints without geocodes.

### A.3.1 Sasanian mints

The location of Sasanian mints and the identification of Sasanian mint signatures are contested. We generally follow the reading of the original hoard descriptions, except in situations where these are dated and the literature nowadays prefers different readings. Regarding the approximate location of the mints, we decided to code the approximate location for most signatures following the consensus in the literature; in some cases where the literature only agrees up to the region we chose Nomisma IDs from mints of that region. As with the other codings, the Nomisma IDs should only be seen as approximating the location of the mint, and do not carry any information on dating. Table A.16 summarizes our signature codings with their approximate mint locations.

## A.4 Political entities and the geography of hoards and mints

### A.4.1 Dynasties/Empires

We record dynasties/empires through the `dynastyname` field of FLAME data, and an equivalent field of the hand-coded data. We aggregate these to 10 more aggregate ("level 1") dynasties/empires, and seven most aggregate ("level 2") dynasties/empires. Figure A.1 shows the breakdown of recorded dynasties in our final sample.

### A.4.2 Location of hoards and mints

Figure A.2 show the location of mints and hoards of our final dataset. Only locations corresponding to coins that were minted after 400 AD are shown. Figure A.3 shows details for western Europe and the eastern Mediterranean.

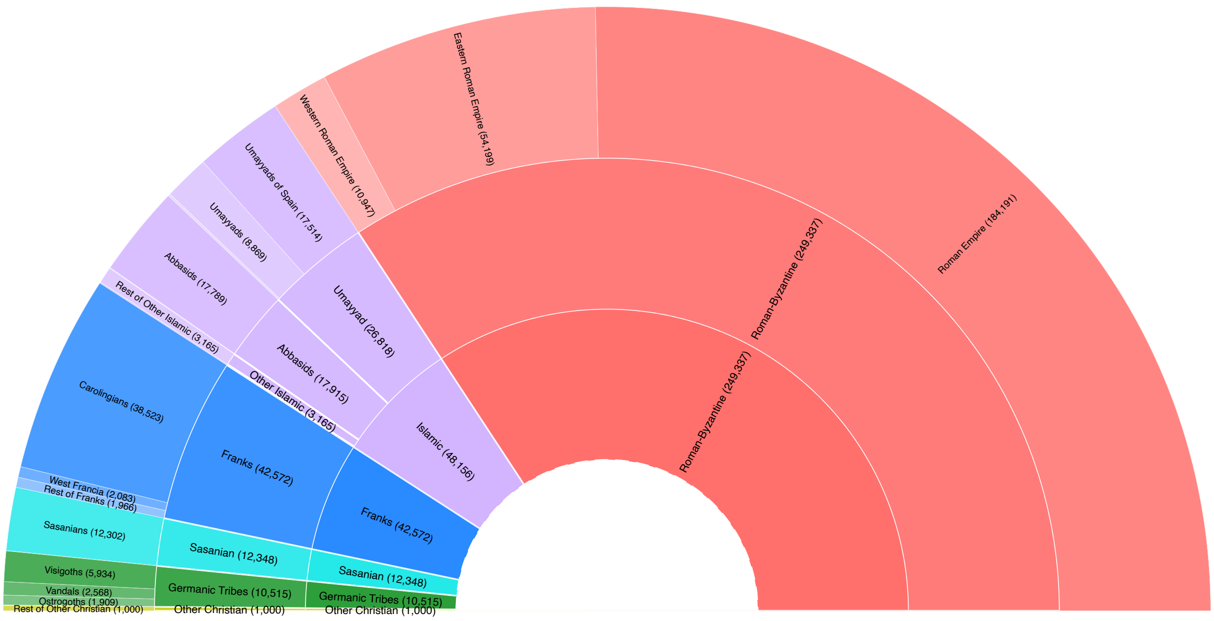


Appendix Figure A.1: Dynasties/Empires

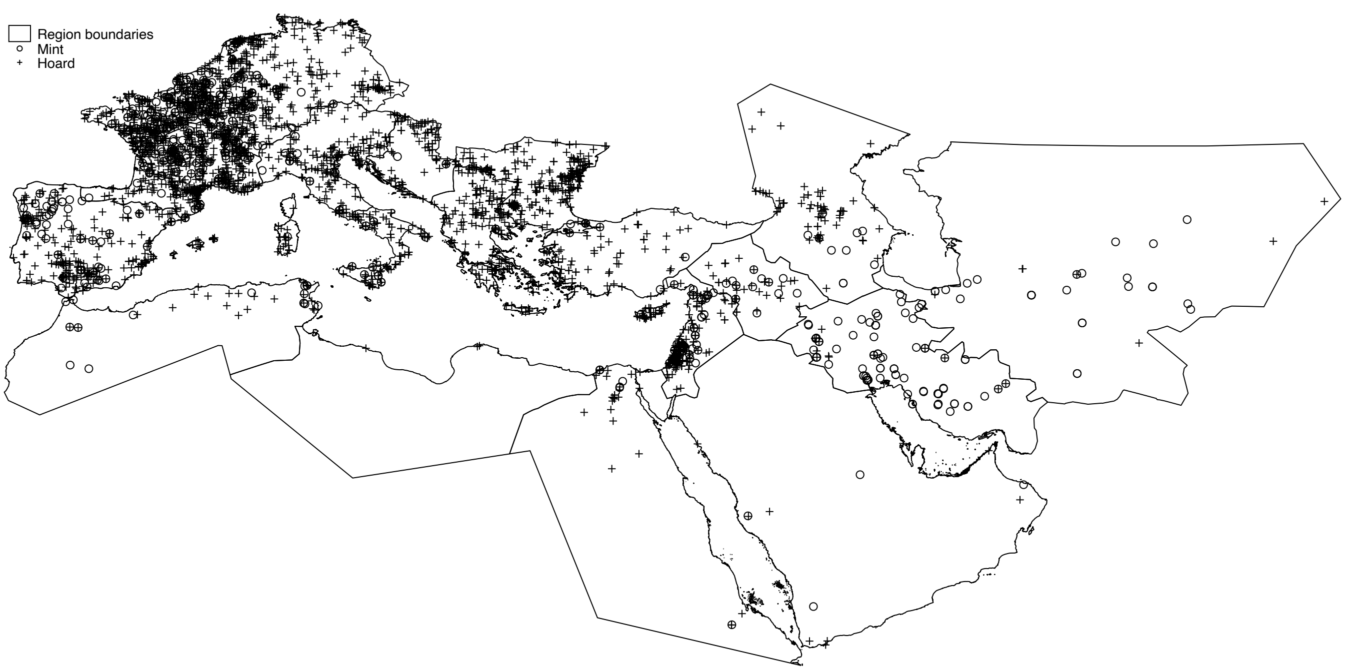


Appendix Figure A.2: Mints and Hoards

Appendix Figure A.3: Mints and Hoards: Details

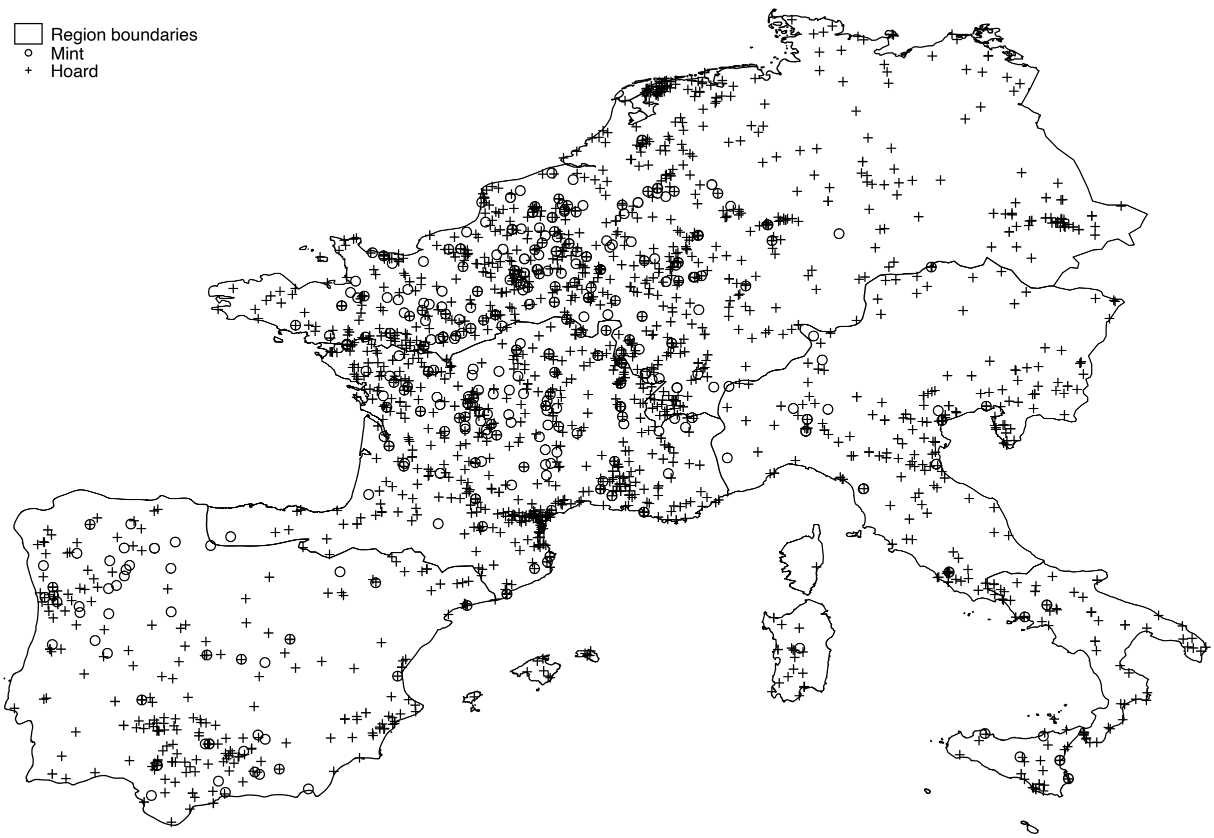


(a) Western Europe

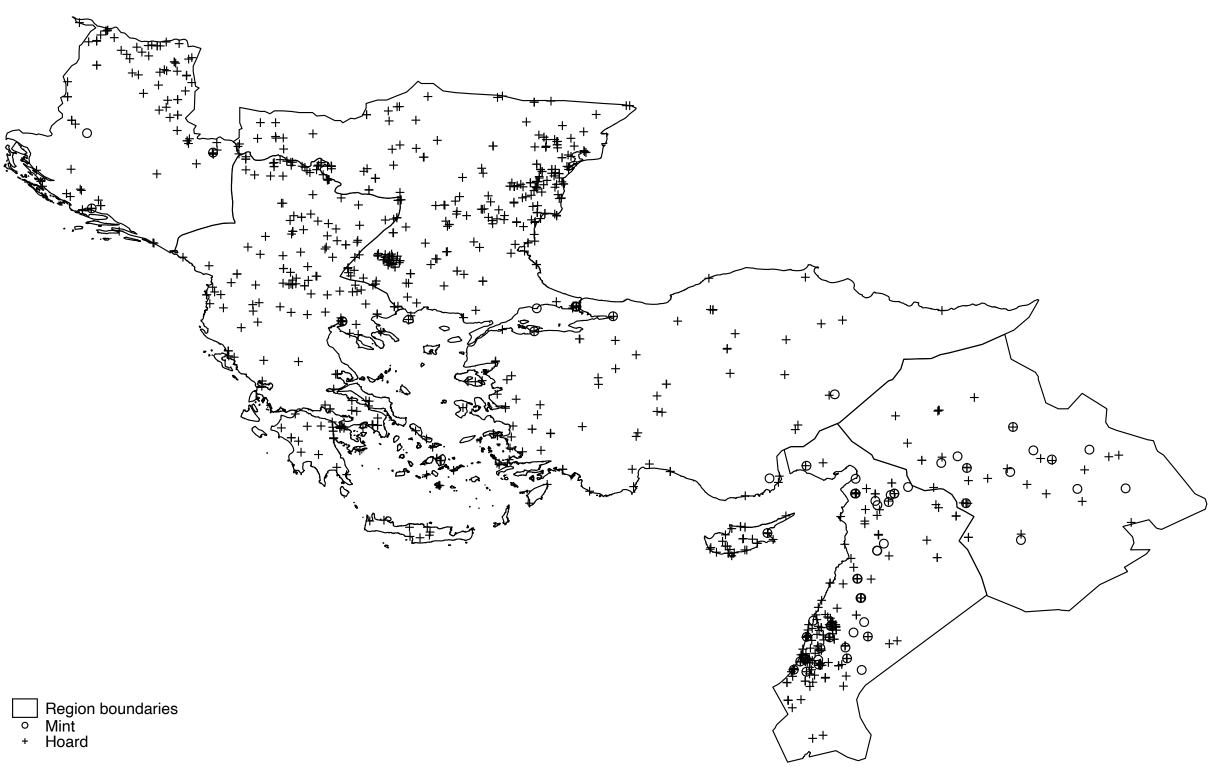


(b) North-eastern Mediterranean

Note: Maps show coins minted after 400 AD

### A.4.3 Comparing hoards with circulation hoards of Banaji (2016)

To support the argument that the coins in our hoards are broadly reflective of coin circulation during Late Antiquity, we compare the age distribution of the hoards in our data with a sample of Byzantine circulation hoards described by Banaji (2016), Chapter 6. These are twelve hoards containing between 12 and 751 Byzantine solidi. Figure A.4 shows the average fraction of coins in each 10-year age bin in these hoards, alongside the distribution of coin ages in Figure 6, showing a similar age profile. Banaji (2016) also reports that on average 44% of the coins in these hoards are older than 33 years at time of deposit; in our data the corresponding share (for hoards with more than ten coins) is 38%.

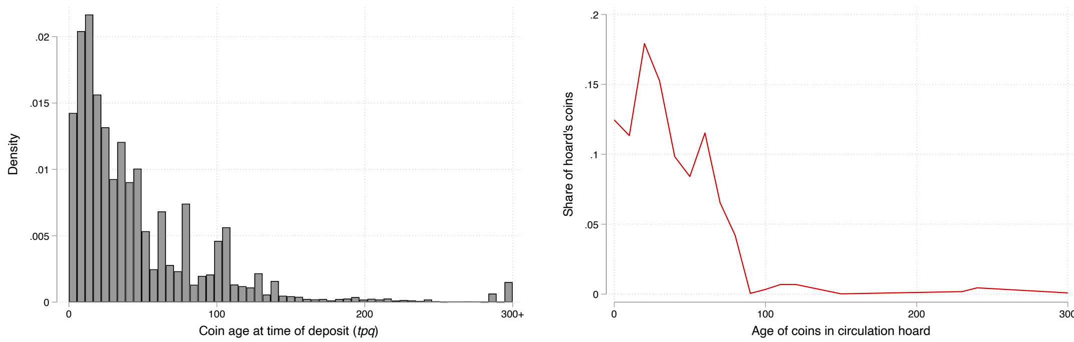


Appendix Figure A.4: Comparison with Circulation Hoards in Banaji (2016)

*Notes:* The left panel is Figure 6. The right panel shows the average share of coins in each 10-year age bin in the circulation hoards of Banaji (2016), Chapter 6, who reports the issuing emperors (but not mint dates) of the coins in these hoards. We draw mint dates uniformly from the ruling years of these emperors.

## A.5 Tables and references

Appendix Table A.1: Summary statistics: Coins

| | count | mean | sd | min | p10 | p50 | p90 | max |
|---|---|---|---|---|---|---|---|---|
| Has mint date interval | 489,259 | 0.85 | 0.36 | 0 | 0 | 1 | 1 | 1 |
| Has mint location | 489,259 | 0.55 | 0.50 | 0 | 0 | 1 | 1 | 1 |
| Has mint location and date interval | 489,259 | 0.54 | 0.50 | 0 | 0 | 1 | 1 | 1 |
| Mint date interval, years | 414,046 | 30.78 | 42.56 | -19 | 1 | 24 | 71 | 432 |
| Mint date interval, start year | 414,046 | 463.68 | 187.10 | 34 | 306 | 375 | 819 | 949 |
| Mint date interval, end year | 414,046 | 494.47 | 184.85 | 79 | 333 | 395 | 840 | 950 |
| Age at tpq | 414,046 | 65.91 | 85.75 | 0 | 6 | 36 | 178 | 805 |
| Has material | 489,259 | 0.98 | 0.15 | 0 | 1 | 1 | 1 | 1 |
| Coin is gold | 489,259 | 0.07 | 0.25 | 0 | 0 | 0 | 0 | 1 |
| Coin is silver | 489,259 | 0.17 | 0.37 | 0 | 0 | 0 | 1 | 1 |
| Coin is copper/bronze | 489,259 | 0.74 | 0.44 | 0 | 0 | 1 | 1 | 1 |
| Has denomination | 489,259 | 0.99 | 0.10 | 0 | 1 | 1 | 1 | 1 |
| Has some empire/dynasty information | 489,259 | 0.69 | 0.46 | 0 | 0 | 1 | 1 | 1 |
| Geodesic distance mint to hoard, km | 268,466 | 773.96 | 789.27 | 0 | 55 | 503 | 1,631 | 6,302 |

*Notes:* Sample consists of all coins from hoards with tpq between 325 and 950. "Age at tpq" is defined as tpq of the hoard minus the midpoint of the mint date interval.

Appendix Table A.2: Summary statistics: Hoards

| | count | mean | sd | min | p10 | p50 | p90 | max |
|---|---|---|---|---|---|---|---|---|
| Hoard tpq | 5,493 | 591.77 | 147.43 | 326 | 378 | 578 | 782 | 950 |
| Number of coins in hoard | 5,493 | 89.07 | 823.91 | 1 | 1 | 1 | 80 | 43,867 |
| Fraction of coins with mint date interval | 5,493 | 0.98 | 0.12 | 0 | 1 | 1 | 1 | 1 |
| Fraction of coins with mint location | 5,493 | 0.87 | 0.27 | 0 | 0 | 1 | 1 | 1 |
| Fraction of coins with mint date interval and mint location | 5,493 | 0.86 | 0.28 | 0 | 0 | 1 | 1 | 1 |
| Average mint date interval | 5,493 | 23.52 | 32.74 | 0 | 1 | 11 | 82 | 377 |
| Average age of coins at tpq | 5,493 | 26.35 | 42.82 | 0 | 0 | 11 | 54 | 522 |
| Fraction of coins with material | 5,493 | 0.99 | 0.08 | 0 | 1 | 1 | 1 | 1 |
| Fraction of coins that are gold | 5,493 | 0.29 | 0.45 | 0 | 0 | 0 | 1 | 1 |
| Fraction of coins that are silver | 5,493 | 0.15 | 0.35 | 0 | 0 | 0 | 1 | 1 |
| Fraction of coins that are bronze | 5,493 | 0.55 | 0.49 | 0 | 0 | 1 | 1 | 1 |
| Fraction of coins with denomination | 5,493 | 0.99 | 0.09 | 0 | 1 | 1 | 1 | 1 |
| Fraction of coins with empire/dynasty information | 5,493 | 0.80 | 0.38 | 0 | 0 | 1 | 1 | 1 |
| Average distance of coins from mint, km | 5,388 | 685.06 | 611.13 | 0 | 88 | 533 | 1,464 | 6,124 |

*Notes:* Sample consists of all coins from hoards with tpq between 325 and 950. "Age at tpq" is defined as tpq of the hoard minus the average coins' midpoint of the mint date interval.

| Mint | id | Location | Latitude | Longitude | Notes |
|---|---|---|---|---|---|
| Abarqubadh | abarqubadh | | 31.28027 | 47.49266 | "This mint was in the district of Khusra-shadh Bahmân (the district of the Tigris) in Irâq, between Wâsit and al-Basra and near the border with Khuzistân." Lloyd (2023) |
| Adurbadagan | adurbadagan | Ganzak | 37.0123 | 46.2019 | Sasanian mint (AT) |
| al Hashimiyah | al-hashimiyah | Kufa | 32.05114 | 44.44017 | Rare Abbasid mint during al-Mansur's reign, situated close to Kufah (138-146 AH). |
| al Rahba | al-rahba | Mayadin | 35.005 | 40.4235 | A mint in Syria, on the Euphrates |
| Arrajan | arrajan | | 30.65388 | 50.27472 | "[Bizamqubadh] was an alternative name for Arrajân in Fars, and also appears to have struck Arab-Sasanian issues." Lloyd (2023) |
| Hulwan | hulwan | | 34.465 | 45.855 | "This mint-name is that of a district (astân) in Irâq, which covered an area to the north-east of Baghdad. Le Strange notes that this district was also known as Shâd Fîrûz - presumably its former Sasanian name. The town of Hulwân itself evidently lay just over the border in Jibâl province, although at this period it appears to have been included with 'Irâq for administrative purposes." Lloyd (2023) |
| Madinat Elvira | madinat_elvira | | 37.23105 | -3.70848 | The archaeological site of Madinat Ilbira. |
| Mah al Basrah | mah-al-basrah | Nihavand, Iran | 34.18879 | 48.37046 | "The term is the Arabic name for Nihavand." (British Museum `x107840`) |
| Mah al Kufah | mah-al-kufah | Dinawar, Iran | 34.583333 | 47.43333 | "Mah al-Kufah = Dinawar (sometimes incorrectly written Daynawar) in the middle ages was one of the most important towns in Djibal (Media); it is now in ruins. The exact location is 34 degrees 35 minutes Lat. N. and 47 degrees 26 minutes E. Long. (Greenwich)." Lockhart (2012) |
| Masabadhan | masabadhan | | 33.52303 | 46.86539 | A district with capital al-Sirawan; the location of al-Sirawan is from Cornu (1983)'s atlas. |
| Maysan | maysan | Naysan | 30.8093 | 47.5628 | Sasanian mint Maysan (MY) |
| Panjshir | panjshir | Panjshir Valley | 35.254095 | 69.456014 | Panjshir Valley, modern-day Afghanistan |
| Rev-Ardashir | rev-ardashir | Bushehr | 28.9119 | 50.8367 | Sasanian mint (LYW/ LYWARTHST/KWN LYW/GNC LYW); the location is from FLAME |
| Roda | roda | | 42.26478 | 3.17887 | A carolingian mint in Rosas, Spain |
| Sarakhs | sarakhs | Sarakhs, Iran | 36.5449 | 61.1577 | "A town in Khurâsân located roughly midway between Marw and Abrashahr. Sarakhs lay on the eastern bank of the Mashhad river, about forty or fifty miles north of its confluence with the Herât river." Lloyd (2023) |
| Uman | oman | Oman | 23.51234 | 58.27000 | Lloyd (2023): "Modern Oman on the Persian Gulf." |

Appendix Table A.3: Manual mint codings I: new mints

| Nomisma ID | Nomisma Note | Latitude | Longitude | Note |
|---|---|---|---|---|
| al-Abbasiyah | “Earfly Abbasid site in North Africa” | 35.62183407 | 10.18089991 | According to Abdul Wahab (2012), three miles south-east of Kairouan. |
| al-Furat | “In the district of Shadh Bahman in Iraq, but its exact location unknown. Klat, 16.” | 30.53269083 | 47.87593421 | Geocodes based on Fig. 11 in Morony (1982). |
| al-Madinat al-Mutawakkiliyah | “al-Madinat al-Mutawakkiliyah is just north of Sammara and was built by the Abbasids.” | 34.2621862 | 43.85500034 | Close to Samarra, Iraq |
| al-Manadhir | “The name of two districts, with tehir chief-towns, named Greater Manadhir & Little Manadhir in Khuzistan, Iran” | 31.97753445 | 48.69644554 | Lloyd (2023): ”Manâdhir was a district within the province of Khuzistân, situated between the Dizfûl and Dujayl rivers above their confluence north of Ahwâz. It was apparently divided into two parts named Greater and Little Manâdhir, each containing a chief town with the same name.” |
| al-Mubarakah (Abbasid) | “Some place in North Africa” | 36.30565739 | 10.13850323 | Unknown location, coding it to modern-day Tunisia |
| al-Samiyah | “Al-Samiya was in the Shatt al-Arab area of lower Iraq. | 30.6617666 | 47.78548511 | Coding to Shatt al-Arab. |
| Bihqubadh af-Asfal | “Lower Bihqubach (sic) in Iraq on the Euphrates” | 31.56718959 | 45.22725183 | Lloyd (2023): ”The three districts of Upper, Middle and Lower Bihqubâdh were located in ‘Iraq to the west of the Euphrates. Bihqubâdh is taken from the Persian meaning ”the good land of king Qubâdh. Al-Asfal means ‘the lower,’ and covered the land next to the Euphrates where it entered the Great Swamp.” Coordinates based on Fig. 8 of Morony (1982). |
| Dastawa | “South of Qazvin” | 35.75554989 | 50.08839336 | |
| Ma’din Bajunays | “Province north of Lake Van” | 40.223509 | 43.8355181 | Location very approximate in western Armenia. |
| Mani | Klat is uncertain of its location although the prefix Mah occurs in older names for Dinavar & Nihavand. Quarter of Jibal. Klat” | 34.38582341 | 47.97904114 | Lloyd (2023) puts it either at Mah al Basrah (Nihavand) or Mah al Kufa (Dinavar). Our chosen geocode is halfway between the two. |
| Nahr Tira | “Exact location on the river or canal of the same name in Khuzistan not know. Klat, p.. 18” | 30.8755 | 49.7131 | From FLAME. |
| Qumis | “A small province which stretches along the foot of the Great Alburz chain of mouintains. Klat, p. 17.” | 35.96088616 | 54.03571139 | Wikipedia “Qumis (region)” |
| Surraq | “Surraq or DAWRAQ (or Dawraq al-Fors), name of a district (k ´ra; Moqaddasf´, pp. 406-07), also known as Sorraq, and of a town that was sometimes its chef-lieu in medieval Islamic times.” | 30.65094882 | 48.67463446 | Coding to Shadegan, Iran. |
| Tabaristan | “Tabaristan, also known as Tapuria, was the name of the former historic region in the southern coasts of Caspian Sea roughly in the location of the northern and southern slopes of Elburz range in Iran.” | 36.5656 | 53.0588 | From FLAME |
| Tudghah | “Unknown location in Morroco” | 31.523 | -5.5313 | al ’Ush (1982) identifies it with “Todr’a”, and cites Renou (1846) (incorrectly as authored by “Lavoix”) saying that it was located fourty kilometers west of Sijilmasa, at a river of the same name. That would place it close to Tinghir, Morocco. |

Appendix Table A.4: Manual mint codings II: geocoding existing Nomisma mints

| Hoard Name | Date | # Coins described | Reference | Location | Latitude | Longitude |
|---|---|---|---|---|---|---|
| Abu Saida | ca. 721 | 15 | Royal Numismatic Society (1975) | Qaryat Abū Şaydā aş Şaghīrah, Iraq | 33.924 | 44.761 |
| Afaq | 773-932 | 1674 | Gachet (1993) | Afak, Iraq | 32.064 | 45.247 |
| Afghanistan | 86-112 AH | 131 | Album (1971) | Afghanistan | 33.000 | 66.000 |
| Agrigenta | 699-828 | 370 | Lagumina (1904) | Agrigento, Italy | 37.311 | 13.577 |
| Al Raqqa | 698-750 | 1187 | Sears (2000) | Ar Raqqah, Syria | 35.953 | 39.008 |
| Al Wajh | | 35 | Hakiem (1977) | Al Wajh, Saudi Arabia | 26.246 | 36.452 |
| Al-Khobar | tpq 784/85 | 42 | Noonan (1980) | Khobar, Saudi Arabia | 26.279 | 50.208 |
| Amman | AH 79-125 | 12 | Kirkbride (1951) | Amman, Jordan | 31.955 | 35.945 |
| Amūda I | tpq 874 | 646 | Ilisch (1990) | ‘Āmūdā, Syria | 37.104 | 40.930 |
| Amūda II | 779-941 | 643 | Ilisch (1990) | ‘Āmūdā, Syria | 37.104 | 40.930 |
| Awarta (Nablus I ) | 602-685 | 29 | Dajani (1951) | ‘Awartā, Palestine | 32.161 | 35.284 |
| Bab Tuma | tpq 748 | 854 | Gyselen and Kalus (1983) | Damascus, Syria | 33.510 | 36.291 |
| Babylone, Egypt | 157 AH - 241 AH | 114 | Jungfleisch (1949) | Cairo, Egypt | 30.063 | 31.250 |
| Buseyra | 769-943 | 3108 | Al Chomari (2020) | Al Buşayrah, Syria | 35.156 | 40.427 |
| Capernaum | | 288 | Wilson (1989) | Kfar Nahum, Israel | 32.881 | 35.575 |
| Damascus | 548-736 | 3815 | al ’Ush (1972b) | Damascus, Syria | 33.510 | 36.291 |
| Damascus | 679-721 | 546 | al ’Ush (1954-1955) | Damascus, Syria | 33.510 | 36.291 |
| Denizbaji | tpq 811 | 2496 | Artuk (1966) | Denizbacı, Turkey | 37.139 | 38.390 |
| Diyarbakir | 802-902 | 224 | Ilisch (1979) | Diyarbakır, Turkey | 37.914 | 40.217 |
| En Nebk | tpq 747 | 102 | Royal Numismatic Society (1977) | An Nabk, Syria | 34.024 | 36.728 |
| Gazira | 3rd to 9th century | 2820 | Gyselen and Nègre (1982) | Al Jazīrah, Iraq | 36.000 | 42.000 |
| Godhlaniya | | 127 | American Numismatic Society (2023) | Syrian Arab Republic, Syria | 35.000 | 38.000 |
| Hamah | tpq 950 | 214 | Ilisch (1990) | Hamāh, Syria | 35.132 | 36.758 |
| Huszt | | 368 | Fomin and Kovács (1987) | Khust, Ukraine | 48.172 | 23.298 |
| Iran 1970 | tpq 820 | 668 | Noonan (1980) | Islamic Republic of Iran, Iran | 32.000 | 53.000 |
| Isfahan | 777-936 | 582 | Lowick (1975) | Isfahan, Iran | 32.652 | 51.675 |
| Jarash | | 36 | Treadwell and Rogan (1994) | Jarash, Jordan | 32.281 | 35.899 |
| Jazira (Illisch) | tpq 886 | 48 | Ilisch (1990) | Al Jazīrah, Iraq | 36.000 | 42.000 |
| Kerman | about 632-651 | 43 | Heidemann et al. (2014) | Kerman, Iran | 30.283 | 57.079 |
| Khdir Elias | tpq 1014 | 2865 | Al-Naqshbandi (1954) | Republic of Iraq, Iraq | 33.000 | 44.000 |
| Khorasan | 705-774 | 196 | Hebert (1966) | Mashhad, Iran | 36.298 | 59.606 |
| Khirbat al-Minya | 716-734 | 2 | Schneider (1952) | Horbat Minnim, Israel | 32.865 | 35.536 |
| Kufah | tpq 808/09 | 178 | Noonan (1980) | Kufa, Iraq | 32.051 | 44.440 |
| Marv | tpq 815 | 855 | Khodzhaniyazov and Treadwell (1998) | Mary, Turkmenistan | 37.594 | 61.830 |
| Near Fez | | 36 | Royal Numismatic Society (1978) | Fès, Morocco | 34.033 | -5.000 |
| Nippur (Bates) | 704-794 | 76 | Bates (1978) | Aţlāl Nafar, Iraq | 32.136 | 45.221 |
| Nippur (Sears) | 597-743 | 97 | Sears (1994) | Aţlāl Nafar, Iraq | 32.136 | 45.221 |
| North Africa (Spain?) | tpq 860 | 87 | Hoge (1997) | Kairouan, Tunisia | 35.678 | 10.096 |
| Orif, Nablus | 691-742 | 19 | Ma’ayeh (1962) | Urif, Palestine, West Bank | 32.159 | 35.224 |
| Ouenza | 789-798 | 12 | Troussel (1942) | Ouenza, Algeria | 35.953 | 8.129 |
| Qamishliyyah | tpq 816 | 1519 | Gyselen and Kalus (1983) | Al Qāmishlī, Syria | 37.052 | 41.231 |
| Ra’s al-Khaimah | 921-975 | 43 | Lowick and Nisbet (1968) | Ras Al Khaimah City, UAE | 25.790 | 55.943 |
| Sinaw | 589-841 | 948 | Lowick (1983) | Sināw, Oman | 22.501 | 58.030 |
| Tabaristan | about 718-760 | 810 | Malek (1996) | Mazandaran Province, Iran | 36.250 | 52.333 |
| Tiflis | ca. 280-330 AH | 112 | Bartolomei (1857) | Tbilisi, Georgia | 41.694 | 44.834 |
| Umm Hajarah | tpq 808/09 | 408 | al ’Ush (1972a) | Umm Hajarah, Syria | 36.195 | 41.074 |
| Utaifiyah | 154-193 AH | 294 | al Bakri (1973) | Baghdad, Iraq | 33.341 | 44.401 |
| Volubilis | tpq 125 AH (742) | 232 | Eustache (1956) | Oualili, Morocco | 34.073 | -5.555 |
| Yarubiyyah | tpq 815/816 | 1415 | American Numismatic Society (2023) | Al Ya‘rubīyah, Syria | 36.811 | 42.062 |
| Zahu/Zakho | tpq 808-9 | 3306 | Al-Naqshbandi (1949, 1950, 1951, 1952) | Zaxo, Iraq | 37.149 | 42.686 |

Appendix Table A.5: Near East and North Africa Hoards

| Hoard name | Date | # Coins described | Reference | Location | Latitude | Longitude |
|---|---|---|---|---|---|---|
| Alcaudete | 698-734 | 14 | Cano Ávila (1989) | Alcaudete | N 37° 35' 27" | W 4° 4' 56" |
| Algeciras | 710-727 | 29 | Canto García and Martín Escudero (2009) | Algeciras | N 36° 7' 59" | W 5° 27' 1" |
| Alhama | 770-876 | 459 | Codera y Zaidín (1892) | Alhama | N 37° 0' 24" | W 3° 59' 22" |
| Arrabal Occidental | 929-1021 | 373 | Canto García et al. (2020a) | Cordoba | N 37° 53' 29" | W 4° 46' 21" |
| Azanuy | 699-733 | 6 | Codera y Zaidín (1913) | Azanuy | N 41° 59' 10" | E 0° 18' 58' |
| Badajoz | 927-1011 | 99 | Prieto (1934) | Badajoz | N 38° 52' 40" | W 6° 58' 14" |
| Baena | 699-754 | 160 | Martín Escudero (2001) | Baena | N 37° 39' 22" | W 4° 20' 4" |
| Barrio de los Olivos Borrachos | 941-1004 | 165 | Marcos Pous and Vicent Zaragoza (1992) | Cordoba | N 37° 53' 29" | W 4° 46' 21" |
| Benferri | 941-958 | 12 | Doménech Belda (1997) | Benferri | N 38° 8' 28" | W 0° 57' 43" |
| Bormujos | 929-965 | 11 | Cano Ávila (2016) | Bormujos | N 37°21'41.9" | W 6° 06' 38.1" |
| Calle San Jose | 936-950 | 16 | Doménech Belda (1997) | Xàtiva | N 38° 59' 25" | W 0° 31' 6" |
| Calle San Pedro | 967-1031 | 19 | Canto García and Jabłońska (2019) | Murcia | N 37° 59' 13" | W 1° 7' 48" |
| Calle Santa Julia | 929-1012 | 263 | Segovia Sopo (2014) | Mérida | N 38° 54' 58" | W 6° 20' 37" |
| Campo de la Verdad | 775-912 | 176 | Martín and Martín (2006) | Cordoba | N 37° 53' 29" | W 4° 46' 21" |
| Carmona | 698-753 | 146 | Canto García and Escudero (2012) | Carmona | N 37°28' 17" | W 5°38' 46" |
| Castillejos de Quintana | 933-1010 | 39 | Cravioto (2016) | Castillejos de Quintana | N 36°46'58.7" | W 4° 41' 30.9" |
| Castro Marim | 788-885 | 53 | Rodrigues Marinho (1995) | Castro-Marim | N 37° 13' 14" | W 7° 26' 36" |
| Cerro da Villa | 831-900 | 239 | Heidemann et al. (2018) | Cerro da Villa | N 37° 4' 48" | W 8° 7' 13" |
| Crevilllent | 770-1269 | 34 | Doménech Belda and Trelis (1990) | Crevillent | N 38° 14' 59" | W 0° 48' 35" |
| Cihuela | 912-1016 | 296 | Navascués y de Palacios (1961a) | Cihuela | N 41° 24' 26" | W 1° 59' 59" |
| Consuegra | 835-1010 | 173 | Martín Escudero (2011) | Consuegra | N 39° 27' 44" | W 3° 36' 28" |
| Cordoba I | 817-1010 | 25 | Navascués y de Palacios (1961b) | Cordoba | N 37° 53' 29" | W 4° 46' 21" |
| Cordoba II | 933-953 | 328 | Navascués y de Palacios (1958) | Cordoba | N 37° 53' 29" | W 4° 46' 21" |
| Cordoba III | 933-1021 | 379 | Navascués y de Palacios (1958) | Cordoba | N 37° 53' 29" | W 4° 46' 21" |
| Cordoba IV | 708-796 | 119 | Canto García (1988) | Cordoba | N 37° 53' 29" | W 4° 46' 21" |
| Cova del Randerro | 768-835 | 54 | Doménech Belda (1997) | Pedreguer | N 38° 47' 35" | E 0° 2' 2" |
| Cuba | 932-1010 | 9 | Martín Escudero (2011) | Cuba | N 38° 10' 24" | W 7° 53' 46" |
| Domingo Perez | 767-865 | 367 | Martín and Martín (2002) | Domingo Pérez | N 37° 29' 45" | W 3° 30' 33" |
| Elche | 841-1173 | 316 | Doménech Belda (1992) | Elche | N 38° 15' 43" | W 0° 42' 3" |
| Electromecanicas I | 941-1005 | 169 | Marcos Pous and Vicent Zaragoza (1992) | Cordoba | N 37° 53' 29" | W 4° 46' 21" |
| Electromecanicas II | 928-1016 | 102 | Marcos Pous and Vicent Zaragoza (1992) | Cordoba | N 37° 53' 29" | W 4° 46' 21" |
| El Pedroso | 928-1021 | 144 | Cano Ávila and Martín Gómez (2006) | Hacienda Montegil, El Pedroso | N 37°43'51.9" | W 5°51'39.8" |
| El Pedroso III | 832-1021 | 144 | Cano Ávila and Gómez (2008) | El Pedroso | N 37° 51' 0" | W 5° 46' 0" |
| El Rebollar | 810-818 | 5 | Salido Domínguez et al. (2020) | Boalo | N 40° 42' 57" | W 3° 54' 59" |
| Finca la Marquesa | 941-1036 | 246 | Doménech Belda (1997) | Montilla | N 37°36'07.2" | W 4°37'11.7" |
| Fontanar | 941-977 | 764 | Canto García and Martín Escudero (2007) | Cordoba | N 37° 53' 29" | W 4° 46' 21" |
| Fuente de Cantos | 837-883 | 15 | Segovia Sopo (2006) | Fuente de Cantos | N 38° 15' 0" | W 6° 18' 0" |
| Hospital Militar | 970-1032 | 23 | Martín Escudero (2003) | Zaragoza | N 41° 39' 21" | W 0° 52' 38" |
| Huesca | 710-756 | 100 | Martín Escudero (2012) | Huesca region | | |
| Izcar | 778-886 | 50 | Ariza Armada (1988) | Cortijo de Izcar | N 37°39'56.1" | W 4°23'41.6" |
| Iznajar | 768-912 | 1047 | Canto García and Marsal Moyano (1988) | Iznajar | N 37° 15' 27" | W 4° 18' 30" |
| Jaen | 711-713 | 4 | González García and Martínez Chico (2017) | Jaen region | | |
| Jerez de los Caballeros | 770-782 | 277 | Canto García (2019) | Jerez de los Caballeros | N 38° 19' 14" | W 6° 46' 21" |
| La Almagra | 820-822 | 7 | Museo Arqueológico de Murcia (2014) | La Almagra | N 38° 2' 15" | W 1° 25' 57" |
| La Fuensanta | 770-812 | 18 | Cravioto and Ayala (1995) | Cerro la Fuensanta | 36°55'13.7"N | 4°23'23.7"W |
| Lantejuela | 773-887 | 175 | Ruiz Asencio (1967) | La Lantejuela | N 37°19'17.5" | W 5°13'27.6" |
| La Rinconada | 770-912 | 315 | Cano Ávila and Martín Gómez (2005) | La Rinconada | N 37° 29' 10" | W 5° 58' 51" |
| Las Torres | 757-976 | 18 | Martínez Enamorado (2004) | Gavilanes | N 40° 15' 44" | W 4° 51' 30" |
| L'Elca | 933-950 | 31 | Doménech Belda (1997) | Oliva | N 38° 55' 10" | W 0° 7' 9" |
| Lleida | 770-1463 | 40 | Soler Balaguero (1993) | Lleida | N 41° 37' 7" | E 0° 34' 29" |
| Lora del Rio | 941-1021 | 165 | Pellicer i Bru (1985) | Lora del Rio | N 37° 39' 32" | W 5° 31' 39" |
| Los Villares | 942-1028 | 112 | Valle (1987) | Caudete de las Fuentes | N 39° 33' 34" | W 1° 16' 42" |

Appendix Table A.6: Hoards in al-Andalus, Part I

| Hoard name | Date | # Coins described | Reference | Location | Latitude | Longitude |
|---|---|---|---|---|---|---|
| Madinat Iyyuh | 711-856 | 20 | Doménech Belda and Gutiérrez Lloret (2006) | El Tolmo de Minateda | N 38° 28’ 34” | W 1° 36’ 20” |
| Marroquies Altos | 933-1010 | 270 | Asencio (1962) | Jaen | N 37° 46’ 9” | W 3° 47’ 25” |
| Marroquies Bajos | 941-1015 | 201 | Canto García et al. (1997) | Jaen | N 37° 46’ 9” | W 3° 47’ 25” |
| Martos | 817-875 | 24 | Canto García (1993) | Cortijo del Mimbre | N 37°38’26.0” | W 3°57’04.9” |
| Merida | 726-901 | 60 | Rodríguez Palomo and Martín Escudero (2022) | Merida | N 38° 54’ 58” | W 6° 20’ 37” |
| Mertola | 932-1036 | 81 | Poiares (2000) | Mertola | N 37° 38’ 34” | W 7° 39’ 40” |
| Mijas Costa | 932-976 | 533 | Ayala Ruiz and Gozalbes Cravioto (1996) | La Cala de Mijas | N 36° 33’ 56” | W 4° 40’ 11” |
| Montellano | 949-1010 | 23 | Cano Ávila (2014) | Montellano | N 37°00’06.1” | W 5°33’02.1” |
| Moraleja | 767-854 | 16 | Álvarez (1993) | Moraleja | N 40° 0’ 58” | W 6° 41’ 51” |
| Moreria | 857-1015 | 134 | Palma García and Segovia Sopo (2007) | Merida | N 38° 54’ 58” | W 6° 20’ 37” |
| Niebla | 805-884 | 36 | Cano Ávila and Martín Gomez (2011) | Sierra de Alcantara | N 37°28’33.8” | W 6°38’36.2” |
| Osuna | 954-1022 | 3 | Alfaro Asins (1992) | Osuna | N 37° 14’ 15” | W 5° 6’ 11” |
| Parque Cruz conde | 852-1021 | 3341 | Canto García et al. (2020b) | Cordoba | N 37° 53’ 29” | W 4° 46’ 21” |
| Partida de Atzbares | 941-970 | 26 | Doménech Belda (1997) | Atzavares Baix (Elche) | N 38° 15’ 43” | W 0° 42’ 3” |
| Pascul de Gayangos | 778-1204 | 159 | Marinho (1993) | Algarve | | |
| Pinos Puente | 770-816 | 169 | Martín Escudero (2011) | Pinos Puente | N 37° 15’ 3” | W 3° 44’ 58” |
| Pozoblanco | 948-976 | 15 | Marcos Pous and Vicent Zaragoza (1992) | Pozoblanco | N 38° 22’ 44” | W 4° 50’ 53” |
| Priego de Cordoba | 770-856 | 54 | Ávila and Pareja (1999) | Priego de Cordoba | N 37° 26’ 17” | W 4° 11’ 42” |
| Puebla de Cazalla | 770-892 | 911 | Ibrahim and Canto García (1991) | La Puebla de Cazalla | N 37° 13’ 17” | W 5° 18’ 41” |
| Puente de Miluze | 934-1057 | 164 | Canto García (2001) | Pamplona | N 42° 49’ 0” | W 1° 38’ 35” |
| Recopolis | 772-785 | 9 | Priego and Enciso (2016) | Recopolis | N 40°19’15.1” | W 2°53’37.7” |
| Sagrada Familia | 945-1012 | 316 | Marcos Pous and Vicent Zaragoza (1992) | Cordoba | N 37° 53’ 29” | W 4° 46’ 21” |
| San Andres de Ordoiz | 782-908 | 167 | Uranga (1950) | Estella-Lizarra | N 42°40’ 19” | W 2°01’ 56” |
| Saqunda | 707-930 | 467 | Martín Escudero et al. (2023) | Cordoba | N 37° 53’ 29” | W 4° 46’ 21” |
| Sevilla | 711-1011 | 497 | Saenz-Diéz (1993) | Sevilla | N 37° 22’ 58” | W 5° 58’ 23” |
| Sierra Cazorla | 928-1021 | 237 | Pellicer i Bru (1982) | Sierra Cazorla | N 37° 54’ 45” | W 2° 58’ 34” |
| Silves | 770-875 | 79 | Miles (1960) | Silves | N 37° 11’ 21” | W 8° 26’ 17” |
| Sinarcas | 942-1037 | 57 | Arroyo Ilera (1989) | Sinarcas | N 39° 44’ 0” | W 1° 14’ 0” |
| Solar del Museo Arqueologico | 953-1007 | 16 | Marcos Pous and Vicent Zaragoza (1992) | Cordoba | N 37° 53’ 29” | W 4° 46’ 21” |
| South France | 692-886 | 204 | Parvérie (2014, 2019) | South France | | |
| Spain single finds (felus) | 699-901 | 57 | Martín Escudero (2012) | Spain | | |
| Tarancon | 929-1014 | 451 | Canto García (2014) | Tarancon | N 40° 0’ 30” | W 3° 0’ 26” |
| Teatro romano | 805-819 | 25 | Segovia Sopo and Jiménez (2011) | Merida | N 38° 54’ 58” | W 6° 20’ 37” |
| Tignar | 864-913 | 35 | Motos Guirao and Díaz García (1985) | Albolote | N 37° 13’ 51” | W 3° 39’ 18” |
| Tijan | 976-1021 | 377 | Fontenla Ballesta (1998) | Sierra de Cabrera | N 37°06’30.3” | W 1°55’49.2” |
| Trujillo | 711-1014 | 384 | Navascués y de Palacios (1957) | Trujillo | N 39° 27’ 28” | W 5° 52’ 55” |
| Valencia de Ventoso | 933-1006 | 7 | Grañeda Miñón (2021) | Valencia del Ventoso | N 38° 16’ 0” | W 6° 28’ 0” |
| Valeria | 936-1009 | 250 | Puertas (1982) | Valeria | N 39° 47’ 0” | W 2° 9’ 0” |
| Valle de Guadajoz | 931-1013 | 204 | Ortega et al. (2006) | Fuentiduena (Baena) | N 37°43’42.1” | W 4°16’54.3” |
| Vega Baja | -200-1500 | 184 | Priego (2020) | Toledo | N 39° 51’ 29” | W 4° 1’ 21” |
| Vera | 941-1024 | 370 | Doménech Belda (1997) | Vera | N 37° 14’ 36” | W 1° 51’ 32” |
| Villaviciosa | 705-817 | 1361 | Peña Martín and Vega Martín (2007) | Villaviciosa de Cordoba | N 38° 5’ 0” | W 5° 1’ 0” |
| Yecla | 705-726 | 5 | Codera y Zaidín (1913) | Yecla | N 38° 39’ 18” | W 1° 7’ 46” |
| Zafra | 789-892 | 43 | Canto García (2019) | Zafra | N 38° 25’ 31” | W 6° 25’ 2” |
| Zamora | 943-999 | 10 | Cerrato and Esquivel (2019) | Zamora | N 41° 30’ 22” | W 5° 44’ 40” |

Appendix Table A.7: Hoards in al-Andalus, Part II

| Hoard Name | Country | Reference | Latitude | Longitude |
|---|---|---|---|---|
| Ankara 1960? | Turkey | Pennas (1991) 122 | 39.9388 | 32.8594 |
| Argos 1983 | Greece | Pennas (1991) 8 | 37.6353 | 22.7277 |
| Ayies Paraskies/Crete 1962 | Greece | Pennas (1991) 59 / Füeg (2007) | 35.209 | 25.2041 |
| Bajagic | Croatia | Mirnik (1981) | 43.7581 | 16.6657 |
| Balchik Stray Find I | Bulgaria | Curta (2005) | 43.4119 | 28.1628 |
| Berezeni | Romania | Oberländer-Târnoveanu (2001) p.67 | 46.378 | 28.1523 |
| Bratimir | Bulgaria | Pennas (1991) 90 | 43.8682 | 26.7044 |
| But | Italy | Arslan (2005) 2280 | 46.4768 | 13.0246 |
| Byala 1954 | Bulgaria | Pennas (1991) 73 | 42.8739 | 27.8886 |
| Calarasi 1947 | Romania | Pennas (1991) 111, Dimian (1957) | 44.2029 | 27.3115 |
| Camarina | Italy | Arslan (2005) 6170 | 36.8279 | 14.5241 |
| Camarina ed. 18 | Italy | Arslan (2005) 6185 | 36.8279 | 14.5241 |
| Camarina ed. 1a | Italy | Arslan (2005) 6181 | 36.8279 | 14.5241 |
| Camarina ed. 6 | Italy | Arslan (2005) 6182 | 36.8279 | 14.5241 |
| Capo Schiso 1950 | Italy | Arslan (2005) 6910 | 37.8244 | 15.2684 |
| Chryse/Edhessa 1935 | Greece | Pennas (1991) 50 / Füeg (2007) | 40.81 | 22.0446 |
| Cleja | Romania | Pennas (1991) 113, Dimian (1957) | 46.4019 | 26.9427 |
| Constanta Stray I | Romania | Dimian (1957) | 44.1777 | 28.6442 |
| Constanta Stray II | Romania | Dimian (1957) | 44.1777 | 28.6442 |
| Corinth 15 May 1934 (South Basilica) | Greece | Pennas (1991) 3 | 37.9373 | 22.932 |
| Corinth 1934 | Greece | Pennas (1991) 7 | 37.9373 | 22.932 |
| Corinth 1965 (Roman Bath) | Greece | Pennas (1991) 1 | 37.9373 | 22.932 |
| Corinth 1965 (Roman Bath) | Greece | Pennas (1991) 4 (BCH 90, 1966, 751, 754) | 37.9373 | 22.932 |
| Corinth (St John's monastery) | Greece | Pennas (1991) 9 | 37.9373 | 22.932 |
| Didyma (single find) | Turkey | Baldus (2006) | 37.3731 | 27.2639 |
| Drobeta - Turnu Severin | Romania | Oberländer-Târnoveanu (2001) p.68 | 44.6425 | 22.6587 |
| Drobeta 1928 | Romania | Oberländer-Târnoveanu (2001) p.67 | 44.6425 | 22.6587 |
| Dubravice | Croatia | Mirnik (1981) | 43.8506 | 15.9398 |
| Dubrovnik 1982 | Croatia | Mosser (1935) p.71 ("Ragusa"), Mirnik (1981) 359 | 42.6489 | 18.094 |
| Elazig | Turkey | Füeg (2007) | 38.6747 | 39.2229 |
| Elbistan | Turkey | Füeg (2007) | 38.2016 | 37.1924 |
| Eskisehir | Turkey | Füeg (2007) | 39.7743 | 30.5138 |
| Gabrica | Bulgaria | Sophoulis (2011) | 43.5082 | 26.9736 |
| Govora | Romania | Oberländer-Târnoveanu (2001) p.68 | 45.0681 | 24.2302 |
| Hadrianoupolis Acropolis Kimistene | Turkey | Laflı et al. (2016) | 40.9231 | 32.4867 |
| Hadrianoupolis Basilica A | Turkey | Laflı et al. (2016) | 40.9231 | 32.4867 |
| Hadrianoupolis Bath A | Turkey | Laflı et al. (2016) | 40.9231 | 32.4867 |
| Hadrianoupolis Bath B | Turkey | Laflı et al. (2016) | 40.9231 | 32.4867 |
| Hadrianoupolis Building 4 | Turkey | Laflı et al. (2016) | 40.9231 | 32.4867 |
| Hadrianoupolis Domus | Turkey | Laflı et al. (2016) | 40.9231 | 32.4867 |
| Hagios Nikolaos, Hydra (Greece) | Greece | Pennas (1996), p. 270 | 37.3011 | 23.3967 |
| Iatrus 1962 | Bulgaria | Pennas (1991) 77 | 43.6262 | 25.587 |
| Iatrus 1975 | Bulgaria | Pennas (1991) 75 | 43.6262 | 25.587 |
| Ipsala | Turkey | Füeg (2007) | 40.9201 | 26.3828 |
| Istria Stray Finds 869-877 | Croatia | Miškec (2002) | 45.1439 | 13.8259 |
| Kavakli | Turkey | Ünal (2018) | 37.755 | 28.305 |
| Kenchreai 1963 | Greece | Pennas (1991) 2 | 37.8833 | 22.9873 |
| Kozojedy, Bohemia | Czechia | Profantova (2009) | 50.2548 | 13.8153 |
| Kyme near Aliaga | Croatia | Carroccio, cited by Morrisson (2017) | 38.7592 | 26.9367 |
| Kyulevcha Grave | Bulgaria | Curta (2005) | 43.2559 | 27.111 |
| Lagbe | Turkey | Füeg (2007), Newell (1945) | 36.8276 | 30.4112 |
| Libice, Bohemia | Czechia | Profantova (2009) | 50.1285 | 15.1815 |
| Liopesi (around 1946) | Greece | Pennas (1991) 35 / Vryonis (1971) | 37.9545 | 23.8521 |
| Ljubimets | Bulgaria | Dimian (1957), Sophoulis (2011) | 41.8466 | 26.0781 |
| Luka Krnicka | Croatia | Miškec (2002) | 44.9723 | 14.0171 |
| Macvanska Mitrovica | Serbia | Pennas (1991) 72 | 44.9655 | 19.5975 |
| Malthi (Dorion) | Greece | Pennas (1991) 6 | 37.267 | 21.8824 |
| Maluk Povorets 1934 | Romania | Pennas (1991) 74 | 43.7133 | 26.7652 |
| Matera Piazza S. Francesco | Italy | Arslan (2005) 4140 | 40.6654 | 16.6087 |
| Medias | Romania | Oberländer-Târnoveanu (2001) p.68, Dimian (1957) | 46.1621 | 24.3567 |
| Melito Porto Salvo | Italy | Arslan (2005) 0450 | 37.9197 | 15.7857 |
| Mikulcice | Czechia | Profantova (2009) | 48.8167 | 17.0516 |
| Monemvasia Stray Find | Greece | Pennas (1996), p. 270 | 36.6876 | 23.0559 |
| Naxos | Greece | Füeg (2007) | 37.0567 | 25.4638 |
| Nea Syllata/Chalkidiki 1977 | Greece | Pennas (1991) 52 | 40.3275 | 23.136 |
| Nin | Croatia | Mirnik (1981) | 44.2392 | 15.1791 |
| Odartsi | Bulgaria | Sophoulis (2011) | 43.44 | 27.9616 |
| Osava near Ram | Serbia | Füeg (2007) | 44.8006 | 21.3433 |
| Osvetimany | Czechia | Profantova (2009) | 49.0562 | 17.2496 |

Appendix Table A.8: Hoards with Byzantine coins, Part I

| Hoard Name | Country | Reference | Latitude | Longitude |
|---|---|---|---|---|
| Oszony, Komarom | Hungary | Oberländer-Târnoveanu (2001) p.68 | 47.7295 | 18.1751 |
| Piran | Italy | Arslan (2005) 2808 | 45.5279 | 13.5694 |
| Pliska | Bulgaria | Füeg (2007) | 43.362 | 27.1228 |
| Prague, Tynsky dur | Czechia | Profantova (2009) | 50.073 | 14.4286 |
| Rakvice (Breclav) | Czechia | Profantova (2009) | 48.8559 | 16.813 |
| Rasova 1934 | Romania | Pennas (1991) 112, Dimian (1957) | 44.2403 | 27.9414 |
| Reggio Calabria | Italy | Arslan (2005) 0670 | 38.0947 | 15.6455 |
| Rhodos Stray Find 859 | Greece | Kasdagli (2018) | 36.436 | 28.2221 |
| Rhodos V.12 (Kattavia) | Greece | Kasdagli (2018) | 35.9534 | 27.7683 |
| Rome / Tiber | Italy | Morrisson and Barrandon (1988) | 41.8882 | 12.4768 |
| Salamis (South of Amphitheatre, 1964-1974) | Turkey | Füeg (2007) | 35.1914 | 33.8979 |
| Santorini (Thira) 1895-1902 | Greece | Pennas (1991) 57 | 36.4058 | 25.4588 |
| Sicily (Fagerlie) | Italy | Fagerlie (1974) | 37.5732 | 14.2114 |
| Songurlu / Mosser | Turkey | Füeg (2007) / Mosser (1935) | 40.1627 | 34.3767 |
| Stare Mesto | Czechia | Profantova (2009) | 49.0727 | 17.4463 |
| Stimanga 1955 | Greece | Pennas (1991) 5 (BCH 80, 1956, 256) | 37.909 | 22.6989 |
| Streda nad Bodrogom | Slovakia | Profantova (2009) | 48.3785 | 21.758 |
| Syracuse Via G. Di Natale | Italy | Arslan (2005) 7335 | 37.0724 | 15.2845 |
| Tegani/Samos 1914 | Greece | Pennas (1991) 58 | 37.6904 | 26.9417 |
| Telerig Stray Miliaresion | Bulgaria | Curta (2005) | 43.8457 | 27.671 |
| Thessaloniki | Greece | Füeg (2007) | 40.652 | 22.9304 |
| Thessaloniki 1891 | Greece | Pennas (1991) 51 | 40.652 | 22.9304 |
| Tichilesti | Romania | Dimian (1957) | 45.1291 | 27.9045 |
| Tralleis/Aydin | Turkey | Ünal (2015) | 37.8591 | 27.8335 |
| Trilj | Croatia | Mirnik (1981) | 43.6187 | 16.7241 |
| Unknown Provenance (Turkey) 1987 | Turkey | Pennas (1991) 123 | 39.2963 | 32.9327 |
| Urluia 1936 | Romania | Dimian (1957), Sophoulis (2011) | 44.1016 | 27.9132 |
| Velul lui Trajan | Romania | Pennas (1991) 105 | 44.1647 | 28.4621 |
| Velul lui Trajan 1999/2000 | Romania | Mănucu-Adameşteanu (2016) | 44.1647 | 28.4621 |
| Voila, Romania | Romania | Dimian (1957) | 45.818 | 24.8405 |
| Vukovar - Lijeva Bara | Croatia | Mirnik (1981) | 45.3382 | 19.0079 |
| Yakimovo (Progorelets) 1960 | Bulgaria | Pennas (1991) 91 | 43.6337 | 23.3621 |
| Yunak | Bulgaria | Pennas (1991) 76 | 43.0763 | 27.6109 |

Appendix Table A.9: Hoards with Byzantine coins, Part II

| Hoard Name | Date | Reference | Location | Latitude | Longitude |
|---|---|---|---|---|---|
| Aalst | 840-855 | Bijsterveld et al. (2000) | Aalst | 51.39611 | 5.477 |
| Aalsum | 814-855 | Morrison and Grunthal (1967) | Aalsum | 53.3403 | 6.00538 |
| Achlum | 768-840 | Morrison and Grunthal (1967) | Achlum | 53.14779 | 5.48239 |
| Alfocea | 943-977 | Parvérie (2018) | Alfocea | 41.724097 | -0.953131 |
| Amerongen | 768-877 | Coupland (2014) | Amerongen | 52.0025 | 5.46024 |
| Ampurias | 768-814 | Doménech-Belda et al. (2013) | Ampurias | 42.134477 | 3.111418 |
| Andalusia | 814-848 | Parvérie (2018) | Andalusia | | |
| Angeac-Champagne | 840-877 | Duplessy (1985) | Angeac-Champagne | 45.60769 | -0.29771 |
| Angers I | 814-840 | Morrison and Grunthal (1967) | Angers | 47.4707 | -0.55324 |
| Angers II (Saint-Julien) | 819-877 | Haertle (1997) | Angers | 47.4707 | -0.55324 |
| Anglure | 864-887 | Morrison and Grunthal (1967) | Anglure | 48.58345 | 3.81356 |
| ANS find | 768-922 | Morrison and Grunthal (1967) | France | | |
| Anse I | 818-823 | Guillemain (1993) | Anse | 45.937639 | 4.717512 |
| Anserall | 768-815 | Doménech-Belda et al. (2013) | Anserall | 42.37829 | 1.456511 |
| Apremont | 793-822 | Morrison and Grunthal (1967) | Apremont-sur-Allier | 46.906 | 3.048 |
| Aquitaine | 814-887 | Coupland (1991) | Aquitaine | | |
| Ardres | 888-923 | Haertle (1997) | Ardres | 50.856432 | 1.978355 |
| Arras | 843-922 | Morrison and Grunthal (1967) | Arras | 50.29039 | 2.778414 |
| Ashdon | 843-898 | Blackburn (1989) | Ashdon | 52.05544 | 0.31373 |
| Aspres-lès-Corps | 901-924 | Schulze (1984) | Aspres-lès-Corps | 44.80162 | 5.98217 |
| Assebroek | 843-877 | Morrison and Grunthal (1967) | Assebroek | 51.18793 | 3.27363 |
| Assen | 800-911 | Morrison and Grunthal (1967) | Assen | 52.99421 | 6.55957 |
| Auxerre | 813-877 | Haertle (1997) | Auxerre | 47.796587 | 3.570535 |
| Auzeville | 814-848 | Sarah et al. (2016) | Auzeville | 43.5257 | 1.49342 |
| Avallon | 843-877 | Coupland (2020) | Avallon | 47.488712 | 3.907758 |
| Avignon | 843-887 | Morrison and Grunthal (1967) | Avignon | 43.95344 | 4.80601 |
| Bakonyszombathely | 898-973 | Morrison and Grunthal (1967) | Bakonyszombathely | 47.47208 | 17.96018 |
| Balloo | 843-855 | Haertle (1997) | Balloo | 54.472363 | -5.69076 |
| Barbentane | 814-840 | Morrison and Grunthal (1967) | Barbentane | 43.89948 | 4.74635 |
| Barcelona | 814-840 | Doménech-Belda et al. (2013) | Barcelona | 41.395937 | 2.174552 |
| Bassenheim | 814-876 | Coupland (2019) | bassenheim | 50.359028 | 7.462443 |
| Bátorove Kosihy | 888-950 | Kovács (1989) | Bátorove Kosihy | 47.83083 | 18.41083 |
| Beaumont | 843-877 | Morrison and Grunthal (1967) | Beaumont (Chalo Saint Mars) | 48.409016 | 2.042742 |
| Bel-Air | 768-814 | Morrison and Grunthal (1967) | Lausanne | 46.57957 | 6.605807 |
| Bellpuig | 887-928 | Doménech-Belda et al. (2013) | Bellpuig | 41.626531 | 1.011607 |
| Belvézet | 768-840 | Morrison and Grunthal (1967) | Belvézet | 44.08433 | 4.36426 |
| Bikbergen | 814-855 | Cruysheer and der Veen (2015) | Bikbergen | 52.287933 | 5.196186 |
| Bjerndrup | 817-924 | Coupland (2020) | Bjerndrup | 54.93391 | 9.32867 |
| Blendecques | 814-840 | Coupland (2020) | Blendecques | 50.716982 | 2.282169 |
| Bligny | 814-887 | Morrison and Grunthal (1967) | Bligny | 48.1725 | 4.6172 |
| Blois | 898-940 | Moesgaard (1997) | Blois | 47.58696 | 1.33139 |
| Bondeno | 768-814 | Morrison and Grunthal (1967) | Bondeno | 44.89098 | 11.41096 |
| Bonnevaux | 800-887 | Morrison and Grunthal (1967) | Bonnevaux | 44.367837 | 4.030289 |
| Borne | 794-813 | Coupland (2011a) | Borne | 52.30137 | 6.75779 |
| Bourges | 840-877 | Morrison and Grunthal (1967) | Bourges | 47.08585 | 2.39293 |
| Bourges | 800-887 | Coupland (2020) | Bourges | 47.08585 | 2.39293 |
| Bourgneuf | 814-888 | Morrison and Grunthal (1967) | Bourgneuf | 46.167624 | -1.022216 |
| Bourgneuf-en-Retz | 843-877 | Coupland (2010) | Bourgneuf-en-Retz | 47.04229 | -1.9543 |
| Bray-sur-Seine | 840-877 | Vandenbossche and Coupland (2012) | Bray-sur-Seine | 48.41451 | 3.24057 |
| Bressuire | 814-840 | Coupland (1995) | Bressuire | 46.84008 | -0.49253 |
| Breuvery-sur-Coole | 768-813 | Dhénin (1989) | Breuvery-sur-Coole | 48.86311 | 4.31164 |
| Brion | 814-840 | Denais (1908) | Brion | 47.4425 | -0.1553 |
| Brioux-sur-Boutonne | 814-840 | Morrison and Grunthal (1967) | Brioux-sur-Boutonne | 46.14349 | -0.21823 |
| Bruère-Allichamps | 814-954 | Morrison and Grunthal (1967) | Bruère-Allichamps | 46.7695 | 2.4325 |
| Burgum | 843-877 | Haertle (1997) | Burgum | 53.19527 | 5.98694 |
| Caden | 843-877 | Coupland (2020) | Caden | 47.630822 | -2.287131 |
| Caen | 936-954 | Coupland (2020) | Caen | 49.183512 | -0.363489 |
| Calatrava la vieja | | Parvérie (2018) | Calatrava la Vieja | 39.074099 | -3.833274 |
| Campeaux | 813-877 | Haertle (1997) | Campeaux | 48.952844 | -0.93197 |
| Carcassonne | 768-814 | Coupland (2014) | Carcassonne | 43.206463 | 2.363268 |
| Castelsarasin | 888-898 | Morrison and Grunthal (1967) and Lafaurie (1965) | Castelsarasin | 44.039071 | 1.106969 |
| Catalonia | 768-905 | Balaguer (1999) and Doménech-Belda et al. (2013) | Calalonia | | |
| Cauroir | 843-882 | Coupland (2011a) | Cauroir | 50.17283 | 3.30174 |
| Cerdanyola | 814-840 | Doménech-Belda et al. (2013) | Cerdanyola | 41.49201 | 2.137338 |
| Cerveník | 826-950 | | Cerveník | 48.45 | 17.75 |

Appendix Table A.10: Carolingian Hoards, Part I

| Hoard Name | Date | Reference | Location | Latitude | Longitude |
|---|---|---|---|---|---|
| Chaley | 936-954 | Morrison and Grunthal (1967) | Chaley | 45.9552 | 5.53122 |
| Chalo-Saint-Mars | 840-877 | Morrison and Grunthal (1967) | Chalo-Saint-Mars | 48.4267 | 2.067 |
| Chalon-sur–Saône I | 800-887 | Morrison and Grunthal (1967) | Chalon-sur-Saône | 46.782132 | 4.858459 |
| Chalon-sur-Saone II | 800-887 | Haertle (1997) | Chalon-sur-Saône | 46.782132 | 4.858459 |
| Charente-Maritime | 888-898 | Coupland (2011a) | Charente-Maritime | | |
| Chartes | 923-977 | Duplessy (1985) | Chartres | 48.446659 | 1.488596 |
| Chartres II | 751-768 | Morrison and Grunthal (1967) | Chartres | 48.446659 | 1.488596 |
| Château Roussillon | 793-877 | Haertle (1997) | Château Roussillon | 42.710278 | 2.946667 |
| Chateauneuf sur Cher | 843-954 | Morrison and Grunthal (1967) | Chateauneuf sur Cher | 46.857333 | 2.320522 |
| Chaumoux-Marcilly | 814-877 | Morrison and Grunthal (1967) | Chaumoux-Marcilly | 47.12628 | 2.77884 |
| Chauvigny | 843-877 | Société des antiquaires de l'Ouest (1982) | Chauvigny | 46.56974 | 0.64345 |
| Chef-Boutonne | 800-922 | Haertle (1997) and Rondier (1869) | Chef-Boutonne | 46.10934 | -0.06806 |
| Chester | 888-924 | Webster et al. (1953) | Chester | 53.1903 | -2.89437 |
| Chézy-sur-Marne | 768-814 | Duplessy (1985) | Chézy-sur-Marne | 48.989611 | 3.366294 |
| Choisy-au-Bac | 888-898 | Haertle (1997) | Choisy-au-Bac | 49.44777 | 2.88097 |
| Ciney Dinant | 898-922 | Coupland (2020) | Ciney | 50.286773 | 5.098966 |
| Clermont Ferrand | 843-918 | Coupland (2020) | Clermont-Ferrand | 45.778063 | 3.083696 |
| Compiègne I | 877-882 | | Compiègne | 49.41762 | 2.82513 |
| Compiègne II | 843-882 | Morrison and Grunthal (1967) | Compiègne | 49.41762 | 2.82513 |
| Corrèze | 843-877 | Coupland (2014) | Corrèze | | |
| Cosne d'Allier | 814-840 | Coupland (2014) | Cosne d'Allier | 46.474799 | 2.830127 |
| Cosne-Cours-sur-Loire II | 814-877 | Morrison and Grunthal (1967) | Cosne-Cours-sur-Loire | 47.40983 | 2.92425 |
| Cosne-Cours-sur-Loire III | 877-840 | Haertle (1997) | Cosne-Cours-sur-Loire | 47.40983 | 2.92425 |
| Croydon | 814-877 | Morrison and Grunthal (1967) | Croydon | 51.379287 | -0.09975 |
| Csorna | 888-947 | Kovács (1989) | Csorna | 47.6167 | 17.25 |
| Cuerdale | 843-922 | Morrison and Grunthal (1967) | Cuerdale | 53.7553 | -2.638 |
| Dalen | 843-976 | Morrison and Grunthal (1967) | Dalen | 52.69847 | 6.75641 |
| Dauphiné | 814-848 | Coupland (2014) | Dauphiné | | |
| Deux-Sèvres | 814-877 | Société de statistique, sciences, lettres et arts du département des Deux-Sèvres (1882) | Deux-Sèvres | | |
| Dijon | 770-780 | Bompaire and Depierre (1989) | Dijon | 47.3268 | 5.04619 |
| Dommartin-Lettrée | 923-936 | Duplessy (1985) | Dommartin-Lettrée | 48.7669 | 4.29933 |
| Dordives | 750-950 | Coupland (2014) | Dordives | 48.144081 | 2.766333 |
| Dorestad | 768-877 | Morrison and Grunthal (1967) | Dorestadt | 51.97212 | 5.344769 |
| Drantum | 814-840 | Haertle (1997) | Drantum | 52.81942 | 8.19537 |
| Eichstetten | 911-922 | Morrison and Grunthal (1967) | Eichstetten | 48.094296 | 7.745429 |
| Ejstrup | 814-840 | Coupland (2020) | Ejstrup | 55.503525 | 9.377413 |
| Ekeren | 819-877 | Haertle (1997) | Ekeren | 51.276405 | 4.417467 |
| Ellikon an der Thur | 887-915 | Zäch (2001) | Ellikon an der Thur | 47.56253 | 8.82386 |
| Emmen | 814-877 | Morrison and Grunthal (1967) | Emmen | 52.49784 | 6.23039 |
| Entrammes | 814-877 | Coupland (2014) | Entrammes | 47.999133 | -0.716154 |
| Espana 1-4 | 800-1009 | Parvérie (2018) | Calatayud | 41.352868 | -1.641101 |
| Etampes | 843-882 | Morrison and Grunthal (1967) | Etampes | 48.434768 | 2.162027 |
| Etréchy | 832-877 | Morrison and Grunthal (1967) | Etrechy | 48.88411 | 3.94374 |
| Evreux | 840-954 | Duplessy (1985) and Moesgaard (2003) | Evreux | 49.02754 | 1.15028 |
| Extremadura | | Parvérie (2018) | Extremadura | | |
| Eyguières | 814-840 | Coupland (2020) | Eyguières | 43.696133 | 5.030134 |
| Fécamp | 900-999 | Duplessy (1985) | Fécamp | 49.75765 | 0.37632 |
| Flacey | 814-840 | Coupland (2020) | Flacey | 48.147247 | 1.349598 |
| Flanders | 814-877 | Coupland (2020) | Flanders | | |
| Florange | | Duplessy (1985) and Simmer (2000) | Florange | 49.32743 | 6.12273 |
| Foissy-lès-Vézelay | 864-877 | | Foissy-lès-Vézelay | 47.43637 | 3.76447 |
| Fontaines | 814-877 | Duplessy (1985) | Fontaines | 46.85083 | 4.773055 |
| Frankfurt | 814-840 | Morrison and Grunthal (1967) | Frankfurt am Main | 50.11208 | 8.68341 |
| Freiburg im Breisgau | 898-922 | Morrison and Grunthal (1967) | Freiburg im Breisgau | 47.99853 | 7.84965 |
| Fresnes | | Duplessy (1985) | Fresnes | 48.75043 | 2.322063 |
| Fridolfing | 768-814 | Coupland (2020) | Fridolfing | 47.998573 | 12.826917 |
| Frisia | 814-855 | Morrison and Grunthal (1967) | Grou | 53.11035 | 5.848604 |
| Gannat | 800-887 | Morrison and Grunthal (1967) | | 46.10192 | 3.19692 |
| Gelderland | 768-814 | Morrison and Grunthal (1967) | Gelderland | | |
| Giekau | 814-911 | Wiechmann (2004) | Giekau | 54.31793 | 10.50529 |
| Glisy | 800-922 | Morrison and Grunthal (1967) | Glisy | 49.8756 | 2.39788 |
| Gnadendorf | 898-905 | Daim and Lauermann (2006) | Gnadendorf | 48.61549 | 16.39885 |
| Goutum | 814-877 | Coupland (2020) | Goutum | 53.178037 | 5.806018 |
| Grisebjerggård | 898-922 | | Slagelse | 55.3028 | 11.2647 |
| Groningen | 814-877 | Morrison and Grunthal (1967) | Groningen | 53.25713 | 6.93525 |
| Guardamiglio | 843-884 | Coupland (2011a) | Guardamiglio | 45.11055 | 9.68215 |

Appendix Table A.11: Carolingian Hoards, Part II

| Hoard Name | Date | Reference | Location | Latitude | Longitude |
|---|---|---|---|---|---|
| Györ I | 888-950 | Kovács (1989) | Györ | 47.69739 | 17.6527 |
| Györ II | 888-951 | Kovács (1989) | Györ | 47.69739 | 17.6527 |
| Halimba | 902-947 | Kovács (1989) | Halimba | 47.03345 | 17.53546 |
| Häljarp | 814-840 | Morrison and Grunthal (1967) | | 55.85578 | 12.910919 |
| Harkirke | 843-905 | Morrison and Grunthal (1967) | Crosby | 53.48919 | -3.048081 |
| Harlingen | 840-855 | Haertle (1997) | Harlingen | 53.1735 | 5.4246 |
| Haute Isle | 814-922 | Morrison and Grunthal (1967) | Haute Isle | 49.083426 | 1.65697 |
| Haza de Carmen | 888-954 | Coupland (2020) | Cordoba | 37.881495 | -4.776125 |
| Hermenches | 822-840 | Morrison and Grunthal (1967) | Hermenches | 46.640456 | 6.757567 |
| Hoen | 814-855 | Morrison and Grunthal (1967) | Hoen | 60.2204 | 10.25852 |
| Hole | 796-840 | Coupland (2020) | Hole | 58.897156 | 6.018229 |
| Holy Family | 800-887 | Parvérie (2018) and Morrison and Grunthal (1967) | Cordoba | 37.888028 | -4.7734 |
| Hradec Hilfort | 768-814 | Coupland (2020) | Hradec-Kralove | 50.209703 | 15.832231 |
| Huriel | 800-887 | Morrison and Grunthal (1967) | Le Moulin-Gargot (Huriel) | 46.37468 | 2.47842 |
| Ibaneta | 800-888 | Doménech-Belda et al. (2013) | Puerto d'Ibaneta | 43.020083 | -1.324207 |
| Ibersheim | 768-814 | Morrison and Grunthal (1967) | Ibersheim | 49.72085 | 8.40065 |
| Ilanz I | 843-905 | Morrison and Grunthal (1967) | Ilanz | 46.77451 | 9.20463 |
| Ilanz II | 664-814 | Bernareggi (1977, 1983), Völckers (1965), McCormick (2001) | Ilanz | 46.77451 | 9.20463 |
| Île Agois | 864-877 | Johnston (1986) | Île Agois | 49.24935 | -2.18641 |
| Île-de-France | 888-936 | Dhénin (2006) | Ile de France | | |
| Imbleville | 864-877 | Haertle (1997) | Imbleville | 49.71539 | 0.95198 |
| Imphy | 751-814 | Morrison and Grunthal (1967) | Imphy | 46.934537 | 3.259903 |
| Indre | 814-865 | Morrison and Grunthal (1967) | Indre | | |
| Indre II | 814-848 | Coupland (2014) | Indre | | |
| Indre-et-Loire | 814-877 | Coupland (2011a) | Indre-et-Loire | | |
| Indre-et-Loire II | 888-910 | Coupland (2011a) | Indre-et-Loire | | |
| Indre-et-Loire III | 888-898 | Coupland (2020) | Indre-et-Loire | | |
| Isle-Aumont I | 814-840 | Haertle (1997) | Isle-Aumont | 48.21131 | 4.12459 |
| Isle-Aumont II | 864-898 | Haertle (1997) | Isle-Aumont | 48.21131 | 4.12459 |
| Issy l'Evêque | 843-922 | Morrison and Grunthal (1967) | Issy l'Evêque | 46.70818 | 3.9734 |
| Jedomelice | 814-840 | Coupland (2020) | Jedomelice | 50.23411 | 13.971234 |
| Jelsum | 768-814 | Morrison and Grunthal (1967) | Jelsum | 53.23455 | 5.783862 |
| Juaye-Mondaye | 800-922 | Morrison and Grunthal (1967) | Juaye-Mondaye | 49.20803 | -0.68508 |
| Jura | 768-814 | Morrison and Grunthal (1967) | Jura | | |
| Karden | 814-822 | Morrison and Grunthal (1967) | Karden | 50.179051 | 7.299583 |
| Karos-Eperjesszög I | 888-915 | Révész (1996) | Karos | 48.32959 | 21.73712 |
| Karos-Eperjesszög II | 900-911 | Gedai (1993) | Karos | 48.32959 | 21.73712 |
| Kättilstorp | 814-877 | Morrison and Grunthal (1967) | Kättilstorp | 58.041694 | 13.711198 |
| Katwijk I | 800-922 | Kluge (1993) | Katwijk | 52.195273 | 4.421091 |
| Katwijk II | 794-800 | Van der Velde (2008) | Katwijk | 52.195273 | 4.421091 |
| Kecel | 888-924 | Huszár (1955) | Kecel | 46.52644 | 19.24647 |
| Kenézlő | 826-950 | Huszár (1955) | Kenézlő | 48.2 | 21.53333 |
| Kimswerd-Pingjum I | 814-877 | Morrison and Grunthal (1967) | Kimswerd | 53.1289 | 5.4387 |
| Kimswerd-Pingjum II | 814-878 | Morrison and Grunthal (1967) | Kimswerd | 53.1289 | 5.4387 |
| Kiskundorozsma-Hosszúhát | 826-950 | Múzeum Móra Ferenc (2002) | Szeged | 46.275 | 20.06278 |
| Kiskunfélegyháza | 881-918 | Kovács (1989) | Kiskunfelegyhaza | 46.71246 | 19.85279 |
| Koblenz | 823-830 | Reinhold Fischer Auktionshaus (2010) | Koblenz | 50.359618 | 7.59383 |
| Krinkberg | 768-814 | Morrison and Grunthal (1967) | Pöschendorf | 54.03055 | 9.472156 |
| La Cornouaille | 814-877 | Coupland (2020) | La Cornouaille | 47.578279 | -0.797543 |
| La Couvertoirade | 881-898 | Coupland (2011a) | La Couvertoirade | 43.91127 | 3.31355 |
| La Roche en Ardenne | 750-950 | Coupland (2014) | La-Roche-en-Ardenne | 50.183528 | 5.575243 |
| La Tessoualle | 814-877 | Haertle (1997) | La Tessoualle | 47.00535 | -0.8494 |
| La Tour-de-Peilz | 755-768 | Geiser (1990) | La-Tour-de-Peilz | 46.45302 | 6.85686 |
| Ladánybene | 888-922 | Huszár (1955) | Ladánybene | 47.03333 | 19.45 |
| Lamairé | 843-877 | Baigl et al. (1995) | Lamairé | 46.75707 | -0.1263 |
| Lamotte Beuvron | 814-877 | Coupland (2020) | Lamotte-Beuvron | 47.602363 | 2.025245 |
| Langon | 814-877 | Morrison and Grunthal (1967) | Langon | 44.55389 | -0.24833 |
| Langres I | 843-922 | Morrison and Grunthal (1967) | Langres | 47.85816 | 5.33113 |
| Langres II | 864-884 | Coupland (2011a) | Langres | 47.85816 | 5.33113 |
| Larino | 768-840 | De Benedittis and Lafaurie (1998) | Larino | 41.7968 | 14.9128 |
| Lauterach | 840-924 | Zäch and Tabernero (2002) | Lauterach | 47.4745 | 9.730031 |
| Lauzès | 814-877 | Morrison and Grunthal (1967) | Lauzès | 47.4707 | -0.55324 |
| Lavelanet | 888-898 | Coupland (2020) | Lavelanet | 42.932652 | 1.848583 |
| Laxfield | 843-877 | Morrison and Grunthal (1967) | Laxfield | 52.30114 | 1.36237 |
| Leiderdorp | 768-840 | Coupland (2020) | Leiderdorp | 52.151653 | 4.529015 |

Appendix Table A.12: Carolingian Hoards, Part III

| Hoard Name | Date | Reference | Location | Latitude | Longitude |
|---|---|---|---|---|---|
| Lésigny-sur-Creuse | 814-898 | Jeanne-Rose (1996) | Lésigny-sur-Creuse | 46.84996 | 0.76421 |
| Levice-Géňa | 926-950 | Minarovicova (2007) | Levice-Géňa | 48.21639 | 18.60806 |
| Lillebonne | 814-877 | Coupland and Moesgaard (2012) | Lillebonne | 49.51802 | 0.53681 |
| Limoux | 849-877 | Haertle (1997) | Limoux | 43.053658 | 2.217421 |
| Lisówek | 848-922 | Morrison and Grunthal (1967) | Lisówek | 51.9 | 20.9333 |
| Llanbedrgoch | 814-878 | Coupland (2020) | Llanbedrgoch | 53.300117 | -4.236622 |
| Llerida | 887-928 | Doménech-Belda et al. (2013) | Lleida | 41.61879 | 0.621737 |
| Loire River Bank | 814-840 | Coupland (2014) | Loire River | | |
| Loiret | 843-1027 | Duplessy (1985) | Loiret | | |
| Lokeren | 843-864 | Haertle (1997) | Lokeren | 51.10473 | 3.9865 |
| Longjumeau | 843-884 | Moesgaard (2010) | Longjumeau | 48.69173 | 2.29005 |
| Loppersum | 814-877 | Morrison and Grunthal (1967) | Loppersum | 53.33276 | 6.74398 |
| Lucca | 947-961 | Saccocci et al. (2004) | Lucca | 43.84201 | 10.51534 |
| Lussac-les-Châteaux | 845-848 | Haertle (1997) | Lussac-les-Châteaux | 46.403093 | 0.723563 |
| Lutkesaaxum | 843-864 | Haertle (1997) | Lutkesaaxum | 53.364638 | 6.489072 |
| Luzancy | 814-877 | Sombart (2008) | Luzancy | 48.97205 | 3.1865 |
| Lyon | 751-771 | Coupland (2020) | Lyon | 45.758973 | 4.830895 |
| Maine et Loire | 751-878 | Coupland (2014) | Maine-et-Loire | | |
| Marçay | 840-898 | Morrison and Grunthal (1967) | Marçay | 47.10002 | 0.21706 |
| Marssum | 814-855 | Coupland (2011a) | Marssum | 53.21056 | 5.73008 |
| Marsum | 814-887 | Morrison and Grunthal (1967) | Marsum | 53.339476 | 5.73008 |
| Matha | 778-877 | Coupland (2014) | Matha | 45.867625 | -0.321187 |
| Melle I | 875-877 | Haertle (1997) | Melle | 46.221471 | -0.147358 |
| Melle II | 843-877 | Haertle (1997) | Melle | 46.221471 | -0.147358 |
| Melle IV | 823-825 | Coupland (2018) | Melle | 46.221471 | -0.147358 |
| Mercurey | 822-877 | Duplessy (1985) and Haertle (1997) | Mercurey | 46.833364 | 4.722119 |
| Méréville | 814-877 | Morrison and Grunthal (1967) | Méréville-Saint-Pierre | 48.59069 | 6.15058 |
| Metz | 843-877 | Morrison and Grunthal (1967) | Metz | 49.11566 | 6.1732 |
| Meurthe et Moselle | 898-922 | Coupland (2014) | Meurthe-et-Moselle | | |
| Midlaren | 814-877 | Morrison and Grunthal (1967), Haertle (1997) | Midlaren | 53.1111 | 6.67616 |
| Midlum | 900-961 | Morrison and Grunthal (1967) | Midlum | 53.18204 | 5.44716 |
| Mikulčice | 887-900 | Slovenská akadémia vied. Archeologickỳ ústav (1979) | Mikulčice | 48.81667 | 17.05 |
| Molliens-Vidame | 817-877 | Haertle (1997) | Molliens-Dreuil | 49.8839 | 2.02 |
| Monchy-au-Bois | 840-922 | Morrison and Grunthal (1967) | Monchy-au-Bois | 50.17999505 | 2.656698281 |
| Montmain | 768-814 | Coupland (2020) | Montmain | 49.410716 | 1.252625 |
| Montrieux-en-Sologne II | 800-922 | Morrison and Grunthal (1967) | Montrieux-en-Sologne | 47.55408 | 1.72638 |
| Montrieux-en-Sologne III | 864-898 | Morrison and Grunthal (1967) | Montrieux-en-Sologne | 47.55408 | 1.72638 |
| Moreria | | Parvérie (2018) | Moreria | 38.916776 | -6.349645 |
| Mourlieu | 900-925 | Caron (1882) | Mourlieu | 46.564931 | 0.512703 |
| Muizen | 822-877 | Morrison and Grunthal (1967) | Muizen | 51.01056 | 4.514722 |
| Mullaghboden | 814-877 | Morrison and Grunthal (1967) | Mullaghboy | 54.83536 | -5.72671 |
| Muret | 814-840 | Coupland (2020) | Muret | 43.460924 | 1.327252 |
| Nagyszokoly | 926-947 | Kovács (1989) | Nagyszokoly | 46.72132 | 18.21182 |
| Nagyvázsony | 902-947 | Kovács (1989) | Nagyvázsony | 46.9835 | 17.69408 |
| Neufchateau I | 800-922 | Coupland (2014) | Neufchateau | 48.356071 | 5.692627 |
| Neufchateau II | 814-848 | Coupland (2014) | Neufchateau | 48.356071 | 5.692627 |
| Neuvy-au-Houlme | 814-877 | Morrison and Grunthal (1967), Duplessy (1985) | Neuvy-au-Houlme | 48.8181 | -0.19966 |
| Niederlahnstein | 855-869 | Coupland (2020) | Niederlahnstein | 50.315193 | 7.598382 |
| Nourray | 843-877 | Morrison and Grunthal (1967) | Nourray | 47.71903 | 1.06023 |
| Nr.Trier | 768-855 | Coupland (2014) and Morrison and Grunthal (1967) | Trier | 49.755513 | 6.640075 |
| Odoorn | 843-961 | Morrison and Grunthal (1967) | Odoorn | 52.85033 | 6.847823 |
| Orléans | 814-864 | Haertle (1997) | Orléans | 47.90143 | 1.90496 |
| Oudwoude | 814-877 | Morrison and Grunthal (1967) | Oudwoude | 53.27968 | 6.11413 |
| Palma de Majorque | 800-888 | Doménech-Belda et al. (2013) | Palma de Majorque | 39.570589 | 2.648991 |
| Paule | 843-877 | Coupland (2014) | Paule | 48.235953 | -3.444348 |
| Pilligerheck | 814-877 | Petry and Wittenbrink (2021), Coupland (2011b) | Muenstermaifeld | 50.20461 | 7.31152 |
| Pingjum | 900-911 | Morrison and Grunthal (1967) | Pingjum | 53.11519 | 5.44004 |
| Place Unknown | 954-986 | Morrison and Grunthal (1967) | | | |
| Plessé | 875-877 | Haertle (1997) | Plessé | 47.54109 | -1.88812 |
| Poitou Charentes | 814-877 | Coupland (2020) | Poitou-Charente | | |
| Pommern | 887-924 | Coupland (2020) | Pommern | 50.169368 | 7.269726 |
| Pont Saint-Pierre | 864-877 | Coupland (2011a) | Pont-Saint-Pierre | 49.33388 | 1.2745 |
| Postsaal | 814-1024 | Coupland (2020) | Bavière | | |
| Pouzauges | 875-898 | Haertle (1997) | Pouzauges | 46.7822 | -0.8361 |

Appendix Table A.13: Carolingian Hoards, Part IV

| Hoard Name | Date | Reference | Location | Latitude | Longitude |
|---|---|---|---|---|---|
| Questembert | 814-877 | Haertle (1997) | Questembert | 47.66097 | -2.4521 |
| Raalte | 814-877 | Coupland (2011a) | Raalte | 52.38724 | 6.27462 |
| Regensburg | 843-877 | Haertle (1997) | Regensburg | 49.016213 | 12.097468 |
| Rennes | 843-922 | Morrison and Grunthal (1967) | Rennes | 48.10761 | -1.68448 |
| Rijs | 814-877 | Morrison and Grunthal (1967) | Rijs | 52.86298 | 5.49838 |
| Rijswijk | 814-840 | Coupland (2020) | Rijswijk | 52.039942 | 4.325633 |
| Rochefort | 900-911 | Coupland (2020) | Rochefort | 45.935077 | -0.962458 |
| Roches l'Evêque | 814-922 | Morrison and Grunthal (1967) | Roches l'Evêque | 47.7772 | 0.8922 |
| Roermond | 222-877 | Haertle (1997), Coupland (2011b), Zuyderwyk and Besteman (2010) | Roermond | 51.193179 | 5.98624 |
| Rome I (Forum) | 887-950 | Metcalf (1992) | Rome | 41.90509 | 12.46194 |
| Rome II (Vatican) | 898-922 | Morrison and Grunthal (1967) | Rome | 41.90509 | 12.46194 |
| Rosas | 814-840 | Doménech-Belda et al. (2013) | Rosas | 42.265002 | 3.178593 |
| Roswinkel | 768-882 | Morrison and Grunthal (1967) | Roswinkel | 52.83787 | 7.03843 |
| Rotterdam | 814-840 | Coupland (2020) | Rotterdam | 51.919909 | 4.47544 |
| Saint Bris le Vineux | 814-877 | Coupland (2020) | Saint-Bris-le-Vineux | 47.74291 | 3.651349 |
| Saint Ponc | 884-887 | Doménech-Belda et al. (2013) | Saint-Ponç | 41.963245 | 1.603627 |
| Saint Yrieix la Perche | 888-898 | Coupland (2020) | Saint-Yrieix-la-Perche | 45.51359 | 1.203618 |
| Saint-Brieuc | 864-875 | Haertle (1997) | Saint-Brieuc | 48.5136 | -2.7653 |
| Saint-Calais | 768-877 | Paty (1848) | Saint-Calais | 47.9211 | 0.7439 |
| Saint-Cyr-en-Talmondais | 814-877 | Morrison and Grunthal (1967) | Saint-Cyr-en-Talmondais | 46.4614 | -1.3356 |
| Saint-Denis | 793-875 | Haertle (1997) | Saint-Denis | 48.9364 | 2.3547 |
| Saint-Martin-sur-le-Pré | | Coupland (2014) | Saint-Martin-sur-le-Pré | 48.9778 | 4.3394 |
| Saint-Même-le-Tenu | 814-877 | Coupland (2014) | Saint-Même-le-Tenu | 47.020808 | -1.794104 |
| Saint-Michel-de-Chavaignes | | Haertle (1997) | Saint-Michel-de-Chavaignes | 48.018584 | 0.570918 |
| Saint-Pierre-de-Maillé | 814-840 | Benoit and Braunstein (1983) | Saint-Pierre-de-Maillé | 46.6797 | 0.8444 |
| Saint-Pierre-des-Fleurs I | 823-877 | Coupland and Moesgaard (2012) | Saint-Pierre-des-Fleurs | 49.2514 | 0.9667 |
| Saint-Pierre-des-Fleurs II | 888-898 | Cardon et al. (2008) | Saint-Pierre-des-Fleurs | 49.2514 | 0.9667 |
| Saint-Seine-l'Abbaye | | Coupland (2014) | Saint-Seine-l'Abbaye | 47.440003 | 4.788637 |
| Santa Elena | 961-966 | Doménech-Belda et al. (2013) | Irun | 43.337137 | -1.786251 |
| Santiago de Compostela | 800-888 | Doménech-Belda et al. (2013) | Santiago de Compostela | 42.880265 | -8.543118 |
| Sarlat | 814-877 | Coupland (2020) | Sarlat-la-Canéda | 44.889865 | 1.216381 |
| Sarzana | 768-814 | Morrison and Grunthal (1967) | Sarzana | 44.11186 | 9.95886 |
| Saumeray | 843-877 | Morrison and Grunthal (1967) | Saumeray | 48.25027 | 1.32157 |
| Saumur-Thouars | 843-898 | Morrison and Grunthal (1967) | Saumur | 47.1218 | -0.1704 |
| Saverne | | Duplessy (1985) | Saverne | 48.73947 | 7.36602 |
| Savigné-sous-le-Lude | 843-898 | Morrison and Grunthal (1967) | Savigné-sous-le-Lude | 47.61845 | 0.05801 |
| Savigny en Véron | 814-877 | Coupland (2020) | Savigny-en-Véron | 47.205554 | 0.147106 |
| Seiches sur le Loir | 751-814 | Coupland (2014) | Seiches-sur-le-Loir | 47.578315 | 0.362977 |
| Séranon | 814-840 | Coupland (2020) | Séranon | 43.772823 | 6.704362 |
| Sevilla region | 888-898 | Parvérie (2018) | Sevilla | 37.393305 | -5.993535 |
| 's-Hertogenbosch | 814-840 | Coupland (2014) | 's-Hertogenbosch | 51.698578 | 5.303773 |
| Sigean | 768-814 | Coupland (2020) | Sigean | 43.0287 | 2.978539 |
| Silverdale | 800-898 | Coupland (2014) | Silverdale | 54.167322 | -2.82505 |
| Minor Finds | 751-1027 | Morrison and Grunthal (1967) | | | |
| Søndre Bø | 814-883 | Morrison and Grunthal (1967) | Søndre Bø | 58.11019 | 6.88224 |
| Strasbourg-Basel | 843-954 | Morrison and Grunthal (1967) | Strasbourg/Basel | 48.171 | 7.6473 |
| Szabadbattyán | 826-950 | Huszár (1955) | Szabadbattyán | 47.11798 | 18.3629 |
| Szabadegyháza | 888-924 | Kovács (1989) | Szabadegyháza | 47.07845 | 18.69228 |
| Szedeg-othalom | 902-924 | Coupland (2014) | Szeged | 46.265179 | 20.140614 |
| Szekszárd | 902-947 | Huszár (1955) | Szekszárd | 46.34779 | 18.70626 |
| Tarrega | 887-928 | Doménech-Belda et al. (2013) | Tarrega | 41.648564 | 1.140707 |
| Taizy | 864-877 | Coupland (2020) | Taizy | 49.51967 | 4.25832 |
| Teloché | 864-877 | Hucher (1845) | Teloché | 47.88987 | 0.26731 |
| Ter Apel | 900-911 | Morrison and Grunthal (1967) | Ter Apel | 52.878359 | 7.063981 |
| Ter Heijde | 814-840 | Coupland (2020) | Ter Heijde | 52.02903 | 4.164265 |
| Terslev | 814-966 | Morrison and Grunthal (1967) | Terslev | 55.37476 | 11.9693 |
| Thoiry | 875-894 | Haertle (1997) | Thoiry | 48.86519 | 1.79463 |
| Thouars | 822-855 | Morrison and Grunthal (1967) | Thouars | 46.977604 | -0.21579 |
| Tiel | 898-922 | Coupland (2011a) | Tiel | 51.88809 | 5.43069 |
| Tiszaeszlàr I | 814-950 | Kovács (1989) | Tiszaeszlàr | 48.05 | 21.46667 |
| Tiszaeszlàr II | 926-950 | Kovács (1989) | Tiszaeszlàr | 48.05 | 21.46667 |
| Tiszanána | 888-946 | Kovács (1989) | Tiszanána | 47.56111 | 20.52382 |

Appendix Table A.14: Carolingian Hoards, Part V

| Hoard Name | Date | Reference | Location | Latitude | Longitude |
|---|---|---|---|---|---|
| Troyes | 814-840 | Coupland (2014) | Troyes | 48.299055 | 4.077872 |
| Troyes II | 843-877 | Coupland (2020) | Troyes | 48.58345 | 3.81356 |
| Tuscany | 888-973 | Ciampoltrini et al. (2001) | Tuscany | | |
| Tytsjerksteradiel | 814-855 | Coupland (2020) | Burgum | 53.195748 | 5.987155 |
| Tzummarum I | 819-855 | Haertle (1997) | Tzummarum | 53.238297 | 5.549116 |
| Tzummarum II | 855-865 | Coupland (2020) | Tzummarum | 53.238297 | 5.549116 |
| Unknown | 954-986 | Morrison and Grunthal (1967) | France | | |
| Vale of York | 898-922 | Williams and Ager (2010) | Vale of York | 54.20361 | -1.36398 |
| Valence | 819-840 | Haertle (1997) | Valence | 44.93347 | 4.890808 |
| Vallée de la Risle | 814-877 | Coupland and Moesgaard (2012) | Vale of Risle | 49.424 | 0.725 |
| Vercelli | 768-814 | Morrison and Grunthal (1967) | Vercelli | 45.32255 | 8.41844 |
| Verdun I | 875-877 | Haertle (1997) | Verdun | 49.15952 | 5.382316 |
| Verdun II | 881-887 | Morrison and Grunthal (1967) | Verdun | 49.15952 | 5.382316 |
| Vereb | 858-024 | Morrison and Grunthal (1967) | Vereb | 47.31867 | 18.61802 |
| Vernon | 814-877 | Coupland (2020) | Vernon | 49.091052 | 1.483426 |
| Vicq sur Gartempe | 814-877 | Coupland (2020) | Vicq sur Gartempe | 46.721302 | 0.862012 |
| Vire | 843-877 | Morrison and Grunthal (1967) | Vire-Normandie | 48.83919 | -0.89 |
| Vrigny | 843-877 | Haertle (1997) | Vrigny | 48.08167 | 2.243889 |
| Wagenborgen | 814-877 | Haertle (1997) | Wagenborgen | 53.25713 | 6.93525 |
| Westerklief I | 814-877 | Sarfatij et al. (1999) | Westerklief | 52.89494 | 4.93322 |
| Westerklief II | 814-877 | Besteman (2006) | Westerklief | 52.89494 | 4.93322 |
| Wiesbaden-Biebrich | 717-814 | Morrison and Grunthal (1967) | Wiesbaden-Biebrich | 50.050115 | 8.237668 |
| Wijk bij Duurstede I | 793-822 | Morrison and Grunthal (1967) | Wijk-Bij-Duurstede | 51.971869 | 5.344562 |
| Wijk bij Duurstede II | 752-768 | Van Es and Verwers (1980) | Wijk-Bij-Duurstede | 51.971869 | 5.344562 |
| Wijk bij Duurstede III | 768-820 | Van Es and Verwers (1980) | Wijk-Bij-Duurstede | 51.971869 | 5.344562 |
| Wijk bij Duurstede IV | 823-840 | Dijkstra (2005) | Wijk-Bij-Duurstede | 51.971869 | 5.344562 |
| Wijk bij Duurstede V | 751-768 | Coupland (2020) | Wijk-Bij-Duurstede | 51.971869 | 5.344562 |
| Wirdum | 814-877 | Coupland (2020) | Wirdum | 53.149585 | 5.803308 |
| Worms | 814-840 | Coupland (2020) | Worms | 49.632241 | 8.36221 |
| Yde | 814-877 | Morrison and Grunthal (1967) | Yde | 53.11143 | 6.58365 |
| Yonne | 814-840 | Coupland (2014) | Yonne | 47.89753 | 3.588695 |
| York | 751-887 | Dolley (1965) | York | 53.95333 | -1.08342 |
| Yronde | 843-877 | Morrison and Grunthal (1967) | Yronde | 45.6133 | 3.25481 |
| Zelzate | 814-877 | Morrison and Grunthal (1967) | Zelzate | 51.19753 | 3.81463 |
| Zetel | 768-793 | Völckers (1965) | Zetel | 53.4146 | 7.9699 |
| Zillis | 888-949 | Zäch (2001) | Zillis | 46.6355 | 9.44514 |
| Zuidlaren | 875-894 | Haertle (1997) | Zuidlaren | 53.09231 | 6.679414 |

Appendix Table A.15: Carolingian Hoards, Part VI

| Signatures | Approx. Location Nomisma ID | Notes |
|---|---|---|
| AHM | hamadhan | |
| AIRAN, AYLAN | hulwan | Eran-asankar-Kavad |
| AM | amol | Amol, Khorasan |
| APL, APR | nishapur | |
| ART, TART | ardashir_khurrah | TART: Tawwaj as dependency of Ardashir Khurra |
| AT | adurbadagan | |
| AU, AW | suq_al-ahwaz | AU is used by Al-Ush, we interpret it as "AW", Hormizd-Ardashir |
| AY, AYL | al-sus | Eran-khvarrah-Shapur. AYL: British Museum says "possibly referring to Susa." |
| AS | ctesiphon | Following the coding in FLAME. |
| BBA | ctesiphon | Court mint, probably at Ctesiphon (Gyselen) |
| BCLA, BJRA, DS, DST | al-basrah | Mallon-McCorgray interprets BCLA as al-Basra. Accoring to Schindel (2005) BJRA is al-Basra. |
| BISH, BYS, BYSH | bishapur | |
| BN, BRMKRMAN, DL, DR, GLM, KL, KLMAN, KLMANLCN, KR, KRAMAN H P, KRMAN, KRMAN W ST, KRMAN-GY, KRMAN-NAR, KRMAN-NAW, NAL, NAR | kirman | Multiple mints that are in Kirman province. |
| D', DA, DAP | darabjird | |
| DAP | fasa | |
| GD | jayy | |
| GU, GW | gorgan | We follow Schindel (2005) in attributing GW to Gorgan (after Yazdegerd I). Gyselen (1977) attributes GU to Gorgan. |
| HL | harat | |
| HWC | jundi_sabur | |
| LAM, RAM | ramhurmuz | |
| LD, RD | rayy | |
| LYW, RIU | rev-ardashir | Bivar (1970) associates RIU with LYW, and confirms Nö's interpretation as Rev-Ardashir |
| MA | masabadhan | |
| MB, MY, PL | maysan | |
| ML, MR | marw | |
| NH, NIHJ, NYHC, WH, WYHC | ctesiphon* | NH, WH: Veh-Ardashir. On WYHC, Album (2011): "A mint in northern Iraq, ostensibly the treasury mint near Ktesiphon prior to the AH50s, and thereafter, for a series dated AH67-73, Arrajan". We follow Album (2011), Schindel (2005), and others in attributing it to Ctesiphon before AH50, then Arrajan. |
| NHR | nahr_tira | |
| NIH, WYH | bihqubadh_af-asfal | |
| NIHJ | arrajan | Almost certainly the same as WYHC. |
| NY, NYH | antiocheia_persis | NY: Nihawand. For NYH, Schindel (2005) suggests Nihawand. |
| SHI | shiraz | |
| SK | zaranj, sijistan | |
| ST | istakhr | |
| SY | fars_shiraz | Unlocated mint, probably in Fars province (or Kirman, as has sometimes been suggested). |
| TPWRSTAN | tabaristan | |
| YZ, ZR, GZ | yazd | |

Appendix Table A.16: Sasanian mint codings

## References


Abdul Wahab, H. (2012): "al-Abbāsiyya," in *Encyclopaedia of Islam*, ed. by P. Bearman, T. Bianquis, C. Bosworth, E. van Donzel, and W. Heinrichs, Brill.

al Bakri, M. D. (1973): "Kanz al-'Utayfiyah al-fiddi," *al-Maskukat*, 4.

Al Chomari, A. A. (2020): *Le commerce régional et international au Xe siècle en Syrie: D'après le trésor monétaire de Buseyra et d'autres trésors de l'époque*, Archaeopress.

Al-Naqshbandi, N. (1949): "Rare Islamic coins in the Iraq Museum," *Sumer*, 5, 199–202.

——— (1950): "The Zakho Treasure," *Sumer*, 6, 177–188.

——— (1951): "The Zakho Treasure," *Sumer*, 7, 165–172.

——— (1952): "The Zakho Treasure," *Sumer*, 8, 220–227.

——— (1954): "Khidr Elias Treasure," *Sumer*, 10, 180–196.

al 'Ush, A.-F. (1954-1955): "Al-Kanz al-dhahabī al-umawī," *Annales Archeologiques de Syrie*, IV-V, 21–28.

——— (1972a): *Kunz umm ḥajarah al-fiḍḍi (Trésor de monnaies d'argent trouvé à Umm Hajarah)*, Damascus.

——— (1972b): *The silver hoard of Damascus: Sasanian, Arab-Sasanian, Khuwarizmian, and Umayyad kept in the National Museum of Damascus*, Damascus: Direction General of Antiquities and Museums.

——— (1982): *Monnaies Aghlabides, étudiées en relation avec l'histoire des Aghlabides*, Institut Français de Damas.

Album, S. (1971): "An Umayyad hoard from Afghanistan," *Museum Notes (American Numismatic Society)*, 17, 241–246.

——— (2011): "Checklist of Islamic Coins, 3rd Edition," .

Alfaro Asins, C. (1992): "La colección de moneda hispano-árabe del Museo Arqueológico Nacional de Madrid," *III Jarique de Numismática hispano-árabe. Actas (Museo Arqueológico Nacional. Madrid, 13-16 diciembre 1990)*, 39–75.

Álvarez, M. d. l. Á. P. (1993): "Tesorillo de monedas árabes de Moraleja (Cáceres)," *Alcántara: revista del Seminario de Estudios Cacereños*, 37–44.

American Numismatic Society (2023): "MANTIS Database," https://numismatics.org/collection, accessed: 2023-07-01.

Ariza Armada, A. (1988): "Un tesorillo de dirhames de Baena (Cordoba)," *Arqueología Medieval*, 2, 137–140.

Arroyo Ilera, R. (1989): "Descripción y análisis de las monedas árabes de Sinarcas (Valencia)," in *Actas del VII Congreso Nacional de Numismática, Madrid, Museo Casa de la Moneda*, 467–479.

Arslan, E. A. (2005): "Il Repertorio dei ritrovamenti di moneta altomedievale (489-1002)," .

Artuk, I. (1966): *Denizbacı definesi*, Ankara: Türk Tarih Kurumu.

Asencio, J. M. R. (1962): "Tesoro de dirhemes califales hallado en Jaén," *Boletín del Instituto de Estudios Giennenses*, 109.

Ávila, R. C. and A. R. H. Pareja (1999): "Un conjunto monetario andalusí de plata emiral procedente de la Junta de los Ríos (Priego de Córdoba)," *Antiquitas*, 125–136.

Ayala Ruiz, J. A. and C. Gozalbes Cravioto (1996): "Un tesorillo califal aparecido en la Cala de Mijas-Costa (Málaga)," *Gaceta Numismática*, 121, 61–76.

Baigl, J.-P., A. Clairand, and O. Jeanne-Rose (1995): "Trouvailles récentes de monnaies carolingiennes dans les Deux-Sèvres: petits trésors et monnaies isolées," *Bulletin de la Société française de numismatique*, 50, 1152–1154.

Balaguer, A. M. (1999): *Història de la moneda dels comtats catalans*, vol. 2, Institut d'Estudis Catalans.

Baldus (2006): *Didyma. III. Ergebnisse der Ausgrabungen und Untersuchungen seit dem Jahre 1962. 3. Fundmünzen aus den Jahren 1962-1998*, Deutsches Archäologisches Institut.

Banaji, J. (2016): *Exploring the Economy of Late Antiquity: Selected Essays*, Cambridge University Press.

Bartolomei, I. A. (1857): "Description d'une trouvaille de 200 dirhems koufiques, faite aux environs de Tiflis, en 1857," *Bulletin de l'Académie impériale des sciences de St. Petersburg*, 3.

Bates, M. L. (1978): "A hoard of dirhams found at Nippur," *Excavations at Nippur, twelfth season*, 126–138.

Benoit, P. and P. Braunstein (1983): *Mines, carrières et métallurgie dans la France médiévale*, Paris: Edition du CNRS.

Bernareggi, E. (1977): "I tremissi longobardi e carolingi del ripostiglio di Ilanz nei Grigioni," *Quaderni ticinesi di numismatica*, VI.

——— (1983): "Carolingian gold coins from the Ilanz hoard," in *Studies Philip Grierson*, 127–135.

Besteman, J. (2006): "Westerklief II, a second Viking silver hoard from the former island of Wieringen; with a contribution by Gert Rispling and Simon Coupland'," *Jaarboek voor Munt-en Penningkunde*, 93, 5–80.

Bijsterveld, A., N. Neufeglise, and B. van der Veen (2000): "Een heilige plaats onder de grond. Aalst en zijn middeleeuwse kerk," *Brabants Heem*, 52, 81–92.

Bivar, A. D. H. (1970): "Appendix: The Sasanian Coin from Qūmis," *Journal of the Royal Asiatic Society of Great Britain and Ireland*, 156–158.

Blackburn, M. A. (1989): "The Ashdon (Essex) hoard and the currency of the Southern Danelaw in the late ninth century," *British Numismatic Journal*, 59, 13–38.

Bompaire and Depierre (1989): "le trésor carolingien de dijon, rue du chapeau rouge," Tech. rep., bulletin de la société française de numismatique.

Cano Ávila, P. (1989): "Algunos dirhemes hallados cerca de Alcaudete (Jaén)," in *VII Congreso Nacional de Numismática: Memoria*, 489–503.

——— (2014): "Hallazgo de dírhemes del califato Omeya de Al-andalus en Montellano (Sevilla)," *Revista Numismática OMNI*, 149–164.

——— (2016): "Hallazgo de dírhems del Califato omeya de al-Andalus en Bormujos (Sevilla)," in *Patrimonio numismático y museos: actas XV Congreso Nacional de Numismática. Madrid, 28-30 de octubre de 2014*, Museo Casa de la Moneda, 1133–1148.

Cano Ávila, P. and C. M. Gómez (2008): "Hallazgo de un tesorillo de dírhemes del imamato fatimí y del califato omeya de al-Andalus en El Pedroso (Sevilla). El Pedroso III," in *Moneda y arqueología: actas XIII Congreso Nacional de Numismática*, Universidad de Cádiz, 799–824.

Cano Ávila, P. and C. Martín Gómez (2006): "Hallazgo de un tesorillo de dírhemes del califato omeya de al-Andalus en El Pedroso (Sevilla)," in *Actas XII Congreso Nacional de Numismática: Madrid. 25-27 de octubre de 2004*, Real Casa de la Moneda, Fábrica Nacional de Moneda y Timbre, 443–464.

Cano Ávila, P. and C. I. Martín Gómez (2005): "Tesoro de dirhemes emirales hallado en La Rinconada (Sevilla)," in *XIII Congreso Internacional de Numismática, Madrid, 2003: actas-proceedings-actes*, Ministerio de Cultura, 1553–1566.

Cano Ávila, P. and C. I. Martín Gomez (2011): "Hallazgo de dírhemes del emirato omeya de al-Ándalus en Niebla (Huelva)," in *Ars metallica. Monedas y medallas: Nules-Valencia, 25-27 de octubre de 2010*, Museo Casa de la Moneda, 817–834.

Canto García, A. (1988): "Tesoro de moneda emiral del siglo II de la Hégira, conservado en el MAn [Museo Arqueológico nacional]," *Actas I Jarique de Estudios Numismáticos Hispano-Árabes, Zaragoza, Institución Fernando el Católico*, 147–162.

——— (1993): "Sobre un pequeño hallazgo de moneda emiral en Martos (Jaén)," *Antiquitas*, 63–66.

——— (2001): "La moneda hispanoárabe y su circulación por Navarra," in *La moneda en Navarra: Museo de Navarra, Pamplona: exposición 31 de mayo a 25 de noviembre de 2001*, Fundación Caja Navarra, 73–82.

——— (2014): "El tesoro de Tarancón (Cuenca, 1893): nuevos datos e imágenes sobre el mismo," *Revista Numismática OMNI*, 21–64.

——— (2019): "Hallazgos de Moneda Andalusi y Documentacion," Tech. rep., Universidad Autónoma de Madrid.

Canto García, A., R. Clapés, and W. Jabłońska (2020a): "Un hallazgo de monedas califales en el arrabal occidental de Córdoba," .

Canto García, A. and F. M. Escudero (2012): "El tesoro de monedas árabes de Carmona y una rectificación de A. Vives Escudero," *Cuadernos de Prehistoria y Arqueología de la Universidad Autónoma de Madrid*, 38.

Canto García, A., G. García Ruiz, and L. Ruiz Quintanar (1997): "Hallazgo de monedas califales de Marroquíes Bajos (Jaén)," *Arqueología y territorio medieval*, 4, 81–101.

Canto García, A. and W. Jabłońska (2019): "Algunas precisiones sobre el hallazgo de dinares califales de la calle San Pedro (Murcia)," *Tudmir: Revista del Museo Santa Clara, Murcia*, 5–13.

Canto García, A. and E. Marsal Moyano (1988): "Hallazgo de moneda emiral de Iznájar (Granada)," *Al-Qantara*, 9, 427.

Canto García, A. and F. Martín Escudero (2007): "El hallazgo de moneda califal de Fontanar (Córdoba)," *Documenta & Instrumenta*, 129–156.

——— (2009): "Hallazgos monetarios islámicos en Algeciras," *Caetaria: revista bianual de Arqueología*, 125–130.

Canto García, A., F. Martín Escudero, and W. Jablonska (2020b): *El hallazgo de monedas califales del Parque Cruz Conde (Córdoba)*, Museo Casa de la Moneda.

Cardon, T., J. C. Moesgaard, R. Prot, and P. Schiesser (2008): "Le premier trésor monétaire de type viking en France. Denier inédit d'Eudes pour Beauvais," *Revue numismatique*, 6, 21–40.

Caron, E. (1882): *Monnaies féodales françaises*, vol. 1, Rollin et Feuardent.

Cerrato, C. B. and A. M. Esquivel (2019): "Conjunto de dírhams califales hallado en Zamora: estudio e interpretación," *Archivo español de arqueología*, 92, 287–306.

Ciampoltrini, G., E. Abela, and S. Bianchini (2001): "Lucca: un contesto con monete del X secolo dell'area dell'ex ospedale Galli Tassi," *Bollettino di Numismatica*, 153–166.

Codera y Zaidín, F. (1892): "Tesoro de monedas árabes, descubierto en Alhama de Granada," *Boletín de la Real Academia de la Historia*, XX, 442–449.

——— (1913): "Monedas árabes orientales encontradas en Aragón," *Boletín de la Real Academia de la Historia*, LXIII, 552–556.

Cornu, G. (1983): *Atlas du monde Arabo-Islamique à l'époque classique: IX.-X. siècles*, Brill.

Coupland, S. (1991): "The early coinage of Charles the Bald, 840-864," *The Numismatic Chronicle (1966-)*, 121–158.

——— (1995): "Bilan Société Française de Numismatique," Tech. rep., Société Française de Numismatique.

——— (2010): "Le trésor de Bourgneuf-en-Retz et les monnaies de Melle au monogramme d'un roi Charles'," *Bulletin de la Société française de numismatique*, 65, 190–3.

——— (2011a): "A checklist of Carolingian coin hoards 751-987," *The Numismatic Chronicle*, 171, 203–256.

——— (2011b): "The Roermond coins reconsidered," *Medieval and Modern Matters*, 2, 25–50.

——— (2014): "A supplement to the checklist of Carolingian coin hoards, 751-987," *The Numismatic Chronicle (1966-)*, 174, 213–222.

——— (2018): "Les monnaies de Melle sous Louis le Pieux'," *Mine, métal, monnaie, Melle. Les voies de la quantification de l'histoire monétaire du haut Moyen Âge*, 259–278.

——— (2019): "Der Karolingschatz von Bassenheim," Tech. rep., Münzfunde aus Rheinland-Pfalz 36.

——— (2020): "A Second Supplement to the Checklist of Carolingian coin hoards, 751-987," *The Numismatic Chronicle*, 180, 259–289.

Coupland, S. and J. C. Moesgaard (2012): "Trésors monétaires peut-être enfouis lors des premiers raids vikings dans la vallée de la Seine'," *Bulletin de la Société française de numismatique*, 67, 222–229.

Cravioto, C. G. (2016): "Tesorillo de monedas andalusíes de Castillejos de Quintana (Pizarra, Málaga)," in *Patrimonio numismático y museos: actas XV Congreso Nacional de Numismática. Madrid, 28-30 de octubre de 2014*, Museo Casa de la Moneda, 1353–1360.

Cravioto, C. G. and J. A. Ayala (1995): "Un tesorillo de monedas del emirato independiente hallado en el Cerro de la Fuensanta (Antequera-Casabermeja-Colmenar. Málaga)," *Mainake*, 235–242.

Cruysheer, A. and B. J. V. der Veen (2015): "De Karolingische schatvondst Bikbergen 1992," Tech. rep., De Beeldenaar.

Curta, F. (2005): "Byzantium in Dark-Age Greece (the numismatic evidence in its Balkan context)," *Byzantine and Modern Greek Studies*, 29, 113–146.

Daim, F. and E. Lauermann (2006): *Das frühungarische Reitergrab von Gnadendorf (Niederösterreich)*, Verlag des Römisch-Germanischen Zentralmuseums.

Dajani, A. (1951): "A hoard of Byzantine gold coins from Awarta, Nablus," *Annual of the Department of Antiquities, Jordan*, 1, 41–43.

De Benedittis, G. and J. Lafaurie (1998): "Trésor de monnaies carolingiennes du VIIIe siécle trouvé à Larino (Italie, Molise)," *Revue Numismatique*, 6, 217–243.

Denais, J. (1908): "Catalogue illustré du musée de Beaufort-en-Vallée," Tech. rep.

Dhénin, M. (1989): "Le trésor monétaire de Breuvery-sur-Coole (Marne)," *Comptes rendus des séances de l'Académie des Inscriptions et Belles-Lettres*, 133, 811–823.

Dhénin, M. (2006): "Les monnaies carolingiennes d'Arpajon (anciennement Chartres), Essonne," *Bulletin de la Société Française de Numismatique*, 61, 226–230.

Dijkstra, M. F. P. (2005): "'Middeleeuwse gulle gaven, greppels en waterputten. De opgraving Wijk bij Duurstede-David van Bourgondieweg.'," *26.*

Dimian, I. (1957): "Cîteva descoperiri monetare bizantine pe teritoriul RPR," *Studii si cercetari de numismatica*, 1, 189–216.

Dolley, M. (1965): "New Light on the Pre-1760 Coney Street (York) Find of Coins of the Duurstede Mint."," *Jaarboek Voor Munt-en Penningkunde*, 52, 1966.

Doménech Belda, C. (1992): "Revisión de un hallazgo de monedas árabes de Elche (Alicante)," .

——— (1997): "Circulación monetaria durante el período islámico en el País Valenciano," .

Doménech Belda, C. and S. Gutiérrez Lloret (2006): "Viejas y nuevas monedas en la ciudad emiral de Madīnat Iyyuh (El Tolmo de Minateda, Hellín, Albacete)," *Al-Qanṭara*, 27, 337–374.

Doménech Belda, C. and J. Trelis (1990): "Hallazgos numismáticos de época islámica en Crevillente (Alicante)," *III Jarique de Numismática Hispano-árabe*.

Doménech-Belda, C. et al. (2013): "La circulation de monnaie carolingienne dans la péninsule ibérique. À propos d'un denier de l'atelier de Roda," *Revue Numismatique*, 6, 383–410.

Duplessy, J. (1985): "Les trésors monétaires médiévaux et modernes découverts en France, vol. 1, 751-1223," .

Eustache, D. (1956): "Monnaies musulmanes trouvées à Volubilis," *Hespéris: Archives berbères et bulletin de l'institut des hautes études-marocaines*, XLIII.

Fagerlie, J. M. (1974): "A Byzantine "Sicilian"' Hoard," in *Studies George C. Miles*, 175–183.

FLAME (2023): "Framing the Late Antique and early Medieval Economy," https://coinage.princeton.edu/, accessed: 2023-07-01.

Fomin, A. V. and L. Kovács (1987): *The tenth century Máramaros County ("Huszt""") dirham hoard*, Magyar Numizmatikai Társulat.

Fontenla Ballesta, S. (1998): "Un tesorillo de plata medieval del Tijan (Turre, Almeria)," Tech. rep., Axarquia 3.

Füeg, F. (2007): *Corpus of the Nomismata from Anastasius II to John I in Constantinople, 713-976*, Classical Numismatic Group.

Gachet, A. (1993): *Présentation d'un trésor monétaire des premiers temps de l'Islam : le trésor d'Afak*.

Gedai, I. (1993): "The denars of Luis the Child in a grave find in Hungary," *Numismatica e antichità classica*, 273–278.

Geiser, A. (1990): *Un trésor de monnaies de Pépin le Bref trouvé à La Tour-de-Peilz (VD), nécropole du Clos d'Aubonne*, Gazette numismatique suisse.

González García, A. and D. Martínez Chico (2017): "Cuatro hallazgos aislados de dinares epigráficos latinos hispano-musulmanes en Jaén," .

Grañeda Miñón, P. (2021): "Reexcavando en el Museo Arqueológico Nacional: los tesoros de Valencia del Ventoso (Badajoz) y Osuna (Sevilla)," Tech. rep., XVI Congreso Nacional de Numismática: Tesoros y hallazgos monetarios: protección, estudio y musealización (Barcelona, 28-30 de noviembre de 2018).

Grierson, P. (1968): *Catalogue of the Byzantine Coins in the Dumbarton Oaks Collection and in the Whittemore Collection, 2: Phocas to Theodosius III, 602-717*, Dumbarton Oaks.

——— (1973): *Catalogue of the Byzantine Coins in the Dumbarton Oaks Collection and in the Whittemore Collection, 3: Leo III to Nicephorus III, 717-1081*, Dumbarton Oaks.

Guillemain, J. (1993): "Deux trouvailles de monnaies médiévales au nord de Lyon," *Bulletin de la Société Française de Numismatique*.

Gyselen, R. (1977): "Trésor de monnaies sasanides trouvé à Suse. I. Inventaire," *Cahiers de la Délégation archéologique française en Iran*, 7, 61–74.

Gyselen, R. and L. Kalus (1983): *Deux trésors monétaires des premiers temps de l'Islam*, Bibliothèque Nationale de France, Paris.

Gyselen, R. and A. Nègre (1982): "Un trésor de Gazīra (Haute-Mésopotamie): monnaies d'argent sasanides et islamiques enfouies au début du IIIe siècle de l'Hégire/IXe siècle de notre ère," *Revue Numismatique*, 6, 170–205.

Haertle, C. M. (1997): *Karolingische Münzfunde aus dem 9. Jahrhundert*, Böhlau.

Hakiem, A. a.-A. D. (1977): "A critical and comparative study of early Arabian coins on the basis of Arabic textual evidence and actual finds," Ph.D. thesis, University of Leeds.

Hebert, R. J. (1966): "Notes on an Umayyad hoard from Khurāsān," *Museum Notes (American Numismatic Society)*, 12, 157–163.

Heidemann, S., J. Riederer, and D. Weber (2014): "A Hoard from the Time of Yazdgard III in Kirmān," *Iran*, 52, 79–124.

Heidemann, S., T. Schierl, and F. Teichner (2018): "Coins from the seaside. An Emiral silver coin hoard from a harbour settlement on the Cerro de Vila (Vilamoura, Algarve, Portugal)," *Al-Qantara*, 39, 169–224.

Hoge, R. (1997): "A Parcel of Mainly'Abbāsid Gold Coins," *The Numismatic Chronicle*, 157, 239–247.

Hucher, E. F. F. (1845): *Essai sur les monnaies frappées dans le Maine*, de Gallienne.

Huszár, L. (1955): *Das Münzmaterial in den Funden der Völkerwanderungszeit im mittleren Donaubecken*, Akadémiai Kiadó.

Ibrahim, T. B. H. and A. Canto García (1991): "Hallazgo emiral en Puebla de Cazalla (Sevilla)," *Numisma: revista de Estudios Numismáticos*, 69–86.

Ilisch, L. (1979): "Ein Dirhamfund des frühen 10. Jahrhunderts aus der Gegend von Diyarbakir," *Münstersche Numismatische Zeitung*.

——— (1990): "Whole and fragmented Dirhams in near eatsern hoards," in *Sigtuna papers: proceedings of the Sigtuna symposium on Viking-age coinage, 1-4 june 1989*, ed. by K. Jonsson and B. Malmer, Kungl. Vitterhets Historie och Antikvitets Akademien.

——— (2005): "Der Steckborner Schatzfund von 1830 und andere Funde nordafrikanischer Dirhams im Bereich des Karlsreiches," in *Simposio Simone Assemani sulla monetazione islamica*, ed. by G. Gorini, Esedra.

Jeanne-Rose, O. (1996): "Trouvailles isolées de monnaies carolingiennes en Poitou: inventaire provisoire," *Revue numismatique*, 6, 241–283.

Johnston, P. (1986): *The archaeology of the Channel Islands*, Phillimore.

Jungfleisch, M. (1949): "La trouvaille du cimetière de Sainte-Barbe à Babylone d'Egypte," *Revue Numismatique*, 11, 165–169.

Kasdagli, A.-M. (2018): *Coins in Rhodes: From the monetary reform of Anastasius I until the Ottoman conquest (498 - 1522)*, Archaeopress.

Khodzhaniyazov, T. and L. Treadwell (1998): "The Marv hoard of early Islamic dirhams," *Iran*, 36, 85–94.

Kirkbride, A. (1951): "Recent Finds of Arabic Coins," *Annual of the Department of Antiquities, Jordan*, 1, 17–19.

Kluge, B. (1993): "Fernhandel und Geldwirtschaft: Beiträge zum deutschen Münzwesen in sächsischer und salischer Zeit," .

Kovács, L. (1989): *Münzen aus der ungarischen Landnahmezeit: archäologische Untersuchung der arabischen, byzantinischen, westeuropäischen und römischen Münzen aus dem Karpatenbecken des 10. Jahrhunderts*, Akadémiai kiadó.

Lafaurie, J. (1965): "Deux trésors monétaires carolingiens: Saumeray (Eure-et-Loir), Rennes (Ille-et-Vilaine)," *Revue Numismatique*, 6, 262–305.

Lafli, E., C. Lightfoot, and M. Ritter (2016): "Byzantine coins from Hadrianoupolis in Paphlagonia," *Byzantine and Modern Greek Studies*, 40, 187–206.

Lagumina, B. (1904): "Ripostiglio di monete arabe rinvenuto in Girgenti," *Archivio storico siciliano*, 29.

Lloyd, S. (2023): "Post-Reform Umayyad Dirhams and their Mint Towns," https://www.angelfire.com/ny3/vaguebrit/, accessed: 2023-07-01.

Lockhart, L. (2012): "Dīnawar," in *Encyclopaedia of Islam*, ed. by P. Bearman, T. Bianquis, C. Bosworth, E. van Donzel, and W. Heinrichs, Brill.

Lowick, N. (1975): "An early tenth century hoard from Isfahan," *The Numismatic Chronicle*, 110–154.

——— (1983): "The Sinaw Hoard of Early Islamic Coins," *The journal of Oman studies*, 6, 199–230.

Lowick, N. and J. Nisbet (1968): "A hoard of dirhems from Ra's al-Khaimah," *The Numismatic Chronicle*, 231–240.

Ma'ayeh, F. S. (1962): "A Hoard of Omayyad Dinars from Orif," *Annual of the Department of Antiquities, Jordan*, 6/7, 76–97.

Malek, H. M. (1996): "A Hoard Group Of Drachms of the Dābūyid Ispahbads and Early'Abbāsid Governors of Ṭabaristān," *The Numismatic Chronicle*, 156, 175–191.

Mănucu-Adameşteanu, G. (2016): *Monede bizantine descoperite în Dobrogea: monede bizantine descoperite în mediul rural din nordul Dobrogei, Secolele VII-XV*, Muzeul Municipiului Bucureşti.

Marcos Pous, A. and A. M. Vicent Zaragoza (1992): "Los tesorillos de moneda hispano-árabe del Museo Arqueológico de Córdoba," *III Jarique de Numismática Hispano-Árabe*, 192–215.

Marinho, J. R. (1993): "As moedas hispano-muçulmanas da colecçao Justino Cumano numa carta de Pascual de Gayangos," Tech. rep., III Jarique de numismatica hispano-arabe.

Martín, M. V. and S. P. Martín (2002): "Del hallazgo de dirhames emirales en Domingo Pérez (Iznalloz, Granada)," *Al-Qanṭara*, 23, 155–192.

——— (2006): "Sobre el hallazgo emiral del Campo de la Verdad (Córdoba)," in *Actas XII Congreso Nacional de Numismática: Madrid. 25-27 de octubre de 2004*, Real Casa de la Moneda, Fábrica Nacional de Moneda y Timbre, 403–416.

Martín Escudero, F. (2001): "El hallazgo omeya de Baena: un tesoro olvidado," in *IV Jarique de numismática andalusí*, Universidad de Jaén, 81–94.

——— (2003): "Sobre el hallazgo de dinares del Hospital Militar de Zaragoza (1858)," in *XI Congreso Nacional de Numismática: actas, Zaragoza, 2002*, Real Casa de la Moneda, Fábrica Nacional de Moneda y Timbre, 257–268.

——— (2011): "Las monedas de Al-Andalus: de actividad ilustrada a disciplina científica," *Las monedas de Al-Andalus*, 1–394.

——— (2012): "Monedas que van, monedas que vienen... circulación monetaria en época de cambios," *De Mahoma a Carlomagno. Los primeros tiempos (siglos vii–ix). XXXIX Semana de Estudios Medievales de Estella*, 311–350.

Martín Escudero, F., M. T. Casal García, and A. Canto García (2023): "Feluses, dírhams y monedas en el arrabal de Šaqunda (Córdoba): análisis y clasificación tipológica," .

Martínez Enamorado, V. (2004): "Frontera de al-Andalus. El Valle del Tiétar en el contexto de la Tagr al-Awsat," .

McCormick, M. (2001): *Origins of the European economy: communications and commerce AD 300-900*, Cambridge University Press.

Metcalf, D. M. (1992): "„The Rome (forum) hoard of 1883 ," *British Numismatic Journal*, 62, 63–96.

Miles, G. C. (1960): "A Hoard of Arab Dirhems from Algarve, Portugal," *Museum Notes (American Numismatic Society)*, 9, 219–230.

Minarovicova, E. (2007): "Novoobjavený rímsky denár z hromad¬ného nálezu rímskych mincí z Vyškoviec nad Ipľom, okr. Levice," Tech. rep., Slovenska Numizmatika.

Mirnik, I. A. (1981): *Coin hoards in Yugoslavia*, BAR Publishing.

Miškec, A. (2002): *Die Fundmünzen der römischen Zeit in Kroatien. Abt. 18. Istrien*, von Zabern.

Moesgaard, J. C. (1997): "A hoard from the Blois region and the proto-feudal coinage of Blois, c. 920/40," *The Numismatic Chronicle (1966-)*, 157, 196–205.

——— (2003): "Le trésor de Saint-Taurin à Evreux (Xe siècle)," *Cahiers Numismatique*, 158, 23–40.

——— (2010): "Le "maillon manquant" entre Quentovic et Rouen?" *Bulletin de la Société française de numismatique*, 65, 57–61.

Morony, M. G. (1982): "Continuity and Change in the Administrative Geography of Late Sasanian and Early Islamic al-'Irāq," *Iran*, 20, 1–49.

Morrison, K. F. and H. Grunthal (1967): *Carolingian Coinage*, New York: American Numismatic Society.

Morrisson, C. (2017): "Coinage in Byzantine Anatolia," in *The Archaeology of Byzantine Anatolia. From the End of Late Antiquity to the Coming of the Turks*, ed. by P. Niewöhner, Oxford University Press.

Morrisson, C. and J.-N. Barrandon (1988): "La trouvaille de monnaies d'argent byzantines de Rome (VIIe-VIIIe s.): Analyses et chronologie," *Revue numismatique*, 6, 149–165.

Morrisson, C., V. Popović, and V. Ivanišević (2006): *Les Trésor monétaires byzantins des Balkans et d'Asie Mineure (491-713)*, Lethielleux.

Mosser, S. M. (1935): *A bibliography of Byzantine coin hoards*, New York: American Numismatic Society.

Motos Guirao, E. and A. Díaz García (1985): "Tesorillo árabe de Tígnar," *Miscelánea de estuios árabes y hebraicos. Sección Árabe-Islam. Vol. 34 (1985)*.

Museo Arqueológico de Murcia (2014): "Tesoros. Materia ley y forma. Catalogue of the exhibition December 2014 to April 2015," Tech. rep., Museo Arqueológico de Murcia.

Múzeum Móra Ferenc (2002): *Studia archaeologica VIII*, Szeged: Múzeum Móra Ferenc.

Navascués y de Palacios, J. (1957): "Tesoro hispano-árabe encontrado en Trujillo (Cáceres)," *Numario Hispánico*, 6, 5–28.

——— (1958): "Tesorillo de monedas de plata del califato cordobés y fatimíes," *Numario Hispánico*, 7, 207–210.

——— (1961a): "Tesoro de Cihuela (Soria)," *Numario Hispánico, X*, 173–175.

——— (1961b): "Tesoro de moneda califal," *Numario Hispánico, X*, 169–173.

Nikolaou, Y. and I. Touratsoglou (2019): *The Circulation of Byzantine Coinage in Mainland Greece and the Balkans. The Hoard Evidence: 5th - 15th centuries*, Athens: Friends of the Numismatic Museum.

Nomisma (2023): "The Nomisma.org project," https://nomisma.org/, accessed: 2023-07-01.

Noonan, T. S. (1980): "When and how dirhams first reached Russia: a numismatic critique of the Pirenne theory," *Cahiers du monde russe et soviétique*, 401–469.

Oberländer-Târnoveanu, E. (2001): "From the Late Antiquity to the Early Middle Ages-the Byzantine Coins in the territories of the Iron Gates of the Danube from the second half of the 6th Century to the first half of the 8th Century," *Etudes byzantines et post-byzantines*, 4, 29–69.

Ortega, M. R. R., J. B. Estella, R. G. Torres, and M. M. M. Marqués (2006): "Estudio de un conjunto monetario de época califal procedente del Valle del Guadajoz (Córdoba)," in *Actas XII Congreso Nacional de Numismática: Madrid. 25-27 de octubre de 2004*, Real Casa de la Moneda, Fábrica Nacional de Moneda y Timbre, 417–441.

Palma García, F. and R. Segovia Sopo (2007): "Un tesorillo de moneda islámica aparecido en Morería (Mérida)," Tech. rep., Biblioteca Virtual Miguel de Cervantes.

Parvérie, M. (2014): "Corpus des monnaies arabo-musulmanes des VIII et IX siècles decouvertes dans le Sud de la France," *Revista Numismática OMNI*, 79–100.

——— (2018): "La circulation des deniers de l'Aquitaine carolingienne en Al-Andalus; un réexamen des trésors 'Espanya-1, 2 et 3'," *Bulletin de la Société numismatique de Limousin*, 25, 4–16.

——— (2019): "Supplément au corpus des monnaies arabomusulmanes découvertes en France," *Revista Numismática OMNI*, 283–294.

Paty, E. (1848): "Étude archéologique sur Saint Calais et son canton," Tech. rep., Bulletin de la Société royale d'agriculture, science et arts de la Sarthe.

Pellicer i Bru, J. (1982): "Un tresor de dirhems àrabs a SC.-J." *Acta numismàtica*, 139–166.

——— (1985): "El tresoret de moneda àrab LR-P dels anys 331-418 AH," *Acta numismàtica*, 157–182.

Peña Martín, S. and M. Vega Martín (2007): "La amonedación canónica del emirato omeya andalusí antes de Abd-al-Rahman II, según el hallazgo de dirhams de Villiciosa (Córdoba)," .

Pennas, V. (1991): "Byzantine Monetary Affairs during the 8th, 9th, 10th and 11th Centuries," D.phil thesis, University of Oxford.

——— (1996): "Life in Byzantine Cities of Peloponnesos: The Numismatic Evidence (8th-12th Century)," in *Mneme Martin Jessop Price*, Hellenic Numismatic Society.

Petry, K. and S. Wittenbrink (2021): *Der karolingische Münzschatzfund von Pilligerheck (Landkreis Mayen-Koblenz), vergraben nach 855*, Verein der Münzfreunde für Westfalen und Nachbargebiete.

Poiares, A. (2000): "Diremes califais encontrados ao norte de Mértola," *Arqueólogo Português*, 201–268.

Priego, M. C. (2020): "Estratos, vellones," feluses" y tremises: Estratigrafía y numismática en el yacimiento de la Vega Baja de Toledo (ss. VII-XV dC)," in *El sitio de las cosas: la Alta Edad Media en contexto*, Servicio de Publicaciones, 123–160.

Priego, M. C. and L. O. Enciso (2016): "Dírhams, feluses y contextualización arqueológica en el centro de la Península: nuevos hallazgos de época emiral (s. VIII-IX dC) en Recópolis," in *Patrimonio numismático y museos: actas XV Congreso Nacional de Numismática. Madrid, 28-30 de octubre de 2014*, Museo Casa de la Moneda, 1097–1114.

Prieto, A. (1934): "Tesoro de monedas musulmanas encontrado en Badajoz," *Al-Andalus*, 2, 299.

PROFANTOVA, N. (2009): “Byzantine Coins from the 9th-10th century from the Czech Republic,” in *Byzantine Coins in Central Europe between the 5th and 10th century*, ed. by M. Wołoszyn, Polish Academy of Arts and Sciences, Institute of Archaeology.

PUERTAS, A. F. (1982): “Catálogo de los fondos numismáticos hispanomusulmanes del Museo de Cuenca,” *Cuadernos de la Alhambra*, 115–142.

REINHOLD FISCHER AUKTIONSHAUS (2010): “Auction 114,” Tech. rep.

RENOU, E. J. (1846): *Description géographique de l’empire de Maroc*, vol. 8, Imprimerie Royale.

RODRIGUES MARINHO, J. (1995): “Um Achado de Dirhames do Emirado Ândalus em Castro Marim,” *O Arqueólogo Português IV*, 13–15.

RODRÍGUEZ PALOMO, D. AND F. MARTÍN ESCUDERO (2022): “Moneda en contexto arqueológico en Mārida (siglos VIII-IX). Estudio e interpretación,” *Arqueología y territorio medieval*, 29.

RONDIER, R. F. (1869): “Trouvailles de monnaies près de Chef-Boutonne,” *Revue de l’Aunis, de la Saintonge et du Poitou.*

ROYAL NUMISMATIC SOCIETY (1975): *Coin Hoards, Volume 1*, London.

——— (1977): *Coin Hoards, Volume 3*, London.

——— (1978): *Coin Hoards, Volume 4*, London.

RUIZ ASENCIO, J. M. (1967): “Tesorillo de dirhemes del Emirato hallado en la Lantejuela,” Tech. rep., nvmisma.

RÉVÉSZ, L. (1996): “A karosi honfoglalás kori temetők : régészeti adatok a Felső-Tisza-vidék X. századi történetéhez,” Tech. rep.

SABATIER, J. (1862): *Description générale des monnaies byzantines frappées sous les empereurs d’Orient depuis Arcadius jusqu’à la prise de Constantinople par Mahomet II*, Rollin et Feuardent.

SACCOCCI, A. (2005): “Ritrovamenti di monete islamiche in Italia continentale e in Sardegna (secc. VII-XVI),” in *Simone Assemani Symposium sulla monetazione islamica. Simone Symposium on Islamic Coinage*, 137–149.

SACCOCCI, A. ET AL. (2004): “Il ripostiglio dall’area “Galli Tassi” di Lucca e la cronologia delle emissioni pavesi e lucchesi di X secolo,” *Bollettino di Numismatica*, 36, 165–203.

SAENZ-DIÉZ, J. I. (1993): “Museo municipal de Sevillla : fondos islamicos de la coleccion Gago,” Tech. rep., III Jarique de numismatica hispano-arabe.

SALIDO DOMÍNGUEZ, J., R.-L. GARCÍA LERGA, R. GÓMEZ OSUNA, E. GARCÍA ARAGÓN, M. BLANCO DOMÍNGUEZ, AND J. BARRIO MARTÍN (2020): “Un nuevo conjunto de monedas emirales del centro peninsular: los dírhams del yacimiento arqueológico de El Rebollar (El Boalo, Madrid),” .

SARAH, G., V. GENEVIÈVE, AND C. GUERROT (2016): “Le trésor carolingien découvert à Auzeville (Haute-Garonne) en 1878. Étude des monnayages toulousains de Charles le Chauve et de Pépin II d’Aquitaine,” *Revue numismatique*, 6, 417–498.

SARFATIJ, H., W. J. H. VERWERS, AND P. WOLTERING (1999): *In discussion with the past: Archaeological studies presented to WA van Es*, Foundation for Promoting Archaeology (Stichting Promotie Archeologie).

SCHINDEL, N. (2005): “Sasanian coinage,” *Encyclopædia Iranica.*

SCHNEIDER, A. M. (1952): “Hirbet el-Minje am See Genesareth,” *Annales Archéologiques Syriennes*, 2, 23–45.

Schulze, M. (1984): “Das ungarische Kriegergrab von Apres-Lès-Corps. Untersuchungen zu den Ungarneinfällen nach Mittel-, West-und Südeuropa (899-955 n. Chr.) mit einem Exkurs zur Münzchronologie altungarischer Gräber,” *Jahrbuch des Römisch-Germanischen Zentralmuseums Mainz*, 31, 473–514.

Sears, S. D. (1994): “A late Umayyad hoard from Nippur,” *The Numismatic Chronicle*, 133–146.

——— (2000): “An Abbasid Revolution Hoard from the Western Jazira (al-Raqqa?),” *American Journal of Numismatics*, 12, 171–193.

Segovia Sopo, R. (2006): “Tesorillo de moneda del Emirato Independiente hallado en Fuente de Cantos y su contextualización en las Guerras de Ibn Marwan contra la corte cordobesa,” in *VI Jornada de Historia de Fuente Cantos: Actas*, Asociación Cultural Lucerna, 145–178.

——— (2014): “El tesorillo numismático andalusí de la C/Santa Julia de Mérida (Badajoz): circulación y ocultación monetaria durante la” Fitna” del Califato de Córdoba,” *Cuadernos emeritenses*, 1–396.

Segovia Sopo, R. and A. V. Jiménez (2011): “Un inédito tesorillo de moneda emiral independiente hallado en el Teatro Romano de Mérida,” in *Ars metallica. Monedas y medallas: Nules-Valencia, 25-27 de octubre de 2010*, Museo Casa de la Moneda, 795–816.

Simmer, A. (2000): “Le trésor carolingien d’Ebange-Florange,” *Les cahiers lorrains*, 3–18.

Slovenská akadémia vied. Archeologickỳ ústav (1979): *Rapports du IIIe Congrès international d’archéologie slave: Bratislava, 7-14 septembre 1975*, vol. 1, Veda.

Société de statistique, sciences, lettres et arts du département des Deux-Sèvres (1882): “Sur un trésor carlovingien provenant de Brioux,” *Bulletins de la Société de statistique du département des Deux-Sèvres*, V.

Société des antiquaires de l’Ouest (1982): “Communications,” *Bulletins de la Société des antiquaires de l’Ouest*, 6.

Soler Balaguero, M. (1993): “Las monedas arabes del gabinete numismatico del IEI,” in *III Jarique de numasmitica hispano-arabe*.

Sombart, S. (2008): “Le trésor carolingien de Luzancy (77138), enfoui ou perdu vers 865-870’,” *Bulletin de la Société française de numismatique*, 63, 128–9.

Sophoulis, P. (2011): “Byzantine coin-circulation in early medieval Bulgaria (mid 8th - early 9th c.),” .

Treadwell, L. and E. Rogan (1994): “An Ottoman report of an Umayyad coin hoard: Jarash, 1898,” *Yarmouk Numismatics*, 6, 20–29.

Troussel, M. (1942): “Monnaies d’argent (dirhams) idrissites et abbassides trouvées à Ouenza,” *Recueil des notices et memoires de la Société archaeologique de Constantine*, 65, 105–123.

Ünal, C. (2015): “The Tralleis Hoard and the Reflection of the Iconoclastic Idea in Byzantine Coin Iconography,” *American Journal of Numismatics*, 27, 199–205.

——— (2018): “Kavaklı Definesi: II. Constans Dönemine Ait Altın Sikkeler,” *Cedrus*, 6, 465–483.

Uranga, J. E. (1950): “El hallazgo de” dírhemes” del Emirato en San Andrés de Ordoiz (Estella, Navarra),” *Príncipe de Viana*, 11, 85–101.

Valle, A. M. (1987): “El tesoro califal de “Los Villares” (Caudete, Valencia),” *Acta numismàtica*, 177–196.

Van der Velde, H. (2008): “Cananefaten en Friezen aan de monding van de Rijn,” *ADC Monografie*, 5, 536.

Van Es, W. A. and W. J. H. Verwers (1980): *Excavations at Dorestad. 1: The Harbour, Hoogstraat*, Amersfoort: Rijksdienst voor het oudheidkundig bodemonderzoek.

Vandenbossche, É. and S. Coupland (2012): "Une trouvaille de deniers carolingiens dans la region de Bray-sur-Seine," *The Numismatic Chronicle*, 172, 307–321.

Völckers, H. H. (1965): *Karolingische Münzfunde der Frühzeit, 751-800: Pippin, Karlmann, Karl der Große, I. und II. Münzperiode.*

Vryonis, S. j. (1971): "An Attic Hoard of Byzantine Gold Coins (668-741) from the Thomas Whittemore Collection and the Numismatic Evidence for the Urban History of Byzantium (1963)," in *Byzantium: its internal history and relations.*

Webster, G., R. Dolley, and G. Dunning (1953): "A Saxon treasure hoard found at Chester, 1950," *The Antiquaries Journal*, 33, 22–32.

Wiechmann, R. (2004): "Karolingische Denare aus Bardowick–Münzumlauf an der nördlichen Peripherie des Frankenreichs," in *Delectat et docet. Festschrift zum 100jährigen Bestehen des Vereins der Münzenfreunde in Hamburg*, Hamburg, 13–44.

Williams and Ager (2010): "The Vale of York Hoard," Tech. rep., British Museum Objects in Focus.

Wilson, J. (1989): "The gold hoard," in *Excavations at Capernaum I (1978-1982)*, ed. by V. Tzaferis, Eisenbrauns.

Wołoszyn, M. (2009): *Byzantine Coins in Central Europe between the 5th and 10th century*, Polish Academy of Arts and Sciences, Institute of Archaeology.

Wroth, W. (1908): *Catalogue of the Imperial Byzantine Coins in the British Museum*, Order of the Trustees, British Museum.

Zäch, B. (2001): *Kanton St. Gallen I: Mittelalterliche und neuzeitliche Münzfunde*, Schweizerische Akademie der Geistes-und Sozialwissenschaften.

Zäch, B. and J. D. Tabernero (2002): "Zwei Münzfunde des 9. und 10. Jahrhunderts aus dem Alpenrheintal: Lauterach (1868) und Chur (1997)," *Schweizerische numismatische rundschau= Revue suisse de numismatique*, 93–128.

Zuyderwyk, J. and J. Besteman (2010): "The Roermond hoard: a Carolingian mixed silver hoard from the ninth century," *Medieval and Modern Matters*, 1, 73–154.

# B Technical appendix and additional results

## B.1 Within-empire coin redistribution before entering circulation?

One potential explanation for why coins flow in particular within empires (i.e. the observed border effect) is that coins could be redistributed across different mints first before they enter circulation. If that were the case, the precise place of minting of a coin should not matter beyond the empire in which it has been minted. Table B.1 investigates this by including hoard cell $\times$ empire (that mints the coin) fixed effects in the specification of equation (2), and finds that distance matters almost to the same degree as in the baseline specification. It it therefore unlikely that a lot of redistribution within an empire happens before coins enter circulation.

## B.2 Coin stocks versus coin flows, a numerical exploration

We describe below the stylized numerical model used to generate figure 7.

Figure B.1 uses our data to empirically explore the hypothesis that gravity regressions with flows of durables over

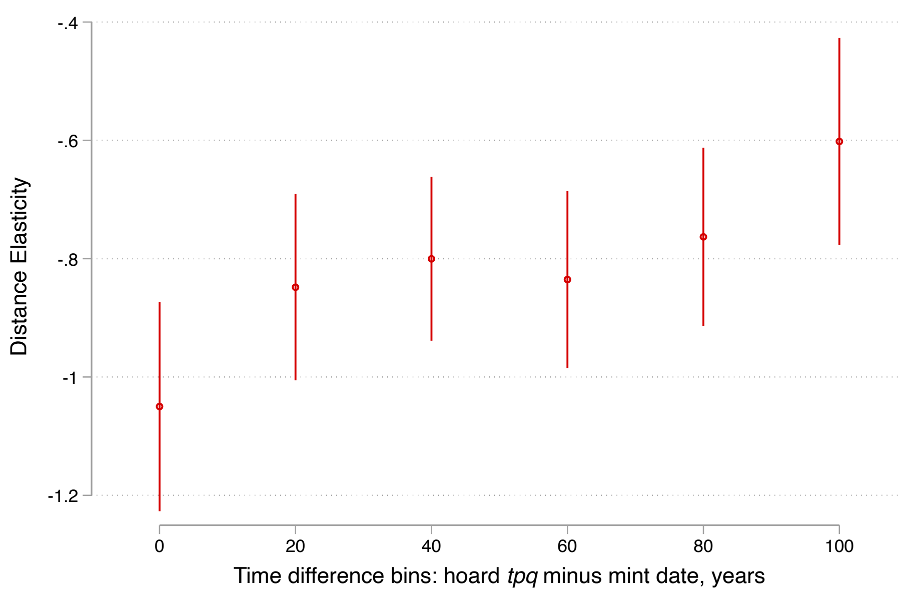


Appendix Figure B.1: The distance elasticity declines as coins age

*Notes:* The figure shows the distance elasticity estimates when estimating equation (B.1) using PPML.

longer horizons bias the distance elasticity towards zero. It shows a coefficient plot of the following regression:

$$\text{count}_{mth\tau} = \exp\left\{\sum_{\tau'\in T} \beta_{\tau'} \log \text{distance}_{mh} \times 1\left(t-\tau=\tau'\right) + \alpha_{mt} + \alpha_{h\tau} + \varepsilon_{mth\tau}\right\} \tag{B.1}$$

where $T = \{0, 20, 40, 60, 80, 100\}$ and mint and hoard *tpq* dates are rounded to 20-year intervals. Coins with longer timespans between mint and hoard *tpq* dates are omitted. We estimate the coefficients using PPML.

The results confirm that the distance elasticity for coins that have travelled for longer is lower (i.e. closer to zero) than for coins that have travelled for shorter periods. Section 2.2 and Figure 7 provide the intuition for this result.

## B.3 Estimation of $\lambda$

To estimate $\lambda$, we divide coins by their age of deposit (using the *tpq* as the date of deposit) into $n$-year bins (for $n = 10$ and $n = 20$). We calculate the fraction $f^{(n)}(k)$ of coins that are in bin $[k, k+n)$, and estimate the parameter of exponential decay from

$$\log f^{(n)}(k) = \tilde{\lambda}^{(n)} \frac{k}{n} + \varepsilon_k.$$

Table B.2 shows the OLS estimation results using 10-year and 20-year bins. The estimates of $\lambda$ can be recovered from $\lambda = 1 - \exp(\tilde{\lambda})$, yielding, respectively, $\hat{\lambda}^{10} = .15$ and $\hat{\lambda}^{20} = .301$.

## B.4 Values versus number of coins

In this subsection we attempt to construct the *equivalent gold weight* of the coins in our data, with the objective of approximating the value of coin flows. Since the relative price of copper/bronze fluctuates heavily during Late Antiquity (see Banaji, 2016, Ch. 5) and copper denominations frequently traded at values different from the intrinsic value based on its metal content, we do this exercise for silver and gold coins only. We also note that FLAME does not record weights of the coins, resulting in only very approximate calculations.

We calculate the equivalent gold weight in two steps. First, we code the reference weights of coins of different denominations in our data.[43] Second, we convert this reference weight into an equivalent gold weight by assuming a constant conversion ratio of 12g of silver for 1g of gold.[44] According to this value metric, gold coins represent 80% of the resulting value in our data, and silver coins represent 20%.

Table B.3 shows the naive gravity regressions, comparing the baseline results from the main text (columns (1) and (2)) with specifications where the dependent variable is the value of coins minted in $m$ by $d$ and found in $h$ (columns (3) and (4)). The distance elasticities are virtually identical when using values as opposed to counting coins.

## B.5 Estimating real consumption

TBD

[43] Note that coins from hoards are often clipped, broken, debased, or abraded, and therefore often weigh less than the reference weight.

[44] This should be seen as a rough approximation. In reality the gold-to-silver ratio fluctuated between 1:10 and 1:16 during Late Antiquity, see Bolin (1953).

## B.6 Tables and references

Appendix Table B.1: Do coins get redistributed within empires before entering circulation?

| | Dependent variable: # $\text{Coins}_{mdh}$ | | | |
|---|---|---|---|---|
| | (1) | (2) | (3) | (4) |
| Log Distance | -0.709** | -0.924** | -0.669** | -0.839** |
| | (0.092) | (0.17) | (0.11) | (0.068) |
| Empire × Hoard Cell FE | Yes | Yes | Yes | Yes |
| Mint × Empire Cell FE | | Yes | | Yes |
| Sample | | | Gold only | Gold only |
| Estimator | PPML | PPML | PPML | PPML |
| $R^2$ | | | | |
| Observations | 41443 | 41443 | 11367 | 11348 |

Standard errors in parentheses, clustered at mint cell × empire and hoard cell level.
$^{+}$ $p < 0.10$, $^{*}$ $p < 0.05$, $^{**}$ $p < 0.01$

*Notes:* This table presents variations of equation (2). The dependent variable is the number of coins in a hoard cell $h$ from a mint cell $m$ issued by a political entity $p$. The regression drops all $(m, d)$ combinations that have no emitted coins. Hoard and mint cells are $1^\circ \times 1^\circ$. Observations only include those that remain after dropping singletons and separated observations. Political entities here are categorized into fourteen divisions.

Appendix Table B.2: Estimation of $\lambda$

| | Dependent variable: Log share of coins in bin $[k, k+n)$ | |
|---|---|---|
| | (1) | (2) |
| $k/n$ | -0.163** | -0.358** |
| | (0.010) | (0.032) |
| Bin size $n$ | 10 | 20 |
| $R^2$ | 0.829 | 0.815 |
| Observations | 55 | 31 |

Standard errors in parentheses.

Appendix Table B.3: Gravity and border effects: # coins vs values of coins

| | Dep. var.: # Coins$_{mdh}$ | | Dep. var.: Value$_{mdh}$ | |
|---|---|---|---|---|
| | (1) | (2) | (3) | (4) |
| Log Distance | -1.138** | -1.002** | -1.146** | -0.991** |
| | (0.12) | (0.13) | (0.076) | (0.069) |
| Political border | | -1.945** | | -1.516** |
| | | (0.62) | | (0.27) |
| Hoard Cell FE | Yes | Yes | Yes | Yes |
| Mint × Empire Cell FE | Yes | Yes | Yes | Yes |
| Sample | | | Gold and Silver | Gold and Silver |
| Estimator | PPML | PPML | PPML | PPML |
| Pseudo-$R^2$ | 0.767 | 0.778 | 0.800 | 0.810 |
| Observations | 217748 | 217748 | 146766 | 146766 |

Standard errors in parentheses, clustered at mint cell × empire and hoard cell level.
$^{+}$ $p < 0.10$, $^{*}$ $p < 0.05$, $^{**}$ $p < 0.01$

*Notes:* This table presents variations of equation (2). The dependent variable is the number of coins in a hoard cell $h$ from a mint cell $m$ issued by a political entity $p$. The regression drops all $(m, d)$ combinations that have no emitted coins. Hoard and mint cells are $1° \times 1°$. Observations only include those that remain after dropping singletons and separated observations. Political entities here are categorized into fourteen divisions. Values are measured in equivalent gold weight.

Appendix Table B.4: Per capita and aggregate consumption, 460-620 AD and 720-900 AD

| | Log real consumption per capita | | Log aggregate real consumption | |
|---|---|---|---|---|
| | 460-620 AD (1) | 720-900 AD (2) | 460-620 AD (3) | 720-900 AD (4) |
| al-Andalus | -0.35 | 0.44 | -1.69 | 2.57 |
| Aquitaine and Basque Country | -0.71 | 0.63 | -3.88 | 3.15 |
| Francia and Germania | -0.97 | 0.66 | -4.80 | 3.90 |
| Northern Italy and Balkans | 0 | 0 | 0 | 0 |
| Southern Italy | -0.38 | -0.35 | -0.40 | -1.19 |
| Byzantine Heartlands | 0.95 | 0.08 | 1.15 | -0.56 |
| al-Sham (Greater Syria) | 0.00 | 0.40 | 1.29 | 2.04 |
| Northern Syria and Caucasus | -0.53 | 0.02 | -0.88 | -0.44 |
| al-Iraq, al-Jibal, Khuzistan, Kirman | 0.08 | 0.53 | 0.88 | 2.93 |
| Eastern Caliphate | -0.62 | 0.11 | -2.39 | 0.91 |
| Jazirat al-arab and al-Yaman | -1.71 | -0.45 | -6.40 | -2.90 |
| Misr (Egypt) | 0.06 | 0.03 | 2.20 | 1.72 |
| al-Maghrib | -0.07 | 0.28 | 0.18 | 0.91 |

*Notes:* TBD.

# References


Banaji, J. (2016): *Exploring the Economy of Late Antiquity: Selected Essays*, Cambridge University Press.

Bolin, S. (1953): "Mohammed, Charlemagne and Ruric," *Scandinavian economic history review*, 1, 5–39.

# C Technical details on operations in spherical geometry

## C.1 Computing 2D distances

Our edges are essentially connecting segments that are characterized by a series of points. To determine the length of each segment, we calculate geodesic distances between the starting point and the ending point. This distance calculation is based on the Haversine equation formula.

$$d_{2D} = 2R \arcsin \sqrt{\mathrm{hav}(\Delta\mathrm{lat}) + \cos(\mathrm{lat}_1)\cos(\mathrm{lat}_2)\,\mathrm{hav}(\Delta\mathrm{lon})}$$

where

$$\mathrm{hav}(x) = \sin^2\left(\frac{x}{2}\right).$$

## C.2 Computing 3D distances

Past efforts to incorporate elevation data into the ORBIS dataset, together with the challenges, has been well-documented here by ORBIS. We follow the documented method, which involves sampling our roads with a series of equidistant points spaced 50 meters apart along the edge. For each sampled point, we retrieve elevation data from the 2019 ASTER project.

As illustrated in the diagram in Figure C.1, we calculate the angle $\alpha = d_{2D}/R$, with known $d_{2D}$, $R$ (assumed to be 6371 kilometers), $h_1$ (the altitude of the start of the line segment) and $h_2$ (that of the end). Using Law of cosines, we have

$$d_{3D} = \sqrt{(R+h_1)^2 + (R+h_2)^2 - 2(R+h_1)(R+h_2)\cos\alpha}$$

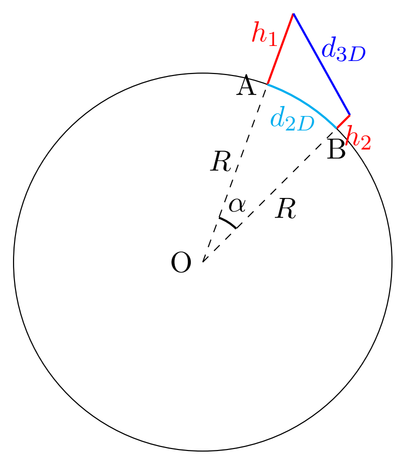


Appendix Figure C.1: The diagram for 3D distance computation. The circle shown in the graph is the great circle defined by A and B

One important consideration of computing the 3D distance is resolution and the sampling technique. It's essential to note that the mesh-grid in the ASTER project does NOT consist of congruent rectangles. As the latitude deviates from zero, the rectangles become elongated. When the latitude is close to zero, it resembles more of a square shape. This distortion is due to the spherical shape of the earth.

It would be also unreliable to simply find all intersecting segments of the routes and the grid, and assign the segments with the grid's height data. Some edges are over-sampled than others. A path that goes from east to west and is close to the pole would gain more resolution comparing to a similar path that are closer to the equator, if segments are sampled this way. To address this issue, we interpolate our path each from start to end every 50 meters (in geodesic distance)[45], use these sampled points to find the corresponding height data.

[45] The choice of 50 meters serves as an optimal compromise because it ensures that consecutive sampled points are placed in different grid cells because 50 meters slightly exceeds the diagonal length of a 30m x 30m square grid cell

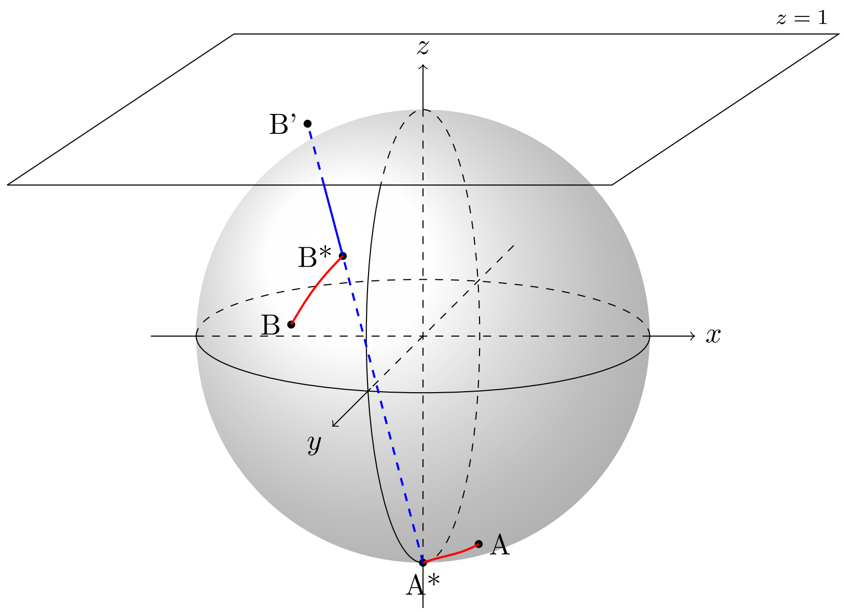


Appendix Figure C.2: Diagram for the stereographic projection

## C.3 Spherical Voronoi tessellation

Na et al. (2002) proved that the spherical Voronoi tessellation can be computed by computing two planar Voronoi diagrams of sites under stereographic projection in the plane. Following Na et al. (2002) and Patel (2018), our Algorithm is described as the following:

1. Choose one arbitrary location among our sites as the center of projection (point A in C.2), or otherwise called the *anchor*.

2. (Drawn in red in C.2) Rotate the globe such that the anchor (A) meets the South pole (A*). In the rotation, all other sites are also rotated (B $\rightarrow$ B*).

3. (Drawn in blue in C.2) Connect the South pole with sites that are not the anchor. Find the intersection (B') of the extended line and the plane $z = 1$. We have now created a mapping (B $\rightarrow$ B') that maps all the sites to points in the plane $z = 1$, except the anchor.

4. Perform Delaunay triangulation on the mapped sites. This can be easily done by the Python package `Shapely`'s function `triangulate()`.

5. Since the anchor is not projected, the triangulation is not complete. One needs to choose another arbitrary location as the anchor and repeat step 1-4. Merge the two different results of triangulation.

6. Map the triangulation back to the unrotated sphere. Find the spherical circumcenter of all the mapped-back triangles (The spherical circumcenter and the Euclidean circumcenter and the center of the sphere lies on the same line. The spherical circumcenter is on the surface of the sphere while the Euclidean circumcenter is inside the sphere).

7. Connect all circumcenter pairs whose corresponding triangles touch.

**Caveat.** Step 6 can potentially cause problems because there are two spherical circumcenters of a triangle. They are antipodal point of each other. If all sites are spaced somewhat evenly around the sphere, it works simply by choosing the spherical circumcenter that is on the same side of the Euclidean circumcenter. However, all our sites can be contained in one hemisphere and Althurayya sites are far from being "placed evenly". Therefore, we are bound to encounter problems with some spherical circumcenter with the unadjusted algorithm. The remedy is that we add an

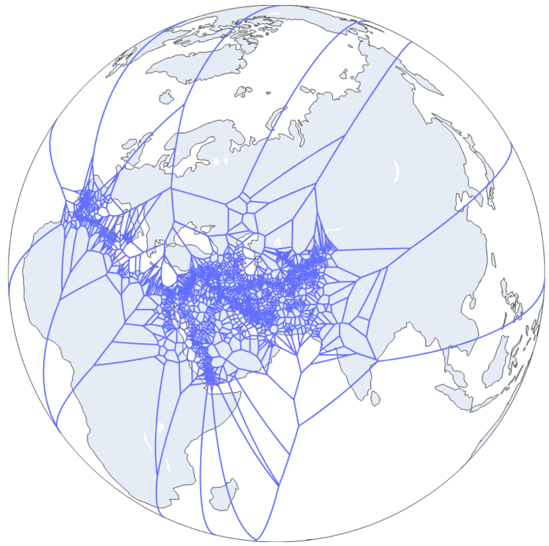

Appendix Figure C.3: The voronoi of all sites in Althurayya

auxiliary site that is far from our original sites[46] when triangulating, and we always choose the spherical circumcenter that is on the same side as the Euclidean circumcenter. Since the auxiliary point is far, the voronoi polygon containing it is outside of our spatial scope of analysis. For instance, in the Voronoi diagram of Althrayya sites, the polygon containing the auxiliary point includes Antarctica, southern part of Australia and South America.

## C.4 Obtaining the arc between two points

This topic is relevant mainly in terms of visualization. We can obtain an approximation of the arc between two point on the globe with the help of the gnomonic projection, because the gnomonic projection projects all great circles into straight lines. For an arc which we only have its two endpoints, we project them on the plane $z = -1$, fill the projected linestring with additional vertices so that segments divided by these additional vertices are no longer than the choice of maximum segment length. This can be easily achieved by Python package `Shapely`'s `segmentize()`. We then map the processed linestring back to the sphere surface. Note that this method can result in uneven resolution. This method can come in handy when even resolution is not important.

## C.5 Other utilities

Since Shapely primarily handles shapes in Euclidean space, we had to develop most of our own utilities. For instance, when dealing with the intersection of two lines on the globe, we treat it as the intersection of two great circles. To achieve this, we transform latitude and longitude coordinates into XYZ coordinates. We then determine the planes that pass through these two lines and find their intersection with the spherical surface.

We also developed our own interpolation function for arcs characterized by a start and an end. To achieve this, we first find all the points on the sphere that are at a certain distance from the start point, effectively creating a circle around the start. We identify the plane that passes through the arc and calculate the intersection points of the plane and the circle. This typically results in two points, and we choose the one inside of the arc.

# References


Na, H.-S., C.-N. Lee, and O. Cheong (2002): "Voronoi diagrams on the sphere," *Computational Geometry*, 23, 183–194.

Patel, A. (2018): "Delaunay+Voronoi on a sphere," .


[46] To decide which auxiliary site to add, we find the mean of longitudes and the mean of latitudes of our original sites, then make the auxiliary site the antipodal of the point (mean of longitude, mean of latitude)

# D Constructing the geospatial model

We build our geospatial model by combining two geospatial models constructed by historians to model travel distances and routes. The first one, ORBIS (Scheidel, 2015), is a geospatial model of the Roman world and spans roughly the maximum extent of Roman conquests. The second, Al-Thurayya (Romanov and Seydi, 2022) is a digitization of Cornu (1983)'s atlas of the Islamic word in the 9th and 10th century. Both geospatial models take the form of undirected graphs; in the case of ORBIS this is augmented by measures of travel costs on each edge. ORBIS also contains sea routes; for the Arab world we augment al-Thurayya with a number of known sea routes. For al-Thurayya we also construct bilateral travel distances ourselves.

## D.1 Vertices

The following links in this document point to the ORBIS city data and Althurayya city data we used in our analysis. ORBIS data labels locations as either actual cities or crossroads. Actual cities are denoted by their authentic names, which correspond to those displayed on the ORBIS website. Crossroads are not designated with a name and are labeled using an "x" and are not visible on the ORBIS website. Similarly, Althurayya locations are characterized by more diverse types, including capitals, metropoles, quarters, sites, towns, villages, waters, waystations, and xroads. Note that some of these locations do not have a name in the dataset.

## D.2 Edges

The edge data for ORBIS and Althurayya is accessible via the respective links provided in this document. We employ the Haversine formula to calculate the length of ORBIS edges, assuming a radius of 6371 km for the Earth. The lengths of Althurayya edges are included within the raw dataset.

## D.3 Merging the graphs

We merge the two graphs by primarily merging vertices shared between them. Some cities hold significance in both the early Islamic world and the Roman world. The challenge of this task is due to differences in location names for the same city within each database. For instance, the city known as Cádiz in Spain is referred to as Gades in ORBIS and Qadis in Althurayya. To address this issue, we implemented a preliminary screening process to identify Althurayya locations situated within a 20km radius of each ORBIS location. We then manually determined whether the location in ORBIS and its counterpart in Althurayya indeed represented the same city. The collection of our refined city pairs and the decisions made can be accessed through the following link.

Apart from the two main data source of routes, we also added the Volga trade route (Section D.4, D.6.1), sea routes in the Caspian Sea and sea routes in the Arab world (Section D.6.2).

During the merge, the geometry of the routes remains unchanged. The only change resulting from the merge is that common locations are treated as identical vertices in the adjacency matrix. All cities are re-indexed and prepared for the computation of least distances and fastest routes after the merge.

## D.4 Construting sea routes for the Arab world

We extend ORBIS's algorithm for sea routes to the Mediterranean Sea and the Black Sea, the Red Sea, the Arabian Sea, the Gulf of Persia, and the Gulf of Oman. Our process begins by creating a grid with a resolution of 0.1 degrees by 0.1 degrees, covering the area of interest in the sea. Each point on the grid can move in eight directions (N, S, W, E, NW, NE, SW, SE). We then manually select Althurayya locations that are close to the coastline as potential ports. Among these candidates, we choose only those whose type is labelled as `capitals`, `metropoles`, `sites`, `towns`, `villages`, or `waystations`, excluding `regions` (centroid of a region) and `xroads`. These selected ports are projected onto the nearest points in the grid, and we calculate the shortest travel time paths along the grid for given routes. The measurement of travel duration is defined in Section D.6.2.

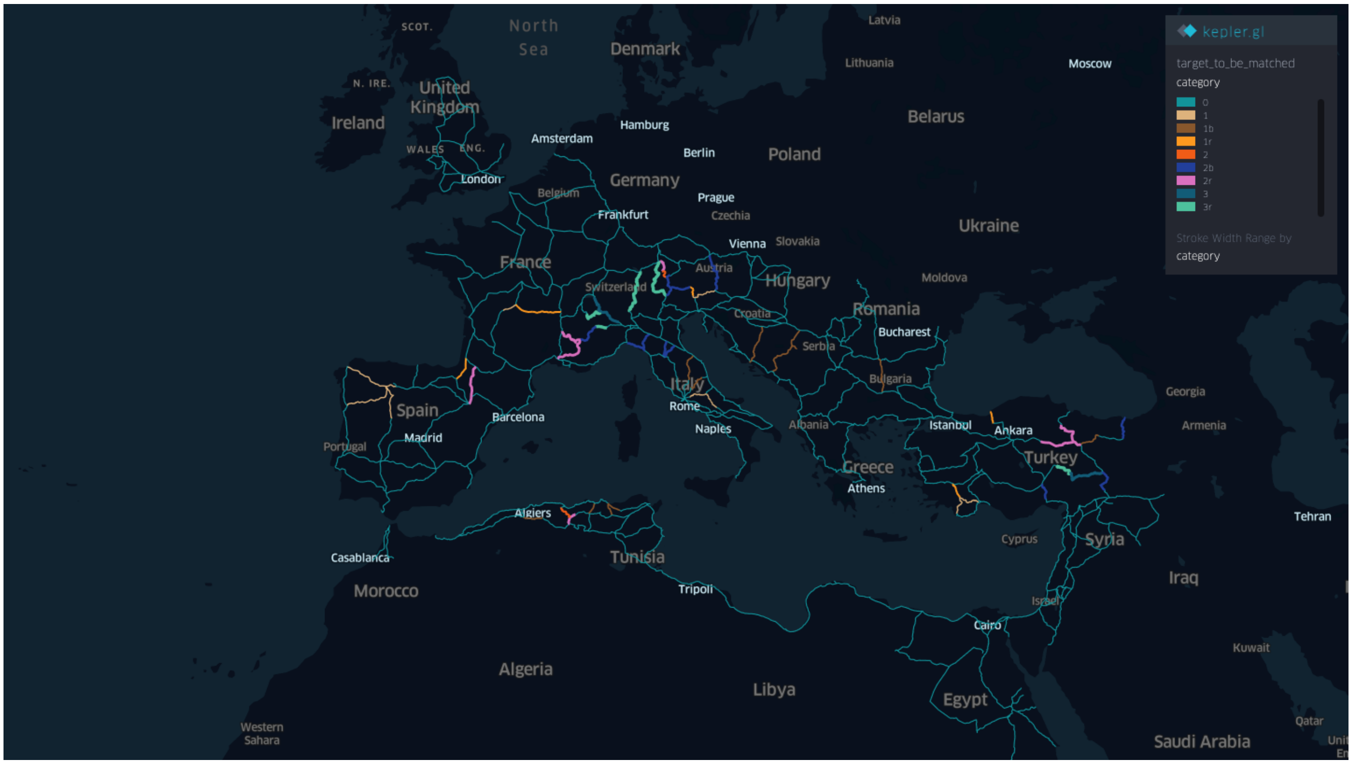


Appendix Figure D.1: The ORBIS adjustment visualized

## D.5 Constructing sea routes for Volga trade route

Volga trade route plays an important role in connecting northern Europe and northwestern Russia with the Caspian Sea via the Volga River. For the segments within the Caspian Sea, we have extended the method outlined in Section D.4. Specifically, we have chosen the following sea routes: Abaskun-Derbent, Derbent-Sasqin, Kuhanrudh-Baku, and Baku-Derbent. To establish a connection between the Caspian Sea and the Black Sea, we have added routes Sasqin-Tanais (via canal), Sarai-Saqsin (via canal), and Sarai-Sarkel (via land). Sasqin-Tanais is represented by a segment in the Don River, which was retrieved from OpenStreetMap here, while Sarai-Saqsin is a segment in the Volga River, retrieved from OpenStreetMap here. Sarai and Sarkel are connected directly since they are in close proximity to each other.

## D.6 Determining weights and speed

### D.6.1 Roads

ORBIS categorizes the weight and speed of terrestrial edges in a categorical manner. Table D.4 shows ten different types of adjustments used by ORBIS, and the locations of these edges are illustrated in Figure D.1. The speed of an edge in ORBIS is defined by Equation D.1.

$$\text{speed} = \text{weight} \times 30km/d, \quad \text{weight} = \frac{\text{unadjusted length}}{\text{adjusted length}} \tag{D.1}$$

ORBIS does not provide explanations for the criteria used to select and categorize edges, otherwise we could simply apply these rules to the Althurayya network. Nevertheless, we have collected various edge-related variables from Stanford EarthWorks and 2019 ASTER project for both ORBIS and Althurayya edges. We run a regression to explain the ORBIS weight defined in Equation D.1 using these variables. We then extrapolate this linear model to the Althurayya data. To put it simply, we use ORBIS as the training set and Althurayya as the test set.

We collect the following variables for all edges and both directions:

**`uphill_3d_2d_ratio`** After properly sampling an edge (as described in Section C.2), we identify all segments that ascend along the specified direction (where the height at the end is greater than the height at the beginning), and then compute the ratio.

$$\text{uphill\_3d\_2d\_ratio} = \frac{\sum_{s \text{ goes uphill}} \text{length\_3D}_s}{\sum_{s \text{ goes uphill}} \text{length\_2D}_s}, \quad s \text{ is a segment in the edge}$$

A large ratio indicates a steep uphill slope.

**`downhill_3d_2d_ratio`** Similar to `uphill_3d_2d_ratio`,

$$\text{downhill\_3d\_2d\_ratio} = \frac{\sum_{s \text{ goes downhill}} \text{length\_3D}_s}{\sum_{s \text{ goes downhill}} \text{length\_2D}_s}$$

**`cityrank_1`** We find the intersection of the edge and the 20 km buffer area of rank 1 cities. Find the ratio of the length of the intersection over the length of the entire edge. The rank of the cities are defined as the following:

| ORBIS | Cumulative Proportion | Althurayya (w/o quaters, regions) | Cumulative Proportion | Harmonized Rank |
|---|---|---|---|---|
| 6 | 25.1% | xroads | 8.6% | 1 |
| | | waystations | 29.0% | |
| 60 | 33.9% | sites | 31.2% | 2 |
| 70 | 48.2% | waters | 37.6% | 3 |
| | | villages | 48.7% | |
| 80 | 83.2% | towns | 94.2% | 4 |
| 90 | 98.2% | capitals | 99.4% | 5 |
| 100 | 100% | metropoles | 100% | 6 |

**`cityrank_2`** Similar to `cityrank_1` but with rank 2 cities.

**`cityrank_3`** Similar to `cityrank_1` but with rank 3 cities.

**`cityrank_4`** Similar to `cityrank_1` but with rank 4 cities.

**`cityrank_5`** Similar to `cityrank_1` but with rank 5 cities.

**`cityrank_6`** Similar to `cityrank_1` but with rank 6 cities.

**`landfeature_Desert`** The percentage of the edge's length that intersects desert polygons, retrieved from Stanford EarthWorks, is calculated. A correction has been manually applied to account for the misidentification of the narrow passage along the Nile as desert

**`landfeature_Plateau`** Percentage of the edge's length that intersects plateau polygons, retrieved from Stanford EarthWorks.

**`landfeature_Plain`** Percentage of the edge's length that intersects plain polygons, retrieved from Stanford EarthWorks.

**`landfeature_Range/mtn`** Percentage of the edge's length that intersects mountain polygons, retrieved from Stanford EarthWorks.

**`near_river`** Percentage of the edge that intersects the 20 km buffer area of rivers.

We fit adjusted ORBIS weights using the mentioned variables (except `leadfeature_Desert` and `near_river` since ORBIS edges does not traverse desert at all, and rivers are modeled separately from the road in ORBIS). To ensure the plausibility of the coefficients and prevent overfitting, we perform least squares regression with the following constraints: (i) `uphill_3d_2d_ratio` has negative effect on the weight, (ii) The effect of `cityrank_*` has positive effect on the weight, (iii) The magnitudes of the effects for `cityrank_*` should follow the ranking `cityrank_1` <

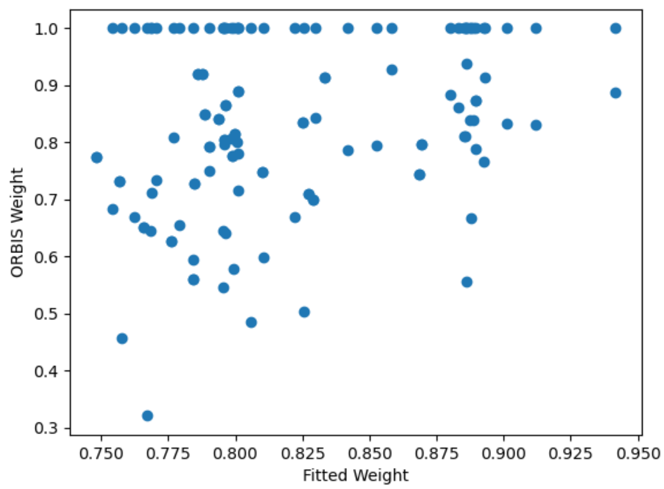


Appendix Figure D.2: Fitted ORBIS weight and actual ORBIS weight

`cityrank_2` < `cityrank_3` < `cityrank_4` < `cityrank_5` < `cityrank_6`, (iv) The effects of `landfeature_Plateau` and `landfeature_Range/mtn` on the weight should be negative, while the effect of `landfeature_Plain` should be positive. Figure D.2 shows a scatter plot between the fitted weight and the ORBIS weight.

We manually set the coefficient for desert to -0.5 and for river to 0.5. This implies that the marching speed is approximately 18.2 km/day for an edge that is 100% within a desert, and the marching speed is roughly 49.5 km/day for an edge near a river[47]. The extrapolated weights and the respective edge locations are displayed in Figure D.3.

The choice of speed not only impacts the total travel time but also influences the traveler's chosen route. For instance, when considering the unweighted shortest route (Figure D.4) from Dimashq to Baghdad, it passes through the Syrian desert. However, with weighted speed considerations, the preferred route would bypass the desert and follow the Euphrates. Similarly, when traveling from Sana to Isfahan, the preferred route (Figure D.5) runs along the coast and includes a stop in Mecca before crossing the Arabian Peninsula.

### D.6.2 Sea

We followed the methodology outlined in Arcenas (2015) to construct sailing speeds at sea, adopting the same steps used by ORBIS. Our data source is the CCMP wind speed data, which provides wind direction and speed information every 6 hours for each cell in a 0.25-degree × 0.25-degree grid, spanning from 1993 to 2023. To align with ORBIS, we focused on speed data for the month of July.

We categorize the wind direction into eight main directions ("N", "NE", "E", "SE", "S", "SW", "W", and "NW"). At the latitude × longitude × direction level, we calculated two key metrics (i) The mean wind speed, and (ii) The proportion of time the wind blew in each direction.

In accordance with Arcenas (2015), scalar wind speeds were classified into four categories: "calm," "light," "moderate," and "heavy," with corresponding Beaufort scale classifications: calm < Beaufort 2; light = Beaufort 2; moderate breeze = Beaufort 3-4; and heavy air ≥ Beaufort 5. Each category corresponds to a specific speed rose (see Figure D.6).

In Figure D.6, the figure on thin arrows denote the scalar velocity of the vessel if the wind blows down the direction of the thin arrow. For instance, when the wind speed is "light," the vessel's speed is 1.0 knot when sailing into the wind, 2.5 knots when the wind blows from the front-right, and 3.4 knots when the wind comes directly from the right. For each coordinate, we calculated the weighted mean of the vessel's speed across the eight wind directions, with the weight determined by the proportion of time the wind blew in each direction. We use the mean vessel speed in eight

[47] This value is considered suitable since ORBIS indicates that a civilian vessel typically travels at around 65 km/day. Although we do not distinguish between river and road in Althurayya, the speed for a mix of different means of transportation should fall within the range of 30 km/day to 65 km/day


Appendix Figure D.3: Al-thurayya edges and their weight

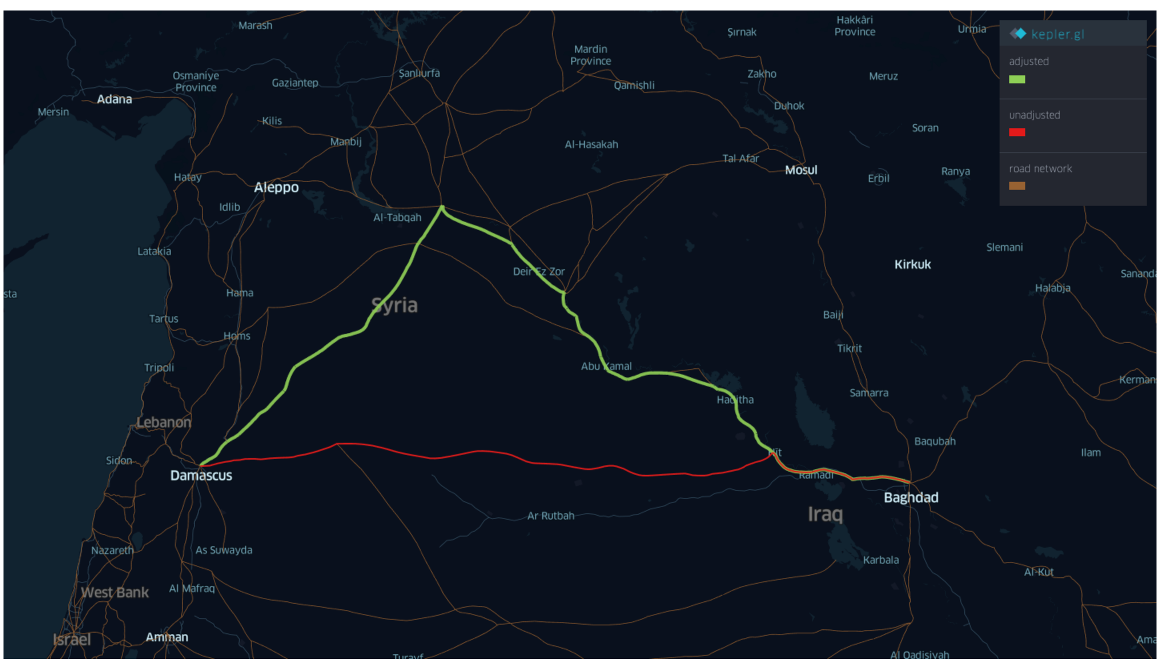


Appendix Figure D.4: Route comparison from Damascus to Baghdad

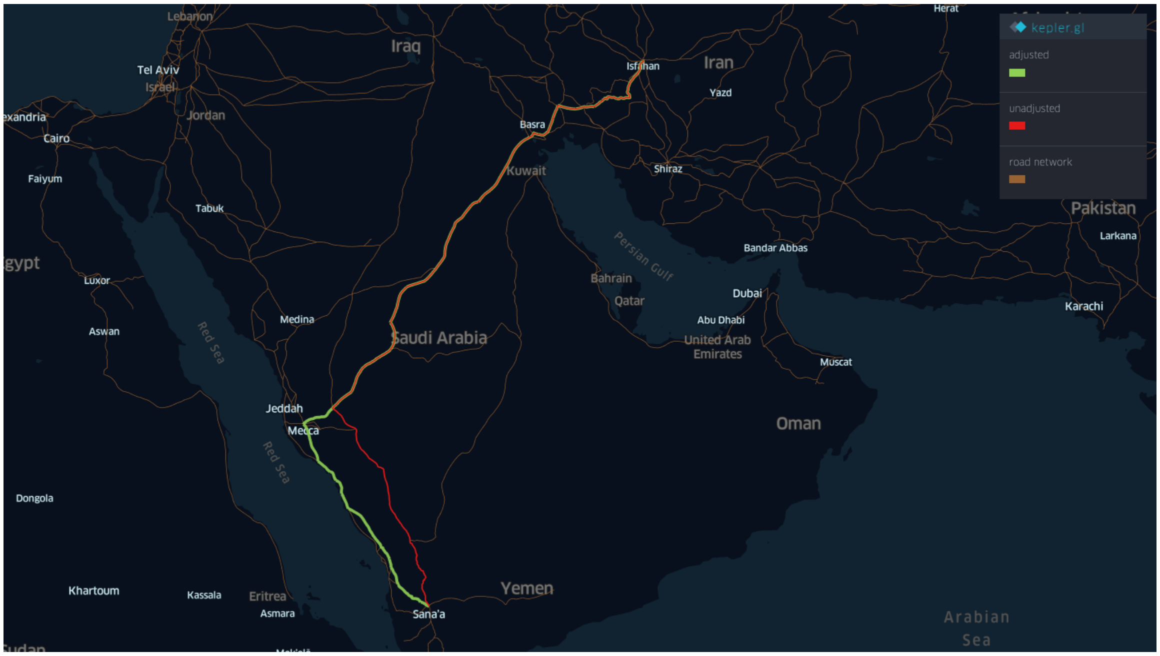


Appendix Figure D.5: Route comparison from Sana'a to Isfahan

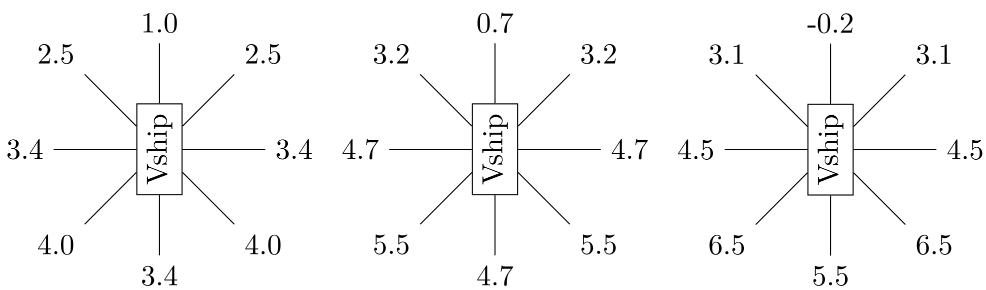


Appendix Figure D.6: Speed rose in light, moderate, and heavy wind (left to right, unit: knot)

directions for each coordinate.

We create a 0.1-degree $\times$ 0.1-degree mesh grid in the area of interest as described in Section D.4. The vessel can go in eight directions at each vertex. The integration of the vessel speed is essential due to the precarity of the wind speed in the sea. The difference of the least time sailing route under uniform speed and varying speed is shown in Figure D.7.

## D.7 Validating the geospatial model

We compare the implied travel times from our geospatial model to those reported by the 10th-century Arab geographer al-Maqdisī in his work *The Best Divisions for the Knowledge of the Regions* (Al-Muqaddasī, 1994).[48] Figure D.8 shows the comparison. Our model generates travel times that are slightly larger for shorter distances, and on average similar for longer routes.

[48] Al-Maqdisī reports cities and (unsystematically) distances (in travel stages, post stages, and *farsakhs*) or travel times (in days, or nights in the desert) between cities in different parts of the Islamic lands. Historians note that it is unlikely that al-Maqdisī did indeed travel to all these regions, and some distances and travel times are unrealistic. We exclude the most egregious outliers.

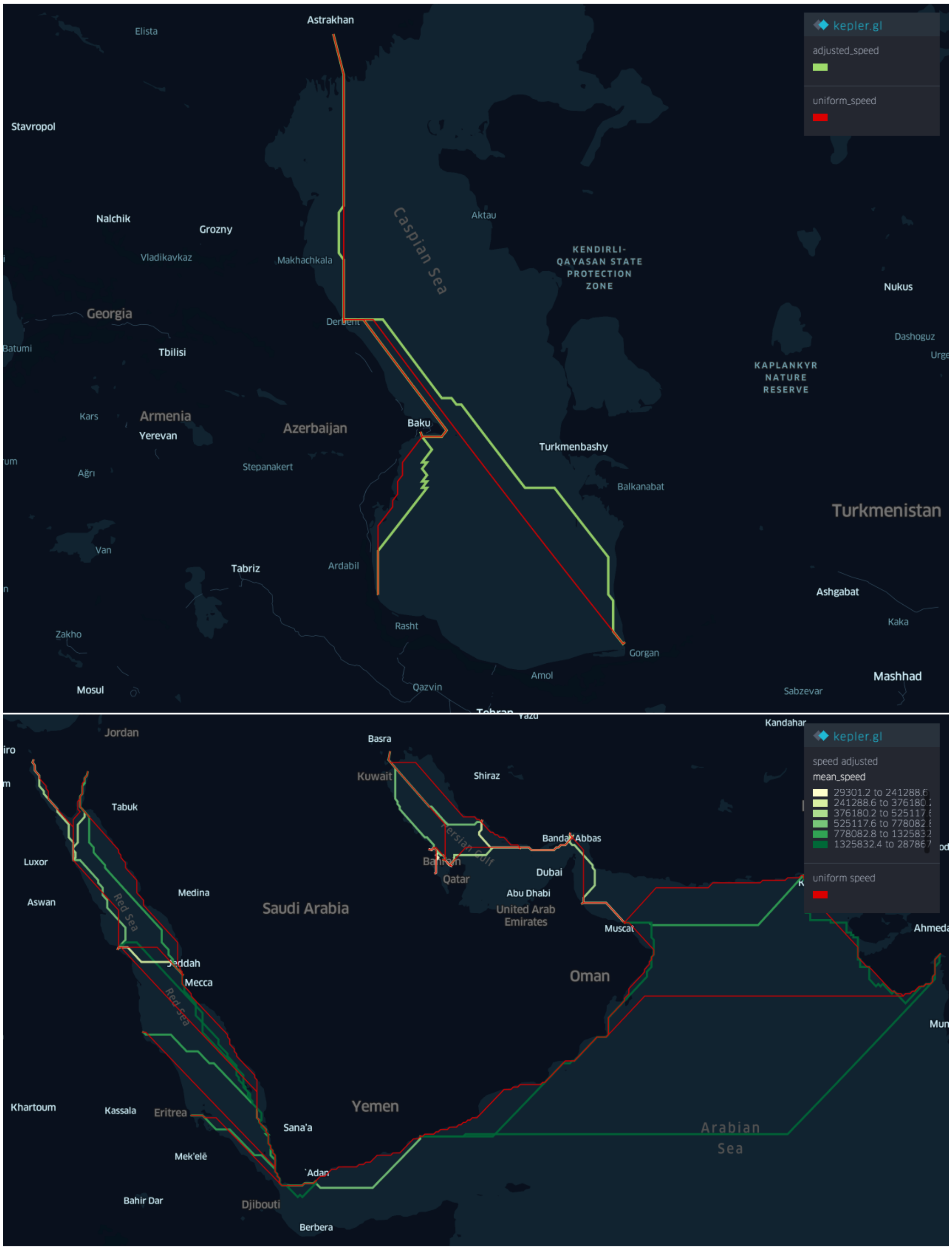


Appendix Figure D.7: Changes of the sailing route before and after incorporating wind speed

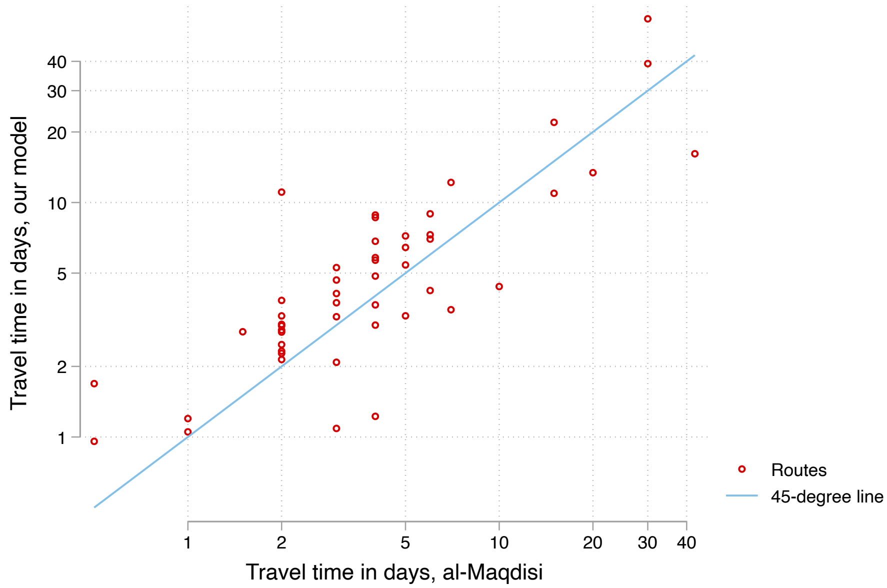


Appendix Figure D.8: Comparison of travel times between our model and those reported by Al-Muqaddasī (1994)

Each dot refers to a city-to-city connection for which Al-Muqaddasī (1994) lists the travel time in days. We exclude desert routes (where he reports travel times in nights or in watering stations, routes with cities cannot be found in al-Thurayya, as well as the route between Tahart and Fes, which he claims can be travelled in three days despite it being a distance of more than 600 kilometers (our model predicts 22 days).

## D.8 Tables and references

| Country | Total | City | Crossroad | Country | Total | City | Crossroad |
|---|---|---|---|---|---|---|---|
| United Kingdom | 200 | 32 | 168 | Cyprus | 7 | 7 | 0 |
| Italy | 119 | 111 | 8 | Serbia | 7 | 7 | 0 |
| Turkey | 88 | 86 | 2 | Hungary | 6 | 4 | 2 |
| Greece | 69 | 69 | 0 | Lebanon | 6 | 5 | 1 |
| France | 50 | 49 | 1 | Ukraine | 6 | 6 | 0 |
| Spain | 43 | 42 | 1 | Bosnia & Herzegovina | 5 | 2 | 3 |
| Egypt | 36 | 36 | 0 | Morocco | 5 | 5 | 0 |
| Algeria | 23 | 23 | 0 | Jordan | 5 | 5 | 0 |
| Tunisia | 18 | 18 | 0 | Slovenia | 4 | 3 | 1 |
| Syria | 17 | 14 | 3 | West Bank | 2 | 2 | 0 |
| Libya | 16 | 16 | 0 | Gaza Strip | 2 | 2 | 0 |
| Germany | 16 | 15 | 1 | Macedonia | 2 | 2 | 0 |
| Romania | 15 | 11 | 4 | Russia | 2 | 2 | 0 |
| Croatia | 15 | 12 | 3 | Georgia | 2 | 2 | 0 |
| Austria | 11 | 11 | 0 | Montenegro | 1 | 1 | 0 |
| Bulgaria | 11 | 10 | 1 | Netherlands | 1 | 1 | 0 |
| Israel | 9 | 9 | 0 | Iraq | 1 | 1 | 0 |
| Portugal | 8 | 5 | 3 | Malta | 1 | 1 | 0 |
| Albania | 8 | 6 | 2 | Total | 844 | 640 | 204 |
| Switzerland | 7 | 7 | 0 | | | | |

Appendix Table D.1: ORBIS cities by their modern country, distinguishing city types (city or crossroad)

| Country | Total | capitals | metrop. | quarters | sites | towns | villages | waters | waystns | xroads |
|---|---|---|---|---|---|---|---|---|---|---|
| Mā-warāᵓ-l-nahr (Transoxiana) | 186 | 17 | 1 | 0 | 3 | 93 | 21 | 0 | 31 | 20 |
| Ḫurāsān | 139 | 12 | 1 | 0 | 0 | 70 | 16 | 1 | 30 | 9 |
| al-Šām (Greater Syria) | 138 | 7 | 1 | 0 | 0 | 57 | 23 | 0 | 27 | 23 |
| Jazīra al-ᶜarab | 122 | 3 | 1 | 0 | 3 | 29 | 16 | 0 | 62 | 8 |
| Fārs(or Fāris) | 114 | 7 | 1 | 0 | 1 | 45 | 15 | 0 | 42 | 3 |
| al-Maġrib | 110 | 6 | 0 | 0 | 0 | 78 | 5 | 0 | 1 | 20 |
| Aqūr (al-Jazīra ) | 94 | 4 | 0 | 1 | 0 | 45 | 9 | 0 | 25 | 10 |
| Miṣr (Egypt) | 88 | 4 | 1 | 1 | 3 | 44 | 23 | 0 | 7 | 5 |
| al-Andalus (Spain) | 83 | 0 | 1 | 0 | 0 | 62 | 3 | 0 | 0 | 17 |
| al-Jibāl | 71 | 9 | 1 | 0 | 1 | 16 | 4 | 0 | 31 | 9 |
| al-ᶜIrāq | 66 | 5 | 1 | 1 | 1 | 37 | 7 | 0 | 11 | 3 |
| al-Riḥāb (Caucasus) | 62 | 2 | 1 | 0 | 0 | 34 | 10 | 0 | 4 | 11 |
| Badiyya al-ᶜarab | 60 | 0 | 0 | 0 | 2 | 4 | 1 | 0 | 48 | 5 |
| al-Sind | 53 | 4 | 0 | 0 | 0 | 36 | 2 | 0 | 1 | 10 |
| al-Daylam | 50 | 3 | 1 | 0 | 0 | 20 | 6 | 0 | 18 | 2 |
| al-Mafāza | 49 | 0 | 0 | 0 | 0 | 3 | 8 | 0 | 33 | 5 |
| Kirmān | 44 | 3 | 1 | 0 | 0 | 26 | 6 | 0 | 5 | 3 |
| Sijistān (Sīstān) | 40 | 4 | 0 | 0 | 0 | 19 | 6 | 0 | 6 | 5 |
| Barqa (Lybia) | 39 | 1 | 0 | 0 | 1 | 8 | 4 | 0 | 24 | 1 |
| Ḫūzistān (al-Ahwāz) | 39 | 7 | 1 | 0 | 0 | 14 | 2 | 0 | 13 | 2 |
| al-Yaman | 31 | 5 | 0 | 0 | 0 | 14 | 2 | 0 | 4 | 6 |
| al-Ḫazar | 8 | 1 | 0 | 0 | 0 | 4 | 0 | 0 | 0 | 3 |
| NoRegion | 6 | 0 | 0 | 0 | 0 | 0 | 0 | 0 | 0 | 6 |
| Total | 1692 | 104 | 13 | 3 | 15 | 758 | 189 | 1 | 423 | 186 |

Appendix Table D.2: Althurayya cities by region, distinguishing city types (capitals, metropoles, quarters, sites, towns, villages, waters, waystations, xroads)

| | count | mean | std | min | 10% | 25% | 50% | 75% | 90% | 99% | max |
|---|---|---|---|---|---|---|---|---|---|---|---|
| ORBIS | 1215 | 144489.0 | 158012.5 | 3827.2 | 31606.2 | 58006.7 | 102353.1 | 168695.0 | 300377.0 | 737576.2 | 2142105.6 |
| Althurayya | 2053 | 55530.4 | 64952.5 | 1687.0 | 13851.8 | 23842.0 | 38387.0 | 62771.0 | 108031.6 | 332197.5 | 861693.0 |

Appendix Table D.3: Summary statistics of the lengths of the edges in graphs

| Type ID | source → target | target → source |
|---|---|---|
| `0` | No adjustment | No adjustment |
| `1` | Add 18 km to the length | No adjustment |
| `2` | Add 36 km to the length | No adjustment |
| `3` | Add 54 km to the length | No adjustment |
| `1r` | No adjustment | Add 18 km to the length |
| `2r` | No adjustment | Add 36 km to the length |
| `3r` | No adjustment | Add 54 km to the length |
| `1b` | Add 18 km to the length | Add 18 km to the length |
| `2b` | Add 36 km to the length | Add 36 km to the length |
| `3b` | Add 54 km to the length | Add 54 km to the length |

Appendix Table D.4: Adjustment by ORBIS

## References


Al-Muqaddasī (1994): *Aḥsan al-taqāsīm fi maʾarfat al-aqalīm (The Best Divisions for Knowledge of the Regions)*, Garnet Publishing (transl. B.A. Collins).

Arcenas, S. (2015): "ORBIS and the sea: A model for maritime transportation under the Roman Empire," *Retrieved February*, 22, 2021.

Cornu, G. (1983): *Atlas du monde Arabo-Islamique à l'époque classique: IX.-X. siècles*, Brill.

Romanov, M. and M. Seydi (2022): "al-Thurayyā," https://althurayya.github.io/ [Accessed: (1 July 2023)].

Scheidel, W. (2015): "ORBIS: The Stanford geospatial network model of the Roman world," Tech. rep.

# E Mapping the Data to the Model

In order to map our data to the model, we need to define which hoard and find locations correspond to which model locations. We define spatial aggregates based on historical political boundaries, geography, and computational feasibility in mind, noting that political boundaries change over time, while our location definition must not. Moreover, administrative boundaries are not available for the same time period for all regions. We therefore proceed in two steps: we first construct region boundaries based on the regions in al-Thurayya, covering the maximum extent of the Umayyad caliphate, and then define regions for the remainder of our area of interest.

## E.1 Constructing regions for the Arab world

We use the `region` tag associated with each Althurayya locations to establish a historical provincial partition of the Arab world.

1. We manually delineated a rough approximation of the Arab world's boundary.
2. We applied spherical voronoi tessellation (see Section C.3) to all al-Thurayya locations within this boundary.
3. The resulting polygons were categorized based on the region information associated with each polygon's corresponding location, aligning them with the 22 regions presented in D.2 (excluding NoRegion).
4. We then take the union of the polygons under the same `region` tag.
5. We intersected the resulting (multi-)polygon with the coastline to remove the portions of the polygon that extended into the sea.
6. The final (multi-)polygon represents the corresponding Arab region.

We also corrected some erroneously labelled region labels[49].

## E.2 Constructing regions for the western world

We construct regions in the western world roughly based on administrative boundaries that we retrieve from the *Digital Atlas of the Roman and Medieval Civilizations* (DARMC) hosted at Harvard Unversity, specifically the AD 200 and 303-325 Roman provincial boundaries (which are based on the Barrington Atlas, Talbert, 2000) and the Medieval kingdom boundaries around AD 814, which are an original contribution of DARMC.

We define the boundaries of our region of interest in Europe by taking the union of the AD 200 Roman provincial boundaries with the 814 boundaries of the Frankish empire and the area of the West Slavs. The resulting border is roughly the modern-day German-Polish border, plus Bohemia, but follows otherwise roughly the AD 200 Roman Empire boundary. In the areas covered by al-Thurayya, the border is delineated roughly by the convex hull of the spatial extent of administriative district boundaries.

## E.3 Aggregating regions

We then merge a number of regions in order to have mints and hoards in all regions (which is important for identification). We merge the realm of Charlemagne with the Frankish lands in Germania; the areas of Byzantine Thracia and Dacia, and combine Sardinia and Corsica. In the east, we combine the administrative districts of the eastern Caliphate where hoard coverage is sparse, the regions of al-Iraq, al-Jibal, Khuzestan, and Kirman; and finally the regions of the Arabian Peninsula. Figure E.1 shows the resulting 21 regions.

## E.4 Defining the coin sample for the structural analysis

We use the same sample of coins as for the reduced-form regressions, with the following exceptions:

- We exclude coins where the mint date interval exceeds 150 years.
- We exclude non-hoard coin finds from excavations (because the *tpq* is meaningless).

[49]See this link.

Appendix Figure E.1: Region Definitions

## References

Talbert, R. J. (2000): *Barrington Atlas of the Greek and Roman World: Map-by-map Directory*, vol. 1, Princeton University Press.